

**The role of hepatic SURF4 in the lipid metabolism and the
development of atherosclerosis**

by

Yishi Shen

A thesis submitted in partial fulfillment of the requirements for the degree of

Doctor of Philosophy

Medical Sciences - Pediatrics

University of Alberta

© Yishi Shen, 2023

Abstract

Atherosclerotic cardiovascular disease (ASCVD) is the leading cause of morbidity and mortality worldwide. Long-term elevated plasma levels of low-density lipoprotein cholesterol (LDL-C) are the major risk factors for developing atherosclerotic lesions, which can eventually lead to myocardial infarction and stroke. Lowering plasma LDL-C levels remains the main way to prevent CVD. LDL is removed from the circulation mainly by the hepatic LDL receptor. Mutations in this receptor cause familial hypercholesterolemia, which is characterized by elevated plasma levels of LDL-C and increased risk of CVD. Statins, the most-prescribed drug lowering plasma cholesterol levels, increase the expression of LDL receptor and reduce cardiovascular events by 20% to 40%. However, about 15% of people treated with statins show statin intolerance and require alternative therapies to lower LDL-C levels. Another option is Proprotein convertase subtilisin/kexin type 9 (PCSK9), which promotes degradation of LDL receptors. Recently approved PCSK9 inhibitors can effectively reduce plasma LDL-C levels, but the treatment is expensive. PCSK9 siRNA therapy may be more affordable, but it is still too expensive for all eligible patients to use for primary prevention. Furthermore, the lipid-lowering effects of both statins and PCSK9 inhibitors depends mainly on enhancing clearance of LDL through increasing expression of LDL receptor. LDL is produced through catabolism of very low-density lipoprotein (VLDL), a triglyceride-rich lipoprotein that is made exclusively by the liver. Triglycerides (TG) on circulating VLDL are hydrolyzed by lipoprotein lipase (LPL), leading to formation of intermediate-density lipoprotein that can then be converted to LDL. The drugs Mipomersen (inhibitor of apolipoprotein B100 (apoB100)) and Lomitapide (inhibitor of microsomal triglyceride transfer protein (MTP)) can reduce VLDL production and secretion, lowering plasma levels of LDL-C. However, both drugs have severe adverse effects such as

hepatic lipid accumulation, liver damage and diarrhea. Thus, the need to identify novel therapeutic targets to reduce plasma cholesterol levels is urgent. This thesis aims to investigate the role of hepatic Surf4, a cargo receptor located in the endoplasmic reticulum (ER) membrane, in regulating plasma lipid levels and the development of atherosclerosis by mediating PCSK9 and VLDL secretion from hepatocytes.

In chapter 3, I investigated the role of Surf4 in PCSK9 secretion *in vitro* and *in vivo*. It has been reported that Surf4 mediates overexpressed PCSK9 secretion in HEK293T cells, which were derived from human embryonic kidney cells. Considering endogenous PCSK9 is mainly expressed and secreted by the liver in normal physiological condition, I determined the role of Surf4 in mediating PCSK9 secretion in human hepatoma derived cell lines, Huh7 and HepG2 cells. Interestingly, I found that knockdown of *SURF4* did not inhibit endogenous PCSK9 secretion; instead, deficiency of *SURF4* upregulated PCSK9 expression in both Huh7 and HepG2 cells. On the other hand, knockdown of hepatic Surf4 in wild type mice (C57BL/6J) has no effects on PCSK9 expression and secretion. Although the results from *in vitro* and *in vivo* studies were completely consistent, these findings indicate a negligible role of hepatic SURF4 in endogenous PCSK9 secretion from the liver and cultured hepatocytes.

In chapter 4, we generated *Surf4* hepatocyte-specific knockout (*Surf4*^{LKO}) mice and found that plasma levels of total cholesterol (TC), TG, non-high-density lipoprotein cholesterol (HDL-C), and apoB were significantly reduced in *Surf4*^{LKO} mice compared to *Surf4*^{Flox} mice. I also found that Surf4 coimmunoprecipitated and colocalized with apoB100, and *SURF4* silencing reduced secretion of apoB100 in cultured human hepatoma cells. Furthermore, knockdown of hepatic *Surf4* in LDL receptor knockout (*Ldlr*^{-/-}) mice significantly reduced TG secretion, plasma levels of TC, non-HDL-C, and apoB, and ameliorated the development of atherosclerosis.

However, both *Surf4*^{LKO} mice and *Ldlr*^{-/-} mice with hepatic *Surf4* knockdown displayed similar levels of liver lipids and plasma alanine aminotransferase (ALT) activity as their control mice, indicating that inhibition of hepatic *Surf4* does not cause notable liver damage. Expression of stearoyl-CoA desaturase-1 (SCD1) was also reduced in the liver of *Surf4* knockdown mice, suggesting a reduction in *de novo* lipogenesis. These findings suggest that deficiency of hepatic *Surf4* reduced VLDL secretion, plasma lipid levels, and the risk of atherosclerosis without causing significant hepatic lipid accumulation or liver damage.

In chapter 5, I investigated the role of hepatic SURF4 in lipoprotein metabolism and the development of atherosclerosis in another commonly used mouse model of atherosclerosis, apolipoprotein E knockout (*apoE*^{-/-}) mice. I found that, in *apoE*^{-/-} mice fed a regular chow diet, knockdown of hepatic *Surf4* expression significantly reduced TG secretion and plasma levels of non-HDL-C and TG without causing obvious hepatic lipid accumulation or liver damage. When hepatic *Surf4* was knocked down in *apoE*^{-/-} mice fed the Western-type diet (WTD), I observed a significant reduction in plasma levels of non-HDL-C, but not TG. Knockdown of hepatic *Surf4* did not increase hepatic TC and TG levels or cause liver damage, but significantly diminished atherosclerotic lesions in *apoE*^{-/-} mice fed with WTD. Therefore, these findings, together with the results from *Ldlr*^{-/-} mice, indicate the potential of hepatic *Surf4* inhibition as a novel therapeutic strategy to reduce plasma lipid levels and the risk of ASCVD.

In summary, the work performed during this Ph.D. thesis will shed light on the novel target of lowering plasma levels of cholesterol and TG and reducing the risk of atherosclerosis without causing obvious hepatic lipid accumulation.

Preface

This thesis is an original work by Yishi Shen. All procedures regarding animal handling, feeding and surgeries were approved by the University of Alberta's Institutional Animal Care Committee in accordance with guidelines of the Canadian Council on Animal Care. The contributions made by the candidate Yishi Shen and co-authors of these studies are described below.

Parts of this thesis have been published and accepted in peer-reviewed journals, listed below in chronological order.

Chapter 1 is modified from a publication: **Yishi Shen**, Hong-mei Gu, Shucun Qin, Da-wei Zhang (2022). 'Surf4, cargo trafficking, lipid metabolism, and therapeutic implications', accepted for publication in *Journal of Molecular Cell Biology*. I conceived and designed the study, drafted and assisted with editing the article, and generated all figures. D.Z helped to conceive and design the study and supervised the final version. All authors participate in the discussion and the preparation of the manuscript.

Chapter 3 is a combination of two publications. Part of this chapter is a copy of the publication: **Yishi Shen**, Bingxiang Wang, Shijun Deng, Lei Zhai, Hong-mei Gu, Adekunle Alabi, Xiaodan Xia, Yongfa Zhao, Xiaole Chang, Shucun Qin, Da-wei Zhang (2020). 'Surf4 regulates expression of proprotein convertase subtilisin/kexin type 9 (PCSK9) but is not required for PCSK9 secretion in cultured human hepatocytes', *Biochimica et Biophysica Acta- Molecular and Cell Biology of Lipids*. 2020 Feb; 1865(2): 158555. doi: doi.org/10.1016/j.bbailip.2019.158555. Part of this chapter is a copy of part of the publication: Bingxiang Wang#, **Yishi Shen**#, Lei Zhai#, Xiaodan Xia#, Hong-mei Gu, Maggie Wang, Yongfa Zhao, Xiaole Chang, Adekunle Alabi, Sijie Xing, Shijun Deng, Boyan Liu, Guiqing

Wang, Shucun Qin, Da-wei Zhang (# **co-first author**). ‘Atherosclerosis-associated hepatic secretion of VLDL but not PCSK9 is dependent on cargo receptor protein Surf4’, *Journal of Lipid Research*. 2021 Jun; 62: 100091. doi: 10.1016/j.jlr.2021.100091. For all data presented in the thesis, I conceived and designed the study, performed most of experiments, drafted and assisted with editing the article, and generated all figures and tables. D.Z helped to conceive and design the study, interpret data, draft, and revise the manuscript for important intellectual content. All authors provided critical feedback and helped shape the research, analysis, and manuscript.

Chapter 4 is a copy of part of the publication: Bingxiang Wang#, **Yishi Shen#**, Lei Zhai#, Xiaodan Xia#, Hong-mei Gu, Maggie Wang, Yongfa Zhao, Xiaole Chang, Adekunle Alabi, Sijie Xing, Shijun Deng, Boyan Liu, Guiqing Wang, Shucun Qin, Da-wei Zhang (# **co-first author**). ‘Atherosclerosis-associated hepatic secretion of VLDL but not PCSK9 is dependent on cargo receptor protein Surf4’, *Journal of Lipid Research*. 2021 Jun; 62: 100091. doi: 10.1016/j.jlr.2021.100091. For all experiments included in the these, I conceived and designed the study, performed most of experiments, drafted and assisted with editing the article, and generated all figures and tables. Bingxiang Wang and Lei Zhai performed the experiments of “Generation of Surf4^{LKO} mice”, “Impact of lacking hepatic Surf4 on plasma lipid levels”, and “Effects of Surf4 deficiency on hepatic lipids”. D.Z helped to conceive and design the study, interpret data, draft, and revise the manuscript for important intellectual content. All authors provided critical feedback and helped shape the research, analysis, and manuscript.

Chapter 5 is a copy of the publication: **Yishi Shen**, Hong-mei Gu, Lei Zhai, Bingxiang Wang, Shucun Qin, and Da-wei Zhang (2022). ‘The role of hepatic Surf4 in lipoprotein metabolism and the development of atherosclerosis in apoE^{-/-} mice’, *Biochimica et Biophysica Acta-*

Molecular and Cell Biology of Lipids. 2022 July; 1867(10): 159196. doi: doi.org/10.1016/j.bbalip.2022.159196. I conceived and designed the study, performed 99% of experiments, drafted and assisted with editing the article, and generated all figures and tables. D.Z helped to conceive and design the study, interpret data, draft, and revise the manuscript for important intellectual content. All authors provided critical feedback and helped shape the research, analysis, and manuscript.

Dedication

I dedicate this thesis to my parents Bingquan Shen and Jun Shi. Thank you for believing in me and investing in my education. Without your support, understanding, and most of all love, the completion of this work would not have been possible.

Acknowledgments

First and foremost, I would like to express deepest gratitude to my supervisor Dr. Da-wei Zhang for his constant support, immense knowledge, and valuable guidance. Thank you for the opportunity to work on this amazing and exciting project which has helped build my robust scientific thinking. I could not have imagined having this work finished without your mentorship. Besides my supervisor, I would also like to extend my appreciation to my supervisory committee Dr. Richard Lehner, Dr. Rene Jacobs, and Dr. Maria Febbraio, thank you for your ongoing assistance, invaluable comments and suggestions to the completion of my thesis.

My enduring appreciation also goes to all members of the Zhang Laboratory especially Mrs. Hong-mei Gu for her mentorship, suggestions, and encouragement. My colleagues and friends always help and motivate me in the laboratory which is hard to put into words. Thank you: Dr. Shijun Deng, Dr. Adekunle Alabi (Jamal), Dr. Xiaodan Xia, Maggie Wang, Suha Jarad, Ziyang Zhang, Govind Gill.

I would also like to express gratitude to the members of the Group on Molecular and Cell Biology of Lipids (MCBL), and the Department of Pediatrics. Many of them helped me for the completion of this work at different moments.

Finally, I would like to thank my parents, Bingquan Shen and Jun Shi, and friends for their unconditional support and always been there for me throughout my life.

Table of Contents

Chapter 1	1
Introduction	1
Abstract	2
1.1 Atherosclerotic cardiovascular disease	3
1.2 Low-density lipoprotein homeostasis	5
1.2.1 Very low-density lipoprotein biosynthesis and secretion	5
1.2.2 Very low-density lipoprotein metabolism	8
1.2.3 Low-density lipoprotein metabolism.....	10
1.3 LDL receptor	10
1.3.1 LDL receptor binding, endocytosis, and recycling.....	10
1.3.2 Transcriptional regulation of the LDL receptor.....	12
1.4 PCSK9	12
1.4.1 The discovery of PCSK9	12
1.4.2 The mechanism of PCSK9-mediated LDL receptor degradation.....	13
1.4.3 PCSK9 biosynthesis, processing, and secretion	15
1.5 Pharmacological treatment for hypercholesterolemia	16
1.5.1 Statins	16
1.5.2 PCSK9 inhibitors.....	17
1.5.3 Very low-density lipoprotein inhibitors.....	17
1.6 Surfeit locus	18
1.6.1 Discovery of Surfeit locus genes	18
1.6.2 Surfeit locus 4.....	19
1.6.3 SURF4 and cargo trafficking.....	22
1.6.4 SURF4, lipid metabolism and atherosclerosis.....	27
1.6.5 Other known physiological and pathophysiological functions of SURF4	28
1.7 Rationale, Hypothesis and Aim of thesis	29
Chapter 2	32
Materials and Methods	32
2.1 Materials	33
2.2 Animal	35

2.3 Culture and treatment of cell lines	35
2.3.1 Cell Culture.....	35
2.3.2 Thawing of frozen cells.....	35
2.3.3 Cryopreservation of immortalized Cells.....	36
2.3.4 Transfection.....	36
2.3.4.1 Lipofectamine 3000 Transfection.....	37
2.3.4.2 RNAiMAX Transfection.....	37
2.3.5 Statin Treatment.....	37
2.4 Quantification of mRNA expression	37
2.4.1 RNA Isolation.....	37
2.4.2 cDNA synthesis.....	38
2.4.3 Quantitative Real-Time PCR (qRT-PCR).....	39
2.5 Western Blot and Protein Expression Analysis	42
2.5.1 Protein extraction from cultured cells.....	42
2.5.2 Protein extraction from animal tissues.....	42
2.5.3 Protein assay and quantification.....	42
2.5.4 Immunoblotting.....	43
2.6 Immunofluorescence	43
2.7 Immunoprecipitation analysis	44
2.8 Measurement of liver lipids	44
2.9 Plasma lipid and Alanine aminotransferase (ALT)	45
2.9.1 ALT determination.....	45
2.9.2 Cholesterol determination.....	45
2.9.3 Triglycerides determination.....	46
2.10 ELISA Measurement of plasma PCSK9	46
2.11 ApoB and TG secretion	47
2.12 Histochemistry	47
2.13 Adeno-associated virus preparation	48
2.14 Atherosclerotic analysis	48
2.15 Statistical analysis	49
Chapter 3 Manuscript I	50

3.1 Introduction.....	52
3.2 Results.....	54
3.2.1 Detection of SURF4	54
3.2.2 Knockdown of <i>SURF4</i> increased PCSK9 expression and secretion in cultured hepatoma cells	57
3.2.3 SURF4 does not directly associate with PCSK9	60
3.2.4 Knockdown of <i>SURF4</i> increased <i>SREBP2</i> transcriptional activity.....	62
3.2.5 Knockdown of hepatic <i>Surf4</i> has no effect on PCSK9 expression and secretion <i>in vivo</i>	64
3.3 Discussion	66
Chapter 4 Manuscript II.....	68
Abstract	70
4.1 Introduction.....	71
4.2 Results	72
4.2.1 Generation of <i>Surf4</i> ^{LKO} mice	72
4.2.2 Impact of lacking hepatic SURF4 on plasma lipid levels.....	74
4.2.3 Effects of SURF4 on apoB secretion.....	77
4.2.4 Effects of <i>Surf4</i> deficiency on hepatic lipids	81
4.2.5 Effects of SURF4 on the development of atherosclerosis	84
4.3 Discussion	90
Chapter 5 Manuscript III	95
Abstract	97
5.1 Introduction.....	98
5.2 Results.....	100
5.2.1 Role of hepatic SURF4 in lipoprotein metabolism in <i>apoE</i> ^{-/-} mice on a regular chow diet	100
5.2.2 Impact of hepatic <i>Surf4</i> silencing on the liver in <i>apoE</i> ^{-/-} mice on a regular chow diet	106
5.2.3 Effects of hepatic SURF4 on the development of atherosclerosis in <i>apoE</i> ^{-/-} mice.....	109
5.2.4 Effects of hepatic SURF4 on lipoprotein metabolism in <i>apoE</i> ^{-/-} mice on the Western-type diet.....	112
5.3 Discussion	117
Chapter 6.....	121
Discussion and Future Perspectives.....	121
6.1 The role of SURF4 in PCSK9 secretion from hepatocytes	122

6.1.1 SURF4 regulates <i>PCSK9</i> expression but is not required for its secretion <i>in vitro</i>	122
6.1.2 Hepatic SURF4 does not affect <i>PCSK9</i> expression and secretion <i>in vivo</i>	123
6.1.3 Conclusion	123
6.2 The role of hepatic SURF4 in lipoprotein metabolism and the development of atherosclerosis in <i>Ldlr</i>^{-/-} mice and <i>apoE</i>^{-/-} mice.....	124
6.2.1 The role of hepatic SURF4 in lipoprotein metabolism and the development of atherosclerosis in <i>Ldlr</i> ^{-/-} mice	124
6.2.2 The role of hepatic SURF4 in lipoprotein metabolism and the development of atherosclerosis in <i>apoE</i> ^{-/-} mice	124
6.2.3 Conclusion	126
6.3 Future Direction.....	128
6.3.1 To investigate the mechanism by which hepatic lipid homeostasis is maintained in <i>Surf4</i> knockdown mice	128
6.3.2 To investigate the role of SURF4 in chylomicron secretion in intestine.....	128
6.3.3 To investigate the role of SURF4 in collagen secretion	129
Reference.....	131

Lists of Figures

Figure 1.1 Development of atherosclerosis.

Figure 1.2 The model for the core lipidation of VLDL particles.

Figure 1.3 VLDL secretion and metabolism.

Figure 1.4 The receptor mediated endocytosis of LDL particles.

Figure 1.5 PCSK9-mediated degradation of LDLR in extracellular pathway.

Figure 1.6. Structure of SURF4.

Figure 1.7. SURF4 and cargo transportation between the ER and Golgi apparatus.

Figure 1.8. Study hypothesis and research objectives.

Figure 3.1. Detection of SURF4.

Figure 3.2. Effect of *SURF4* knockdown on PCSK9 secretion.

Figure 3.3. Immunoprecipitation of SURF4.

Figure 3.4. Effect of *SURF4* knockdown on *SREBP2* transcriptional activity.

Figure 3.5. The effect of hepatic knockdown of *Surf4* on PCSK9 secretion *in vivo*.

Figure 4.1. Generation of *Surf4*^{LKO} mice.

Figure 4.2. Impact of lacking hepatic SURF4 on plasma lipid and blood glucose levels.

Figure 4.3. The effect of *SURF4* knockdown on the level of apoB and apoA-I in cultured cells.

Figure 4.4. Effect of hepatic *Surf4* silencing on liver lipids and gene expression.

Figure 4.5. The effect of *Surf4* knockdown on plasma lipid levels and the expression of apoB and apoA-I in *Ldlr*^{-/-} mice.

Figure 4.6. The effect of *Surf4* knockdown on the levels of liver lipids and the development of atherosclerosis in *Ldlr*^{-/-} mice.

Figure 5.1. Effect of hepatic *Surf4* silencing on plasma lipid levels.

Figure 5.2. Effect of hepatic *Surf4* deficiency on TG secretion.

Figure 5.3. Effect of hepatic *Surf4* silencing on the liver.

Figure 5.4. Effect of hepatic *Surf4* silencing on the development of atherosclerosis.

Figure 5.5. Effects of hepatic *Surf4* deficiency on plasma lipids.

Figure 5.6. Effects of hepatic *Surf4* silencing on liver lipids and gene expression.

Figure 6.1. Final model of proposed role of hepatic SURF4 in mediating lipoprotein metabolism and the development of atherosclerosis.

Lists of Tables

Table 2.1 Used antibodies and dilutions.

Table 2.2 DsiRNAs for knocking down experiments.

Table 2.3. Reverse transcription reaction mixture.

Table 2.4. qRT-PCR reaction mixture.

Table 2.5. qRT-PCR running parameters.

Table 2.6. Primers for qRT-PCR.

Table 2.7. shRNAs for AAV preparation.

List of Abbreviations

AAV	Adeno-associated virus
ALT	Alanine aminotransferase
AMELX	Amelogenin, X-linked
ApoB	Apolipoprotein B
ApoE	Apolipoprotein E
ASCVD	Atherosclerotic cardiovascular disease
BSA	Bovine serum albumin
cDNA	Complementary DNA
CE	Cholesteryl ester
COPII	Coat protein complex II
CPT1A	Carnitine palmitoyltransferase 1A
DMEM	Dulbecco's Modified Eagle Medium
DMSO	Dimethyl Sulfoxide
DsiRNA	Dicer-Substrate siRNA
DSPP	Dentin sialophosphoprotein
EDTA	Ethylenediaminetetraacetic acid
ELISA	Enzyme-linked immunosorbent assay
ER	Endoplasmic reticulum
ERES	ER exit sites
ERGIC	ER-Golgi intermediate compartment
FASN	Fatty acid synthase

FBS	Fetal bovine serum
FH	Familial Hypercholesterinemia
FPLC	Fast protein liquid chromatography
GH	Growth hormone
GRP78	Glucose regulated protein 78
HDL	High density lipoprotein
HL	Hepatic lipase
HMGCR	3-hydroxy-3-methylglutaryl-CoA reductase
IDL	Intermediate-density lipoprotein
INSIG	Insulin Induced gene
iPSC	Induced pluripotent stem cell
KLHL12	Kelch-like protein 12
LDL-C	Low-density lipoprotein cholesterol
LDLR	Low-density lipoprotein receptor
LPL	Lipoprotein lipase
LRP	LDL receptor related protein
MTP	Microsomal triglyceride transfer protein
ox-LDL	Oxidized low-density lipoprotein
PBS	Phosphate-buffered saline
PCSK9	Proprotein convertase subtilisin/kexin type 9
PVDF	Polyvinyl difluoride
qRT-PCR	Quantitative Real-Time PCR
S1P & S2P	Site 1 & 2 proteases

SCAP	SREBP cleavage-activating protein
SCD1	Stearoyl-CoA desaturase-1
SREBP-1c	Sterol regulatory element-binding protein 1c
SREBP-2	Sterol regulatory element-binding protein 2
SURF4	Surfeit locus 4
SVIP	Small valosin-containing protein-interacting protein
TALI	TANGO1-Like
TANGO1	Transport and Golgi Organization 1
TC	Total cholesterol
TFR	Transferrin receptor
TG	Triglyceride
VLDL	Very low-density lipoprotein
VTV	VLDL transport vesicle

Chapter 1

Introduction

Abstract

Plasma levels of low-density lipoprotein cholesterol (LDL-C) are positively correlated with the risk of atherosclerotic cardiovascular disease (ASCVD), one of the leading causes of morbidity and mortality worldwide. Numerous studies have demonstrated and reached the consensus that lowering plasma levels of LDL-C can effectively prevent and delay the development of atherosclerosis. LDL-C is catabolized from very low-density lipoprotein (VLDL), which is mainly secreted from the liver, and primarily cleared by low density lipoprotein receptor (LDLR) on the surface of hepatocytes. Based on these results, currently, most drugs in the market are designed to reduce the production of LDL catabolized from VLDL or increase the clearance of LDL by LDLR. Statins, the most prescribed lipid-lowering drugs aim to increase *LDLR* expression and subsequently reduce plasma LDL-C levels. As reported, statins reduce cardiovascular events by ranged from 20% to 40%. However, approximately 15% of the patients show statin intolerance due to severe side-effects, such as muscle pain and impaired liver function. An alternative method enhancing LDL clearance is inhibition of proprotein convertase subtilisin/kexin type 9 (PCSK9). PCSK9 promotes LDLR degradation in the lysosome by preventing LDLR from recycling after its endocytosis. Although PCSK9 inhibitors are very effective as dramatically reducing plasma LDL-C levels and cardiovascular events, the treatment is not cost-effectiveness and financially infeasible. Furthermore, familial hypercholesterolemia (FH) patients cannot be benefitted from these drugs due to mutant LDLR expressed in them. Mipomersen (inhibitor of apolipoprotein B100 (apoB100)) and Lomitapide (inhibitor of microsomal triglyceride transfer protein (MTP)) are viable alternatives in the market; however, both drugs can cause severe side effects, such as hepatic lipid accumulation, and liver damage etc. Besides LDL-C levels, more and more evidence is emerging that

hypertriglyceridemia is also an important risk factor for atherosclerosis. Thus, it is urgent to identify new alternative targets to effectively reduce plasma LDL-C and triglyceride (TG) levels.

1.1 Atherosclerotic cardiovascular disease

Atherosclerosis is the underlying cause of myocardial infarction and stroke. Numerous studies have demonstrated that long term elevated plasma levels of LDL-C and apoB100, the main structure protein of LDL, are positively associated with the risk of developing ASCVD [1, 2]. Transcytosis of LDL particles from the blood stream into the subendothelial space of the vessel wall is the critical initial step of the atherosclerotic plaque formation. Arterial injury induced endothelial dysfunction and pro-inflammatory conditions promote infiltration of monocytes into subendothelial space where they differentiate into macrophages. The retained LDL particles can be oxidized to oxidatively modified LDL (ox-LDL) which can be internalized by macrophages promoting foam cells formation, the hallmark of the fatty streak phase of atherosclerosis. Foam cells cause enhanced oxidative stress and secrete pro-inflammatory cytokines/chemokines, such as tumor necrosis factor- α and interleukin-1, which cause more LDL oxidation, monocyte recruitment and foam cell formation. Unresolved inflammation results in foam cell apoptosis and formation of necrotic core of the plaques. To stabilize the plaque surface, macrophages secreted chemoattractants stimulate infiltration and proliferation of smooth muscle cells which produce the extracellular matrix providing a stable fibrous barrier for the plaque (Figure 1.1) [3]. The fibrous cap is eventually ruptured due to collagen degradation by macrophage proteases, increased smooth muscle cell/macrophage death, and mechanical shear stress from the blood stream. Plaque rupture leads to acute exposure of procoagulant and prothrombotic factors from the necrotic core of the lesion to platelets and procoagulant factors in the lumen, thereby causing thrombus formation. Thrombus formation at sites of plaque rupture accounts for most clinical events with acute occlusive luminal

thrombosis causing myocardial infarction, unstable angina, sudden cardiac death, and stroke [4]. Thus, lowering plasma levels of LDL-C by increasing its clearance or reducing its production is the primary target to reducing atherosclerosis formation and CVD events.

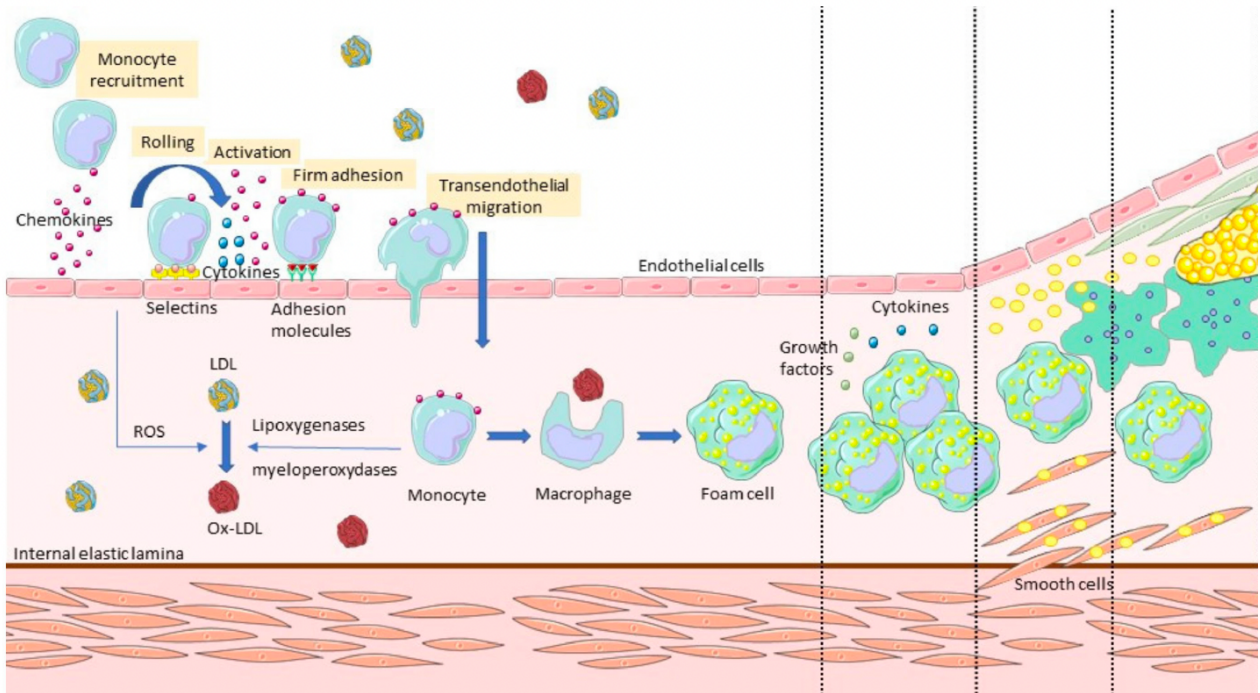


Figure 1.1 Development of atherosclerosis. LDL particles enter the intima and then become oxidized resulting in the formation of ox-LDL. The monocytes enter the intima and differentiate into macrophages which take up ox-LDL forming foam cells enhancing LDL oxidation, monocyte recruitment, and foam cell formation. Macrophages also secreted chemoattractants that stimulate infiltration and proliferation of smooth muscle cells, which produce the extracellular matrix providing a stable fibrous barrier for the plaque. This figure is modified from Thayse et al [5].

1.2 Low-density lipoprotein homeostasis

1.2.1 Very low-density lipoprotein biosynthesis and secretion

VLDL is a TG-rich lipoprotein mainly synthesized and secreted by hepatocytes for energy delivery to peripheral tissues, such as the heart and muscle. Secretion of VLDL is also one main way for the liver to remove excessive TG [6]. ApoB100 is an essential structural protein of VLDL and is mainly expressed in hepatocytes. Rodent hepatocytes express both apoB100 and apoB48, while apoB48 is only expressed in human enterocytes since the absence of APOBEC1 in human hepatocytes, which edits *apoB* mRNA converting a CAA codon to a UAA stop codon generating apoB48 [7, 8]. VLDL biogenesis occurs in the endoplasmic reticulum (ER) lumen of hepatocytes, starting with the translocation of newly synthesized apoB100 through rough ER membrane. Nascent apoB100 is partially lipidated to form nascent VLDL particles cotranslationally. This step is mediated by MTP, a lipid transfer protein that transfers both neutral and polar lipids to newly synthesized apoB100. In the absence of sufficient lipids, unlipidated apoB100 is rapidly degraded mainly through the proteasome pathway. Nascent VLDL particles can acquire more lipids from ER lumen lipid droplets to generate mature VLDL and then be transported to the Golgi apparatus, where they undergo several modifications, such as phosphorylation and glycosylation, before being secreted into the circulation [9, 10] (Figure 1.2). Another key player in VLDL assembly and secretion is apolipoprotein C-III (apoC-III). ApoC-III is an inhibitor of LPL and increases plasma TG levels. However, it was reported that overexpression of apoC-III enhanced VLDL biosynthesis and secretion under lipid-rich conditions in McArdle RH7777 cells, implicating its role in recruiting additional TG to the nascent apoB100 particles prior to secretion [11, 12].

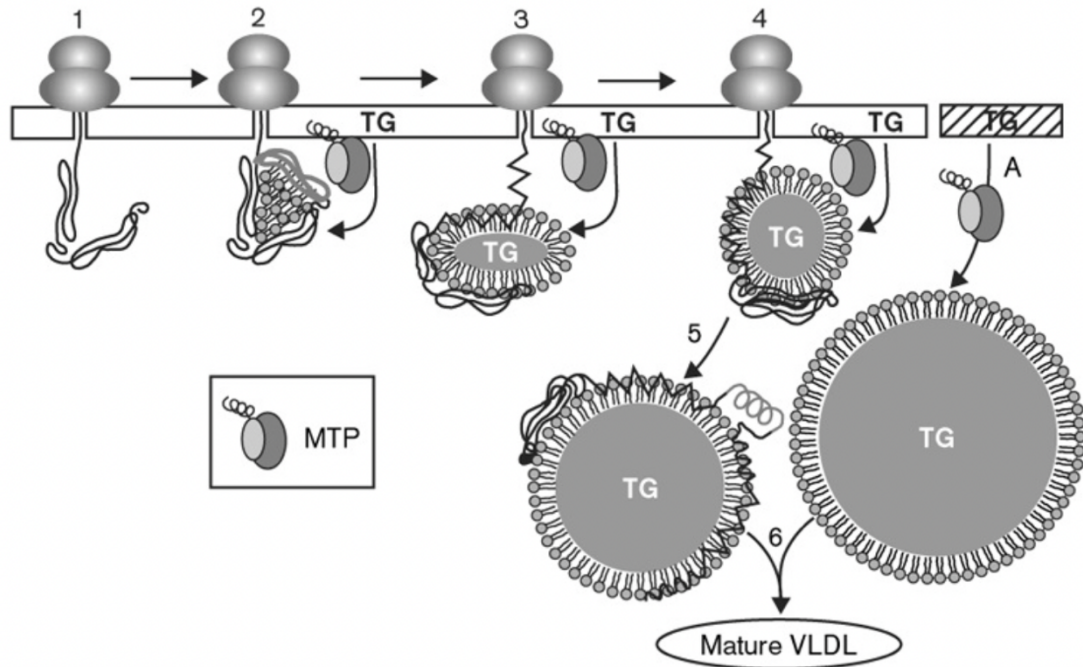


Figure 1.2. The model for the core lipidation of VLDL particles.

This figure is adapted from Shelness et al [13]. VLDL biogenesis occurs in the ER lumen of hepatocytes, starting with the translocation of newly synthesized apoB100 through rough ER membrane. Nascent apoB100 is partially lipidated to form nascent VLDL particles cotranslationally. This step is mediated by MTP. Nascent VLDL particles can acquire more lipids from ER lumen lipid droplets to generate mature VLDL and then be transported to the Golgi apparatus, and then being secreted into the circulation.

VLDL is a large particle up to 100-nm in diameter; therefore, it cannot be transported via the classical coat protein complex II (COPII) vesicles, which are only approximately 60-70 nm in diameter [14]. Based on the findings obtained from cryo-electron microscopy, Balch and colleagues reported that the geometry of COPII vesicles was flexible enough to form enlarged vesicles for cargoes up to ~100 nm in diameter [15]. However, several lines of evidence show that VLDL does not exit the ER via classic COPII vesicles. Instead, VLDL departs the ER in a specialized vesicle, the VLDL transport vesicle (VTV) [9, 16, 17]. VTV ranges between 100-120 nm in diameter and can readily accommodate VLDL-sized cargoes. VTV formation requires the COPII components, Transport and Golgi Organization 1 (TANGO1), SAR1B, and Kelch-like protein 12 (KLHL12). Silencing of KLHL12 significantly reduced secretion of apoB100 and resulted in accumulation of apoB in the ER of McArdle RH7777 cells, indicating its role in VLDL secretion [18]. KLHL12 is a key substrate adaptor protein for a Cul3-Ring ligase complex. Jin et al. reported that the KLHL12-Cul3 ubiquitin ligase mediates monoubiquitylation of SEC31, promoting the assembly of large COPII vesicles for procollagen secretion [19]. It will be of interest to assess whether the same mechanism exists for KLHL12-mediated VLDL secretion. On the other hand, TANGO1 is a transmembrane protein residing in the ER exit site (ERES). Its N-terminal ER luminal SH3-like domain can bring bulky molecules, such as collagens, to the ER exit site, facilitating the ER export of these bulky cargoes [16, 20-22]. Santos et al. reported that TANGO1 and TANGO1-Like (TALI) protein were required for the formation of VTV and VLDL secretion in HepG2 cells. Depletion of TANGO1 impaired the ER export of apoB100 in HepG2 cells [16]. However, whether and how the SH3-like domain of TANGO1 directly recognizes and then brings VLDL to the ER exit site remains elusive. In addition, several other proteins, such as Transmembrane 6 super family member 2 (TM6SF2) [23], Cideb [24, 25], and Small valosin-containing protein-interacting protein (SVIP)

[17], have been implicated in VLDL production as well. Most recently, we demonstrated that Surfeit locus 4 (Surf4) mediates VLDL secretion (Figure 1.3). Whether other critical factors participating in the formation of VTV are still unknown.

1.2.2 Very low-density lipoprotein metabolism

In circulation, VLDL particles are transported to peripheral tissues where TGs on the VLDL particles are hydrolyzed by lipoprotein lipase (LPL) and fatty acids are released. The removal of TG from VLDL results in the formation of VLDL remnants (Intermediate density lipoproteins (IDL)). These IDL particles are relatively enriched in cholesteryl esters (CE) and acquire apolipoprotein E (apoE) from high-density lipoprotein (HDL) particles. Only a fraction of the IDL particles (approximately 50%) can be removed from the circulation by the liver via binding of apoE to LDLR and LDL receptor related protein (LRP) receptors. The remaining TG on the IDL particles are hydrolyzed by hepatic lipase (HL) and LPL, and exchangeable apolipoproteins (such as apoE) are transferred from the IDL to other lipoproteins leading to the formation of LDL. These LDL particles predominantly contain CE and apoB100 [9, 10, 26]. Thus, LDL is a product of VLDL metabolism (Figure 1.3).

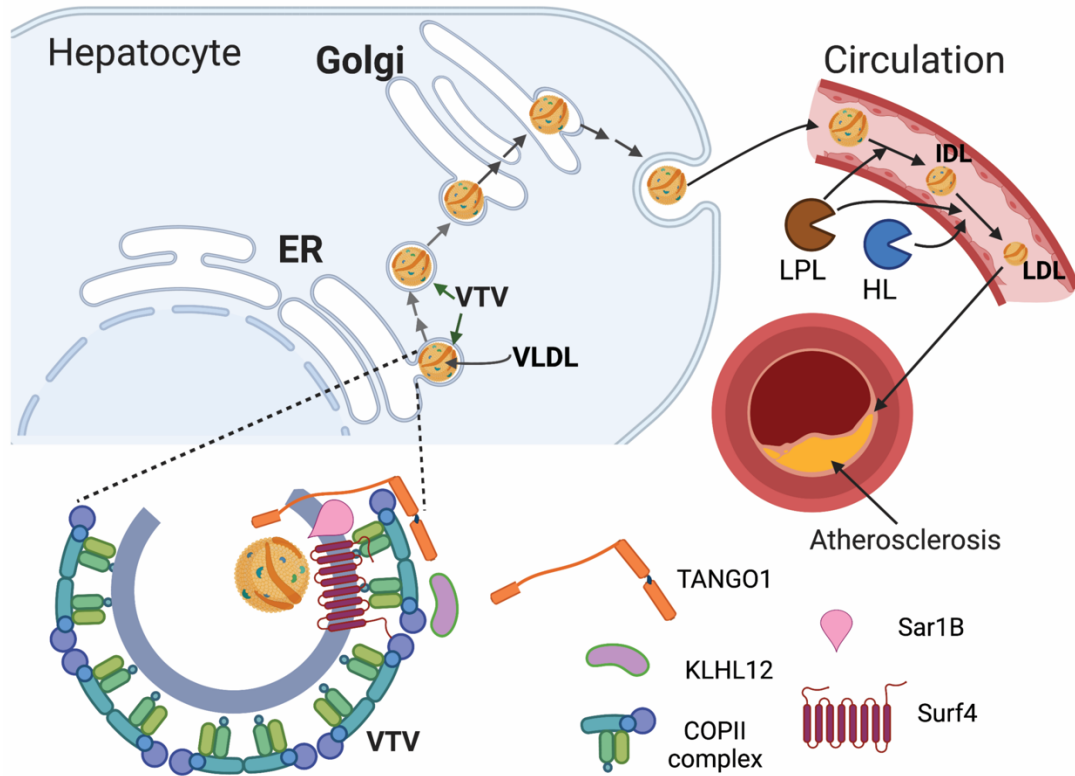


Figure 1.3. VLDL secretion and metabolism. The transport of VLDL from the ER to the Golgi apparatus is mediated by VTV, which is formed in the ERES and ranges from 100-120 nm in diameter. The biogenesis of VTV requires several factors, such as COPII components, KLHL12, TANGO1 and SAR1B. VLDL is then transported to the Golgi apparatus and secreted into the circulation from hepatocytes. In the circulation, TG on VLDL is hydrolyzed by LPL to IDL. TG on IDL can be further hydrolyzed by LPL and HL to form LDL. Elevated LDL can be deposited in the arterial intima and then oxidized to ox-LDL, promoting the development of atherosclerosis. This figure is created with BioRender.com.

1.2.3 Low-density lipoprotein metabolism

Plasma levels of LDL are determined by its production and clearance. The production of LDL from VLDL is partially regulated by the number of hepatic LDLR with a high LDLR number lead to decreased LDL production due to increased IDL uptake [27]. For LDL clearance, approximately 70% of circulating LDL is cleared by hepatic LDLR-mediated endocytosis with the remaining taken up by LDLR on peripheral tissues [28]. An increase in the number of hepatic LDLR increases LDL clearance leading to a decrease in plasma levels of LDL. Thus, the level of hepatic LDLR plays a critical role in regulating plasma LDL levels.

1.3 LDL receptor

1.3.1 LDL receptor binding, endocytosis, and recycling

The LDLR is an integral membrane glycoprotein, which binds to and mediates the internalization of its ligands on the cell surface, such as lipoprotein particles containing apoB100 or apoE. Lipoproteins internalized by the LDLR include LDL, VLDL, IDL and chylomicron remnants [29]. After binding to its ligands on the cell surface, the LDLR undergoes receptor-mediated endocytosis by associating with clathrin-coated pits [30, 31]. The LDLR/ligand complex is then internalized and transported to the endosome. In the acidic environment of the endosome, LDLR separates from its ligand, and the ligand is delivered to the lysosome, where CEs are hydrolyzed into free cholesterol and fatty acids while the apolipoproteins are degraded into free amino acids. The LDLR, on the other hand, is quickly recycled back to the cell surface, where it can initiate another ligand binding [27]. Every 10 to 20 minutes, the LDLR undergoes a complete cycle of ligand binding, endocytosis, endosomal discharge of ligand and recycling [32] (Figure 1.4).

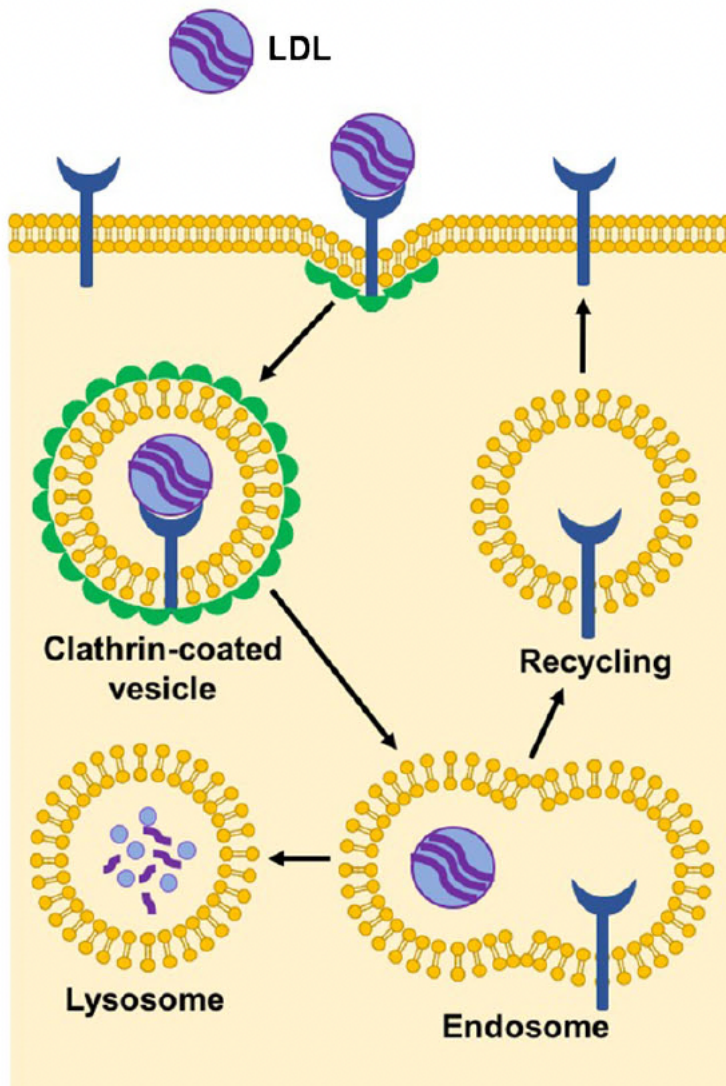


Figure 1.4. The receptor mediated endocytosis of LDL particles. Once binding to the LDL receptor on the cell surface, LDL is internalized via clathrin-mediated endocytosis. In the acidic environment of early endosome, LDLs dissociates from LDL receptors and most of the LDL receptors are recycled back to the cell surface for another round of ligand binding. LDL particles remain in the maturing endosome and then delivered to the lysosome for degradation. This figure is adapted from Chadwick et al [33].

1.3.2 Transcriptional regulation of the LDL receptor

The transcription of the *LDLR* gene is mainly regulated by the transcription factor sterol regulatory element-binding protein 2 (SREBP2), the master transcription factor for cholesterol homeostasis [34, 35]. SREBP2, unlike other transcription factors, is synthesized as a membrane bound protein attached to the ER. SREBP2 in the ER membrane associates with a sterol sensing protein SREBP-cleavage activating protein (SCAP) which, in turn, is bound to another ER protein, Insulin induced gene (INSIG-1). SREBP2 processing is tightly regulated by cholesterol levels in the ER. When cholesterol levels are higher than 5% of total lipids, SCAP binds tightly to SREBP2 and INSIG-1. When the levels of cholesterol in the ER decrease below the 5% threshold, INSIG-1 dissociates from SCAP, and SREBP2/SCAP complex can be transported to the Golgi apparatus, where SREBP2 is cleaved by Site 1 & 2 proteases (S1P & S2P) sequentially, releasing the active N-terminal domain of SREBP2 (nSREBP2). The nSREBP2 is then translocated to the nucleus and binds to the promotor region containing a Sterol regulatory element (SRE) sequence, activating the transcription of its target genes, such as *LDLR*, *HMGCR*, *PCSK9*, etc. [27, 36].

1.4 PCSK9

1.4.1 The discovery of PCSK9

PCSK9 is a member of the subtilisin-like serine protease family, which includes 7 basic amino acid-specific proprotein convertases and two members (site-1 protease and PCSK9) that cleave at the carboxyl terminus of nonbasic residues in their substrates [37-40]. PCSK9 is a secretory glycoprotein of 692 amino acids [41]. The *PCSK9* gene was first cloned by Seidah et al. in 2002. In 2003, Abifadel et al. reported that gain-of-function mutations in the *PCSK9* gene cause severe hypercholesterolemia [42]. In contrast, loss-of-function mutations in *PCSK9* result in a reduction in plasma LDL-C levels and are associated with reduced risk of coronary artery disease [43].

Shortly thereafter, three independent groups from Norway, the United States, and the United Kingdom reported that a D373Y mutation in *PCSK9* causes FH [44-46]. FH is a common genetic disease with significantly increased risk of premature ASCVD. Mutations in the *PCSK9* gene cause autosomal dominant hypercholesterolemia, making it the third genetic cause of FH in addition to *LDLR* and *apoB100* [42, 47].

1.4.2 The mechanism of PCSK9-mediated LDL receptor degradation

PCSK9 is known to bind to LDLR and promote its degradation in hepatocytes. The process is initiated when the catalytic domain of PCSK9 binds to the EGF-A domain of LDLR, and the pro-domain of PCSK9 then binds to YWTD repeat of the LDLR at the cell surface. After, the PCSK9/LDLR undergoes clathrin-dependent endocytosis and is delivered to the endosome. In the acid environment of the endosome, PCSK9 undergoes a conformational change which increases its affinity for LDLR, thereby preventing dissociation of the PCSK9/LDLR complex and then precluding LDLR from being recycled back to the cell surface. Consequently, the PCSK9/LDLR is transported to the lysosome for degradation [48-51] (Figure 1.5). While PCSK9, as a secretory protein, mainly binds to the LDLR extracellularly, it has also been reported that PCSK9 might interact and bind to LDLR intracellularly to promote LDLR degradation in the lysosome. Within the secretory pathway, PCSK9 may interact with LDLR, and then the PCSK9/LDLR complex can be transported to the lysosome for degradation. This process is blocked by the binding of PCSK9 to glucose-regulated protein 94 (GRP94) in the ER [52, 53].

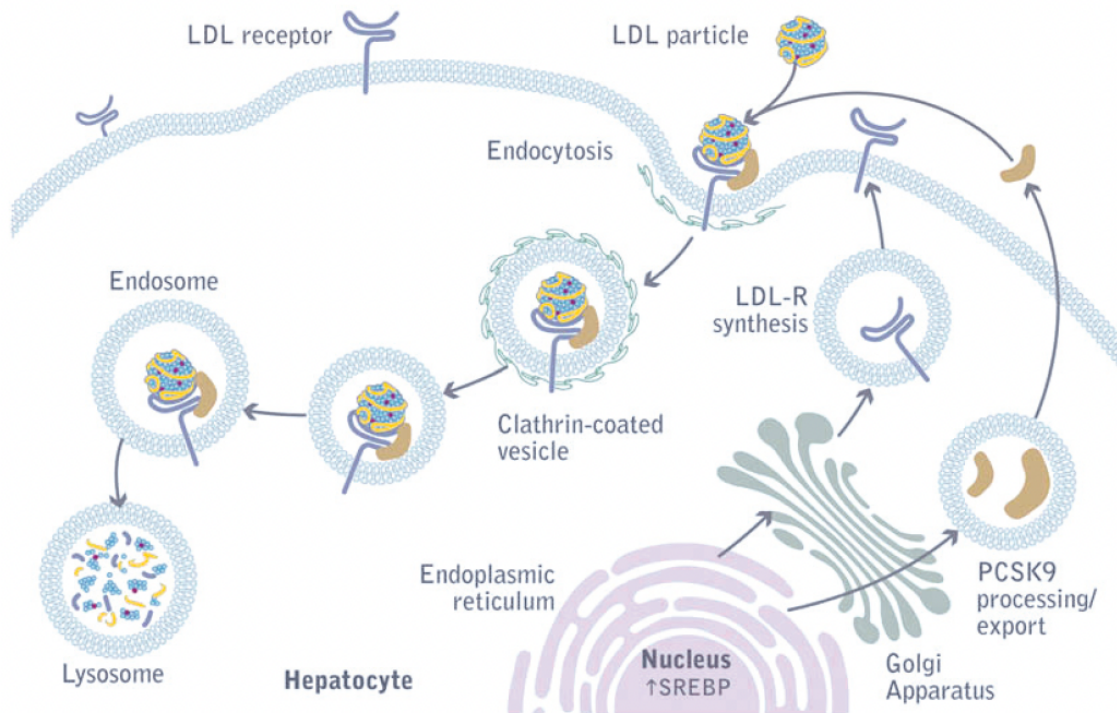


Figure 1.5. PCSK9-mediated degradation of LDLR in extracellular pathway. PCSK9 is transcriptionally regulated by SREBP2 and secreted into circulation. Once PCSK9 binds to LDLR at the cell surface, the PCSK9/LDLR complex enters cells by endocytosis and then delivered to the endosome. In the acidic environment of endosome, PCSK9 binds to LDLR with a much higher affinity, and the LDLR is consequently delivered to the lysosome for degradation, rather than being recycled. This figure is adapted from Lambert et al [54].

1.4.3 PCSK9 biosynthesis, processing, and secretion

PCSK9 is synthesized as a 692-amino-acid (74 kDa) zymogen, composed of a signal peptide, a prodomain, a catalytic domain and C-terminal cysteine-histidine rich domain. It undergoes autocatalytic cleavage in the ER, which is required for PCSK9 maturation and secretion [40]. PCSK9 is expressed in various tissues, such as the liver, kidneys, and intestine [55]. However, circulating PCSK9 is primarily secreted by hepatocytes and has a very short half-life of approximately 5 minutes [56, 57]. Furthermore, subjects carrying loss-of-function mutations in *PCSK9* which impair PCSK9 secretion demonstrated reduced plasma levels of PCSK9 and LDL-C but did not show notable health problems [58]. Overexpression of mutant PCSK9 retained in the ER also did not cause unfolded protein response or ER stress [59]. Therefore, inhibition of PCSK9 secretion represents a promising strategy for reducing plasma PCSK9 levels. However, the mechanism of PCSK9 secretion is not fully understood. Our group and other have reported that SEC24, an adaptor protein of COPII vesicles, was required for PCSK9 secretion. Furthermore, knockdown of *SEC24A*, *SEC24B* or *SEC24C* significantly reduced secretion of the wild-type PCSK9 but not mutant PCSK9 without the C-terminal histidine-rich domain, suggesting the requirement of the C-terminal domain for SEC24-mediated PCSK9 secretion [60, 61]. SEC24, an essential subunit of COPII vesicles, is localized in the cytosol and forms a complex with SAR1 and SEC23 to constitute the inner layer of the COPII vesicles. The cargo-binding sites on SEC24 recognize and directly interact with the cytosolic ER export signals present in transmembrane proteins or cargo receptors to selectively recruit cargos into COPII vesicles for ER-Golgi transport [62]. Cargo receptors are transmembrane proteins with an ER lumen domain that binds ER luminal cargos and a cytosolic domain that interacts with COPII components, thereby sorting cargo into COPII vesicles. Sec24A, assisting PCSK9 secretion via COPII vesicles, recognizes the ER exit

signal present in the cytosol region of a transmembrane protein [61]. However, Sec24A is not a transmembrane protein, and a cargo receptor is always present to assist it to perform its appropriate function. Thus, it is reasonable to speculate that it needs a cargo receptor to bridge its interaction with cytosolic SEC24.

1.5 Pharmacological treatment for hypercholesterolemia

1.5.1 Statins

Statins, which were firstly introduced in 1987, are currently the primary therapy for the treatment of hypercholesterolemia [63]. Statins exert their action by inhibiting HMG-CoA reductase (HMGCR), which is the rate-limiting enzyme of the cholesterol biosynthetic pathway. Consequently, inhibition of the enzyme reduces cellular cholesterol levels, leading to cellular processing of SREBP2. The transcriptionally active nSREBP2 translocates to the nucleus and binds to the SRE in the promoter of the *LDLR* gene enhancing its transcriptional activity, increasing the levels of LDLR on the cell surface and consequently reducing plasma LDL-C levels [64]. The efficacy of statin treatment has been consistently demonstrated by numerous randomized clinical trials that each 1 mmol/L reduction in plasma LDL-C levels results in 20-22% reduction in CVD risk [65, 66]. Despite its efficiency for the treatment of hypercholesterolemia, usually the target plasma LDL-C concentrations cannot be achieved with statin monotherapy in many patients, especially with FH. And its side effects have also been noticed in more than 10% of the patients on the medication, referred as “statin intolerance”. The most common side effects include muscle pain, nausea, new-onset type 2 diabetes [67, 68]. Due to these unexpected side effects, current research in the field focuses on developing alternative therapies for lowering plasma LDL-C levels.

1.5.2 PCSK9 inhibitors

PCSK9 has emerged as a critical regulator of cholesterol homeostasis. Humanized monoclonal antibodies against PCSK9 have been developed with impressive results, reducing plasma LDL-C levels by ~60% and a further ~15% reduction in cardiovascular events when combined with statins [69]. However, the treatment is expensive because it requires multiple injections of a large amount of anti-PCSK9 antibodies [70]. PCSK9 siRNA (Inclisiran) is also effective in reducing plasma LDL-C levels by approximately 50%, while it only requires two injections per year, and may therefore be more affordable than PCSK9 antibodies [71, 72]. However, it remains a financial burden as a primary prevention measure for all eligible patients. In addition, siRNAs, when at high doses, may exhibit miRNA-like off-target activity and trigger an innate immune response [73]. Patients with Inclisiran treatment show an increase in mild-to-moderate bronchitis (4.3% vs 2.7% for Inclisiran and placebo, respectively) [74]. Therefore, potential long-term side effects of using siRNAs as a lifelong primary prevention strategy still need to be assessed, and there is an urgent need for a new strategy to inhibit PCSK9 as an affordable and safe primary prevention measure for all eligible patients.

1.5.3 Very low-density lipoprotein inhibitors

It has long been interested in reducing plasma levels of LDL-C in a manner which is independent of LDLR, such as reducing its production by inhibiting VLDL production and secretion. In the last few years, two new drugs have been approved by the US Food and Drug Administration which aim at reducing plasma LDL-C levels by inhibiting VLDL production through distinct mechanisms. One is Mipomersen, an antisense oligonucleotide targeting apoB100, and another one is Lomitapide which is a small inhibitor of MTP. Several clinical trials have demonstrated that Mipomersen and Lomitapide are effective in reducing plasma LDL-C levels in homozygous FH patients, however,

both drugs cause severe side effects, such as hepatic lipid accumulation and liver damage [75-79]. Mipomersen even has been recently withdrawn from the market due to its severe side effects. There also several available potential therapeutic targets for VLDL secretion have been reported, such as TM6SF2, carboxylesterase 3/triacylglycerol hydrolase (TGH), CTP: phosphocholine cytidyltransferase alpha (CT α), and phosphatidylethanolamine N-methyltransferase (PEMT). TM6SF2 was reported to participate in bulk lipidation of VLDL and deficiency of TM6SF2 reduced hepatic TG secretion but not VLDL-apoB in mouse model, suggesting that the amount of TG loaded per particle was reduced [80-82]. TGH participates in VLDL assembly and deficiency of hepatic TGH significantly reduces VLDL secretion from hepatocytes and the development of atherosclerosis without causing obvious hepatic steatosis due to increased FA oxidation [83, 84]. CT α is key enzyme in CDP-choline pathway for the biosynthesis of phosphatidylcholine (PC) and knockout of hepatic CT α dramatically reduced apoB secretion and plasma levels of TG [85, 86]. PEMT catalyzes the conversion of phosphatidylethanolamine (PE) to PC and deficiency of PEMT dramatically reduced VLDL secretion from hepatocytes but had no effects on PC levels in the liver [87-89]. However, lacking hepatic CT α or PEMT causes TG accumulation in the liver. Nevertheless, it would be of interest to investigate if any other critical players are involved in VLDL assembly and secretion, and identify novel potential therapeutic targets to controlling plasma lipid levels.

1.6 Surfeit locus

1.6.1 Discovery of Surfeit locus genes

The mouse Surfeit locus was firstly reported by Williams et al. in 1986. They observed that Mes-1, a murine enhancer element, is located within 15-73 base pairs between the heterogenous 5' ends of two different genes, *Surf1* and *Surf2*. They then found that the 3' end of the third transcription,

Surf3, is located 70bp from the 3' end of *Surf1*, and the 3' end of the fourth transcription, *Surf4*, overlaps with the 3' end of *Surf2* by 133bp [90, 91]. The same lab identified *Surf5* and *Surf6* in 1990. The 5' end of *Surf6* is located within a CpG-rich island about 8 kilobases from a CpG-rich island containing the 5' end of *Surf3*, and *Surf5* resides between *Surf3* and *Surf6*. The surfeit cluster contains all *Surf1-6* genes flanked by a CpG-rich island [92]. *Surf1* encodes an integral membrane protein, and mutations in *Surf1* cause Leigh syndrome, a severe neurological disorder characterized by progressive loss of mental and movement abilities [93, 94]. *Surf3* encodes a ribosomal protein called L7a, which promotes tumorigenesis, such as in breast cancer and osteosarcoma [95-97]. *Surf5*, now named *MED22*, has three different transcripts, Surf-5a, Surf-5b, and Surf-5c, due to alternative splicing [98-100]. Disruption of *MED22* has been reported to be associated with the formation of intracellular vacuoles in podocytes, and *MED22* is required to maintain podocyte health [58]. *Surf6* is in the nucleolus, participates in rRNA processing during ribosome biogenesis, and may promote tumorigenesis [101].

1.6.2 Surfeit locus 4

Surf4 is highly conserved across species. Human SURF4 shares 99 % amino acid identity with the monkey, hamster, rat and mouse protein, and 93, 88 and 58% amino acid identity with the chicken, zebrafish and *C. elegans* homologues, respectively [102] (Figures 1.6A and 1.6B). SURF4 is a mammalian homology of Erv29p, a cargo receptor in yeast; both share approximately 30% amino acid identity [103]. SURF4 consists of 269 amino acids with a molecular weight of 30 kDa and is primarily localized in the ER. It is a polytopic transmembrane protein with 8 putative transmembrane α -helices and a cytosolic exposed N- and C-terminal domain [102, 104]. The N-terminal domain begins with a 21 amino acid- α -helix, followed by a short 3-amino acid loop connecting the first transmembrane α -helix. The C-terminal domain has a short α -helix of 8 amino

acid residues connected to the last transmembrane α -helix by a 6-amino acid loop. A di-lysine ER localization motif is located near the end of the C-terminal domain (Figure 1.6C) [104, 105]. Although *Surf4* has been discovered for over three decades, its physiological function has not been well studied until the last 10 years.

blue); low confidence (yellow); very low confidence (red). The alignment was performed using CLUSTAL O (1.2.4) (Madeira et al., 2022).

1.6.3 SURF4 and cargo trafficking

In 2008, Mitrovic and his colleagues found that SURF4 was mainly localized within the ER Golgi Intermediate Compartment (ERGIC-53)-associated structure with some overlapping with early Golgi domains in Hela cells. They also reported that SURF4 appeared to cycle between the ER and the Golgi apparatus, as replacement of the three lysine residues in the C-terminal di-lysine ER localization motif with a serine residue caused accumulation of SURF4 in the Golgi apparatus [106]. Later, Yin et al. observed that SURF4 could recognize and bind an amino-terminal tripeptide motif in secretory proteins, such as dentin sialophosphoprotein (DSPP), amelogenin, X-linked (AMELX), and growth hormone (GH). The consensus motif of the amino-terminal tripeptide, named the ER-ESCAPE motif, consists of bulky hydrophobic-proline-bulky hydrophobic amino acid (Φ -P- Φ) and is exposed after removal of the signal peptide in cargos. The bulky hydrophobic amino acid residues include Ile, Leu, Val, and Phe. Removal of Pro in the middle of the motif or the presence of an acidic amino acid residue in the motif significantly reduces binding of these proteins to SURF4. Upon binding to the ER-ESCAPE motif in the cargo, SURF4 is proposed to undergo a conformational change in the transmembrane domains, enabling it to interact with COPII proteins, such as Sec24, which subsequently facilitates the incorporation of the cargo into the COPII vesicle for ER export [107]. Many properties of the extracellular environment of higher eukaryotes, such as neutral pH and a calcium concentration of approximately 1 mM, are similar to those within the ER lumen, which allows the premature assembly of monomers to form large protein complexes [108]. To prevent premature aggregation, proteins most likely to aggregate in the ER lumen, such as DSPP, GH, AMELX, have a strong ER-ESCAPE motif to facilitate their secretion and keep

their concentration in the ER lumen low, while less susceptible cargos have a weaker ER-ESCAPE motif [107].

SURF4 has been implicated in ER export of diverse cargos, such as erythropoietin (EPO), α 1-antitrypsin (α 1AT), and proinsulin [109-111]. EPO is mainly secreted into the blood by interstitial cells in the peritubular capillary bed of the renal cortex. EPO binds to the erythropoietin receptor on erythroid precursors to promote cell proliferation and differentiation. Lack of circulating EPO, such as in patients with chronic kidney disease, can lead to severe anemia [112-115]. Deficiency of *SURF4* in Human Embryonic Kidney (HEK) 293T cells caused ER accumulation and extracellular depletion of EPO, whereas *Surf4* overexpression in mice increased serum EPO levels, indicating the important role of SURF4 in EPO secretion [109]. α 1AT is mainly produced and secreted as a monomer or polymer by hepatocytes. Circulating α 1AT monomer functions as a serine protease inhibitor to suppress the activity of neutrophil elastase, while α 1AT polymer acts as a neutrophil chemo-attractant to stimulate inflammation [116]. Mutations that impair α 1AT secretion result in accumulation of α 1AT polymers in the ER of hepatocytes, increasing the risk of neonatal hepatitis and hepatocellular carcinoma [117]. Ordonez et al. reported that SURF4 mediated ER-Golgi transport of both α 1AT monomer and polymer in Chinese Hamster Ovary (CHO) cells, with a preference for the polymer [110]. In addition, Saegusa et al. reported that *Surf4* directly interacted with proinsulin and mediated the transport of proinsulin from the ER to the Golgi apparatus in cultured rat pancreatic beta cells. Silencing of *Surf4* reduced insulin secretion and caused ER retention of proinsulin [111]. Furthermore, SURF4 is required for the trafficking of progranulin to lysosomes. Progranulin can promote wound healing, stimulate tumor growth and migration, modulate the immune response, and prevent neurodegeneration. Insufficiency in progranulin also causes frontotemporal dementia and increases the risk of Alzheimer's and Parkinson's disease [118-

121]. Devireddy et al. reported that newly synthesized progranulin and prosaposin formed a complex in the ER lumen, then prosaposin bound to SURF4 for the export of the complex from the ER [122].

Notably, progranulin contains, whereas EPO and proinsulin do not have the N-terminal ER-ESCAPE motif, and α 1AT even has an unfavorable N-terminal ER-ESCAPE motif (EDPQ). These findings indicate that the ER-ESCAPE motif is required for the ER export of some but not all SURF4's substrates. SURF4 is located in the ERES and is involved in the formation of COPII-positive ERES [123]. It may interact with the ER-export motif on cargos and Sec24 in COPII to mediate ER-Golgi transport of cargos via the classical COPII vesicles (Figure 1.7A). In addition, SURF4 is involved in the formation of the tubular network of ER-Golgi protein transport, another important carrier for the ER export of secretory proteins. ERES induces the formation of a network of tubules that, unlike COPII vesicles, contain secretory cargoes, but do not have COPII components. COPII components are present only in the neck of the tubules to concentrate secretory proteins and then promote their entry into the tubular carriers [124, 125]. Yan et al. reported that SURF4 induced the formation of a highly elongated tubular ER-Golgi Intermediate Compartment (t-ERGIC), accelerating ER-to-Golgi transport of soluble cargoes [126] (Figure 1.7B). It will be of interest to determine whether and how SURF4 decides which of the two different ER-to-Golgi transport systems is used for ER export of different cargos.

In addition to its important role in regulating anterograde trafficking of cargos, SURF4 is critical for intracellular retrograde trafficking (Figure 1.7C). The C-terminal cytosolic region of SURF4 has a triple-lysine COPI sorting motif that can interact with COPI subunit α -COP to transport SURF4 back to the ER [127]. SURF4 with a mutant COPI sorting motif, in which the C-terminal three lysine residues are substituted with an alanine residue, exhibits reduced binding to α -COP

and is trapped in the Golgi apparatus instead of being returned to the ER. Furthermore, deficiency of *SURF4* impairs the interaction between stimulator of interferon genes (STING) and α -COP, leading to Golgi accumulation of STING and subsequent activation of the STING signaling pathway [128]. This may shed light on the pathogenesis of COPA syndrome, a rare immune disorder characterized by high titer antibodies and inflammatory arthritis [129]. Therefore, SURF4 acts as a cargo receptor for STING in the COPI-mediated retrograde trafficking and may be a potential target for the diagnosis and treatment of COPA syndrome [128, 129]. Interestingly, it has been reported that the tubular ER-to-Golgi complex is positive for COPI and acquires COPI while it moves toward the Golgi apparatus, suggesting initiation of retrograde trafficking back to the ER [130]. However, we cannot exclude the possibility that COPI may have a potential role in anterograde ER-to-Golgi transport in the tubular network [124, 125]. Nevertheless, these findings indicate that SURF4 has a broad substrate spectrum, traffics bidirectionally, and mediates both vesicle and tubular anterograde ER-to-Golgi transport (Figure 1.7).

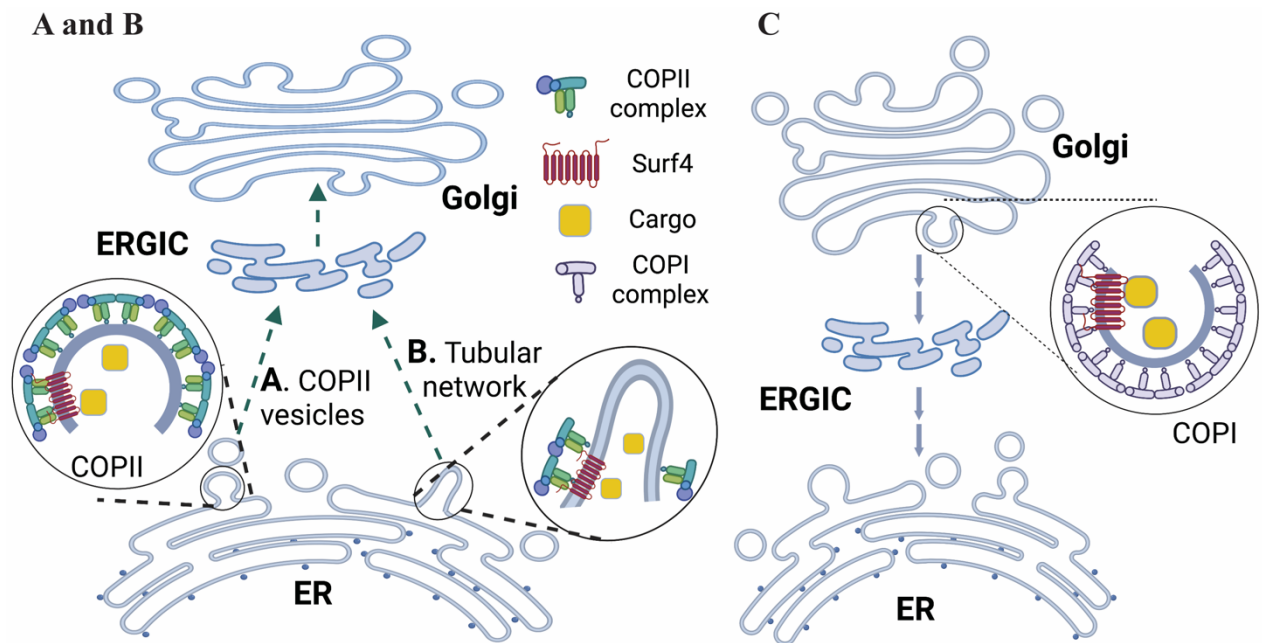


Figure 1.7. SURF4 and cargo transportation between the ER and Golgi apparatus. (A) The canonical COPII vesicle-mediated ER-to-Golgi cargo transport. Newly synthesized cargoes in the ER lumen are sorted by SURF4 into the canonical COPII vesicle. Sec23/24 coat protein forms the inner layer and recruits Sec13/31 forming the second coat layer to complete COPII vesicle assembling. (B) The tubular network mediated ER to-Golgi cargo transport. A network of tubules is formed at ERES. COPII components present in the neck of the tubules to concentrate secretory proteins and then promote their entry into the tubular carriers, but do not present in the tubules. SURF4 may recognize cargoes and mediate their incorporation into the tubular transport carrier. (C) The COPI vesicle-mediated Golgi-to-ER cargo transport. SURF4 interacts with α -COP in the COPI complex and facilitates the incorporation of cargoes into the COPI vesicle for the retrograde transport from the Golgi apparatus to the ER. This figure is created with BioRender.com.

1.6.4 SURF4, lipid metabolism and atherosclerosis

Recently, Emmer et al. combined proximity-dependent biotinylation with CRISPR mediated functional genomic screening to identify SURF4 as a cargo receptor for facilitating PCSK9 secretion in HEK293T cells. They found that inactivation of *SURF4* led to intracellular accumulation of PCSK9 overexpressed in HEK293T cells. However, lack of SURF4 only partially reduced PCSK9 secretion. The authors proposed that SURF4 actively recruited PCSK9 into COPII vesicles, and the residual SURF4-independent secretion was possibly due to bulk flow or alternative ER cargo receptors [131]. Furthermore, Wolf et al. reported that SURF4 facilitated PCSK9 secretion from cardiomyocytes, which then damaged cardiac function in an autocrine manner. They silenced *Surf4* expression in ventricular cardiomyocytes isolated from adult Wistar rats and found that deficiency of *Surf4* reduced the levels of PCSK9 released from cardiomyocytes and protected heart function [132]. In their studies, Emmer et al. investigated secretion of PCSK9 overexpressed in HEK293T cells that do not express endogenous PCSK9 and Wolf et al. studied secretion of endogenous PCSK9 from cardiomyocytes that express PCSK9 at very low levels. Considering circulating PCSK9 is mainly secreted by hepatocytes, further studies are required to investigate the role of hepatic SURF4 in mediating PCSK9 secretion and regulating plasma lipid levels.

In addition to PCSK9, SURF4 has also been reported to interact with apoB100 and mediate its secretion from HepG2 cell. Saegusa et al. reported that SURF4 predominately localizes at ERES. Deficiency of *SURF4* results in ER accumulation of apoB100 and reduced number of COPII positive ERES in HepG2 cells [123]. ApoB100 is the essential structure protein of VLDL, it is of interest to further investigate if SURF4 participate in mediating VLDL secretion from hepatocytes and manipulating lipoprotein metabolism. Furthermore, a SNP (rs3758348) within the first intron

of human *SURF4* is significantly associated with a reduction in plasma total cholesterol (TC) and LDL-C levels [133]. These reports indicate a critical role of SURF4 in regulating lipid metabolism.

1.6.5 Other known physiological and pathophysiological functions of SURF4

Global *Surf4* knockout (*Surf4*^{-/-}) mice die as early as embryonic day 3.5 (E3.5) [134]. Knockout of *apoB* also results in embryonic lethality, but at a later stage (E9.5) [135]. Therefore, the impact of *Surf4* deficiency on embryonic development may not be related to its role in apoB secretion. SURF4 can promote cellular reprogramming and stimulate the generation of induced pluripotent stem cells (iPSCs). Its expression is high in metaphase II oocytes and early embryos prior to the two-cell stage [136-138]. These findings indicate a critical role for SURF4 in embryonic development. Deficiency of *SURF4* may lead to embryonic lethality due to embryonic dysplasia [134, 136]. Alternatively, SURF4 may mediate secretion of unidentified cargoes that are important for early embryonic development.

SURF4 has also been shown to participate in the replication of positive-strand RNA viruses, such as hepatitis C virus (HCV) and poliovirus. *SURF4* silencing significantly reduces virus replication but does not alter viral entry, translation, assembly or release. SURF4 can be recruited into virus RNA replication complex via the HCV non-structural 4B protein, contributing to the formation of double-membrane vesicles (DMVs) that serves as a platform for viral replication [139-141]. Furthermore, SURF4 has been reported to have oncogenic potential in NIH3T3 cells. *SURF4* is highly expressed in human cancer tissues, and patients with higher SURF4 levels have shorter overall survival. Consistently, overexpression of *SURF4* increased cell proliferation and migration *in vitro*, and introduction of *SURF4*-overexpressing NIH3T3 cells into mice induced tumor growth [142]. *SURF4* expression is also upregulated in ovarian cancer stem cells, and knockdown of *SURF4* inhibits tumorigenesis. How SURF4, a cargo receptor, possesses oncogenic potential

remains elusive. Several recent studies have shed light on this question. Yue et al. used RNA-sequencing and bioinformatics to identify BIRC3 as a downstream regulator of *SURF4*. *SURF4*-knockdown human ovarian cancer cell lines, A2780 and 3AO, showed reduced protein and mRNA levels of BIRC3, suppressed self-renewal ability, and improved sensitivity to chemotherapeutic drugs [143]. BIRC3 is an apoptosis inhibitor and functions through inhibiting caspase activation [144]. In addition, Tang et al. demonstrated that SURF4 was required for sonic hedgehog (Shh) export from the ER in HeLa and HEK293T cells [145]. Shh is an important signaling molecule that plays a critical role in cell differentiation and contributes to the development and progression of numerous cancers [146]. Therefore, SURF4 may exert its oncogenic role by upregulating BIRC3 expression and/or promoting ER-Golgi trafficking of Shh.

1.7 Rationale, Hypothesis and Aim of thesis

Plasma LDL-C levels are mainly determined by its production from VLDL and clearance through LDL receptor as described above. Most drugs on the market are focusing on enhancing LDL clearance by increasing LDL receptor on the cell surface, such as statins (inhibiting HMGCR and increasing SREBP2 processing) and PCSK9 inhibitors (inhibiting PCSK9-promoted LDL receptor degradation). However, as aforementioned, these treatments have their own limits and side effects. Furthermore, homozygous FH patients cannot benefit from these drugs due to lacking functional LDL receptor. Mipomersen and Lomitapide are two first-in-class drugs which are aiming at reducing VLDL production and demonstrate impressive LDL-C lowering effects. However, both drugs cause severe side effects, such as hepatic lipid accumulation and liver damage. Thus, the need for developing novel targets with more efficiency and less side effects are urgently needed.

SURF4 was reported to interact with PCSK9 and apoB100 (the core protein of VLDL) and mediate their secretion in cultured cells. However, the role of SURF4 in mediating endogenous PCSK9

secretion from the hepatocytes, where most of circulating PCSK9 is secreted, has yet to be determined. Thus, we propose that SURF4 mediates PCSK9 secretion from hepatocytes and reduces LDLR on the hepatocyte surface, leading to increased plasma LDL-C levels. In addition, the potential role of SURF4 in VLDL secretion from the hepatocytes and regulating lipoprotein metabolism was still elusive. Therefore, we also propose that SURF4 mediates VLDL secretion from hepatocytes and regulates plasma lipoprotein metabolism, subsequently influencing the development of atherosclerosis. To test my hypothesis, I developed the following research aims.

- 1. To investigate the role of SURF4 in PCSK9 secretion from hepatocytes *in vitro* and *in vivo*.**
- 2. To investigate the role of hepatic SURF4 in lipoprotein metabolism and the development of atherosclerosis in *Ldlr*^{-/-} mice.**
- 3. To investigate the role of hepatic SURF4 in lipoprotein metabolism and the development of atherosclerosis in *apoE*^{-/-} mice.**

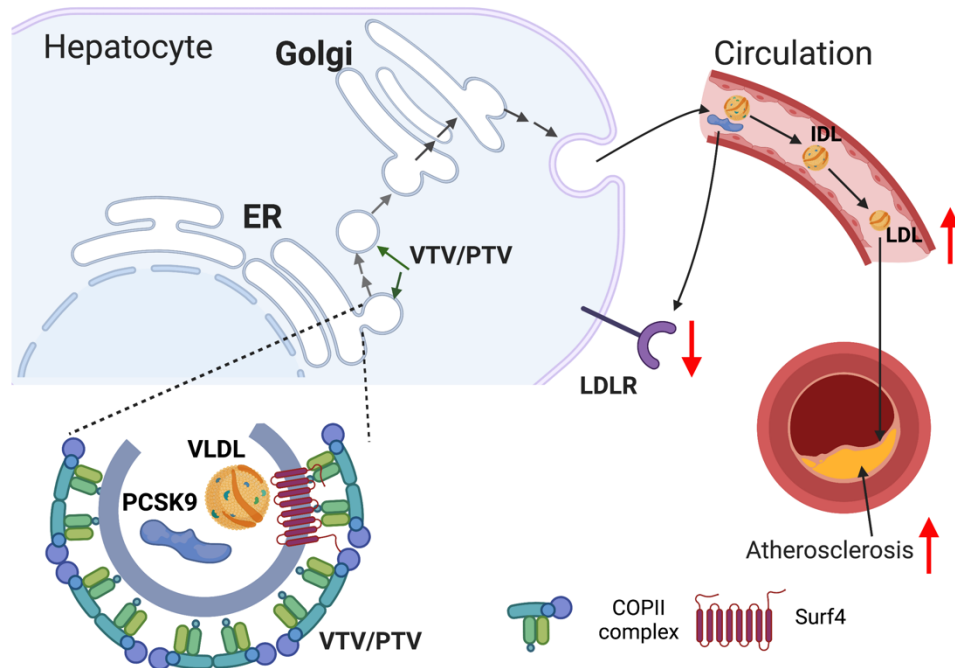


Figure 1.8. Study hypothesis and research objectives.

This dissertation aims to determine the role of hepatic SURF4 in mediating PCSK9 and VLDL secretion, and the development of atherosclerosis. In Chapter 3, data demonstrated that SURF4 plays a negligible role in mediating PCSK9 secretion from hepatocytes *in vitro* and *in vivo*. In Chapter 4&5, SURF4 is identified to interact with apoB100 and mediating VLDL secretion from the liver, regulating plasma lipid levels and the development of atherosclerosis in both *Ldlr*^{-/-} and *apoE*^{-/-} mice. These results not only reveal the important role of hepatic SURF4 in regulating plasma cholesterol levels but also shed important light on developing alternative therapeutic target for lowering plasma cholesterol levels and reducing the risk of atherosclerosis. This Figure is created with BioRender.com.

Chapter 2

Materials and Methods

2.1 Materials

DMEM, fetal bovine serum (FBS), Bovine serum albumin (BSA), and cComplete™ EDTA-free protease inhibitors were purchased from Millipore Sigma or Hyclone. Penicillin-streptomycin, trypsin-EDTA solution, Lipofectamine® 3000, Lipofectamine® RNAiMAX, High Capacity cDNA Reverse Transcription Kit, SYBR® Select Master Mix, PureLink™ HiPure Plasmid Miniprep and Maxiprep Kits, BCA Protein Assay Kit, TRIzol®, PVDF (polyvinyl difluoride) membranes, Alexa Fluor 488 donkey anti-rabbit IgG, Alexa Fluor 647 goat anti-mouse IgG, and Alexa Fluor 647 donkey anti-goat IgG were obtained from Thermo Fisher Scientific. IRDye Secondary Antibodies (IRDye 800CW Goat anti-Rabbit IgG and IRDye 680 Goat anti-Mouse IgG) were purchased from Licor Biosciences. Quick ligation kit, T4 DNA polymerase, and high-fidelity restriction enzymes were purchased from New England Biolabs. Mouse PCSK9 ELISA Kit was from abcam. Total Cholesterol E Kit and Triglyceride (TG) Kit (Triglyceride M Enzyme Color A (L-Type) and Triglyceride M Enzyme Color B (L-Type)) were from FIJIFILM Wako Diagnostics. Alanine transaminase (ALT) colorimetric activity assay kit was obtained from Cayman Chemical. All other reagents were obtained from Fisher Scientific unless otherwise indicated.

Antibodies were obtained from Proteintech, Abcam, Novus, Biologicals, MilliporeSigma, and Invitrogen (Table 2.1). The custom-made rabbit polyclonal anti Surf4 antibody, 1195Sa, was produced and purified by GenScript using a peptide that is completely conserved among different species [147].

Table 2.1 Used antibodies and dilutions

Antibody	Company	Catalogue No	Dilutions	Notes
Mouse anti-PCSK9	N/A	15A6	1:1000/1:100	WB/IP
Rabbit anti-Surf4	Custom-made	N/A	1:2000/1:100/1:200	WB/IP/IF
Mouse anti-TFR	BD Bioscience	612125	1:10,000/1:100	WB/IP
Mouse anti-actin	BD Bioscience	612657	1:10,000	WB
Goat anti-albumin	Invitrogen	PA129338	1:10,000	WB
Rabbit anti-GRP78	abcam	ab108615	1:1000	WB
Anti-DYK	Proteintech	20543-1-AP	1:1000	WB
Rabbit anti-Surf4	abcam	ab150327	1:500	WB
Rabbit anti-Surf4	abcam	ab192611	1:500	WB
Rabbit anti-Surf4	Abnova	H00006836-M01	1:500	WB
Rabbit anti-HA	Proteintech	51064-2-AP	1:5000	WB
Goat anti-apoB	MilliporeSigm a	AB742	1:2000	WB
Goat anti-apoB	abcam	Ab7616	1:100	IP/IF
Mouse anti-apoA-I	Invitrogen	MIA1405	1:2000	WB
Rabbit anti-calnexin	Proteintech	10427-2-AP	1:5000	WB
Rabbit anti-SCD1	abcam	ab236868	1:1000	WB
Rabbit anti-HMGCR	abcam	ab174830	1:1000	WB
Goat anti-CPT1A	Novus Biologicals	NB100-53791	1:1000	WB
Rabbit anti-FASN	Proteintech	10624-2-AP	1:2000	WB

IF, immunofluorescence; IP, immunoprecipitation; N/A, not available; WB, Western blot.

2.2 Animal

The wild-type C57BL6/J, *Ldlr*^{-/-}, *Pcsk9*^{-/-} and *apoE*^{-/-} mice were purchased from the Jackson Laboratory, housed and bred in the animal facility at the University of Alberta. Three to five mice were housed per cage with free access to H₂O in a climate-controlled facility with a 12-h light/dark cycle. After weaning, mice were fed ad libitum a chow diet containing 20 % protein, 5 % fat, and 48.7 % carbohydrates (LabDiet, PICO Laboratory Rodent Diet 20). For the high fat/high cholesterol experiment, mice were fed the Western-Type Diet containing 0.15 % cholesterol (TestDiet 1,813,029, kcal from fat 40 %, protein 16 %, and carbohydrate 44 %) for 14 weeks. All animal procedures were approved by the University of Alberta's Animal Care and Use Committee and were conducted per the guidelines of the Canadian Council on Animal Care. Mice used in all experiments were 10–14-weeks old and fasted for 10 h before the endpoint unless otherwise indicated.

2.3 Culture and treatment of cell lines

2.3.1 Cell Culture

A humidified incubator with 5% CO₂ was used to culture all cells at 37°C. A Class II laminar flow cabinets were used to conduct cell culture experiments under aseptic conditions.

2.3.2 Thawing of frozen cells

Cells stored in -80 °C freezer or liquid nitrogen in cryovials were rapidly transferred into a 37 °C water bath to thaw for 30 seconds. The content was then transferred into a 15 ml conical tube containing 9 ml appropriate culture media for the cell. Cells and media were then transferred into a 100 mm culture dish and placed in an incubator.

2.3.3 Cryopreservation of immortalized Cells

Cells in 100 mm plates with 90 to 100% confluence had their culture media withdrawn, and cells were then given a 10 ml PBS wash. Following a 5-minute trypsin treatment (Sigma), the cells were suspended in 9 ml of the proper growth medium and placed in a 15 ml conical tube for a 5-minute 150 x g centrifugation. The pellet was resuspended in 1 ml of freezing solution (DMEM or MEM + 10% FBS + 10% DMSO). After that, the cells were put into cryovials. The vials were kept in a Nalgene® freezing container filled with isopropanol to be frozen overnight in a -80°C freezer and then kept in liquid nitrogen.

2.3.4 Transfection

Dicer-Substrate siRNA (DsiRNA) and plasmid DNA were introduced into cells using Lipofectamine™ RNAiMAX (HEK293, Huh7, and HepG2 cells) or Lipofectamine™ 3000, respectively, according to the manufacturer's instructions and briefly described below for 6 well culture plates. Scrambled and predesigned DsiRNAs against Surf4 were purchased from IDT® and listed in **Table 2.2**.

Table 2.2 DsiRNAs for knocking down experiments

Target	Forward	Reverse
Scramble	5'-AUUAGUGUGCGAUGUACCCAGGAAC-3'	5'-GUUCCUGGGUACAUCGCACACUAAU-3'
Human Surf4-1	5'-CGCAUUGGUAUUUCAUCAAAGCA-3'	5'-UGC UUUGAAUGAUAAUACCA AUGCGUC-3'
Human Surf4-2	5'-AUGACUCCUGAAAACGACUUCTT-3'	5'-AAGAAGUCGUUUUCAGGAAGUCAUGC-3'

2.3.4.1 Lipofectamine 3000 Transfection

2 µg DNA and 4 µl P3000 reagent was added to 125 µl serum reduced Opti-MEM medium and vortexed (Transfection mixture A). 3 µl Lipofectamine 3000 reagent was then added to 125 µl Opti-MEM medium and vortexed (Transfection mixture B). Transfection mixture A and B were then combined and vortexed briefly, followed by a 15 min incubation at room temperature. The Mixture was then added drop by drop to cells.

2.3.4.2 RNAiMAX Transfection

2 µl of 10 µM siRNA solution was added to 125 µl Opti-MEM medium and vortexed (Transfection Solution A). 6 µl RNAiMAX reagent was then added to 125 µl Opti-MEM medium and vortexed (Transfection Solution B). Solution A and B were then combined and vortexed briefly, and incubated for 5 min at room temperature. The solution mixture was then added drop by drop to cells.

2.3.5 Statin Treatment

24h before cell lysis for collection, culture medium was replaced with fresh medium containing Lovastatin (J&K scientific) dissolved in Dimethylformamide (DMF) at a final concentration of 7.5 µg/ml and mevalonate (5 µg/ml). Same amount of DMF was added into the control group.

2.4 Quantification of mRNA expression

2.4.1 RNA Isolation

Following the manufacturer's instructions, total RNAs were extracted from mouse tissue and cultured cells using Trizol (Life Technologies). Briefly, 1ml of Trizol was added to a 2 ml tube

containing 50 mg of animal tissue, which was then homogenised with a PowerGen 500 Homogenizer (Fischer Scientific). For RNA extraction from cultured cells, the growth medium had to be removed, and 0.4 ml of Trizol had to be added to every 1×10^5 - 10^7 cells in the culture plates. After that, the culture plate's contents were pipetted up and down many times to homogenise each well's contents. Lysate from animal tissue and cultured cell were then incubated for 5 min at room temperature. For each 1 ml of Trizol used for lysis, 0.2 ml of chloroform was added and incubated at room temperature for 2 min. The aqueous phase and the phenol red-chloroform phase were separated from the mixture by centrifuging it at $12,000 \times g$, $4^\circ C$, for 15 min. After moving the RNA-containing aqueous phase into a new tube, isopropanol (0.5 ml per 1 ml of Trizol originally used for lysis) was added. The mixture was then incubated for 10 min at room temperature. The sample was then centrifuged at $12,000 \times g$ and $4^\circ C$ for 10 min. After removing the supernatant, 1ml of 75% ethanol was used to wash the RNA pellet. The sample was centrifuged at $7,500 \times g$ for 5 min at $4^\circ C$ after being vortexed for 5 sec. The supernatant was then discarded. The pellet was air-dried for 10 min and then dissolved in 50 μ l of RNase Free water for further analysis. RNA concentration was quantified using Nanodrop spectrophotometer (Nanoview Plus, GE).

2.4.2 cDNA synthesis

cDNA was synthesized using High-Capacity cDNA Reverse Transcription Kit (Applied Biosystems). Samples were mixed with reagent as indicated in (Table 2.3) in PCR tubes in a thermal cycler (C1000, Biorad) under the following condition: $25^\circ C$ for 10 min, $37^\circ C$ for 120 min, $85^\circ C$ for 5 min and $4^\circ C$ as the holding temperature.

Table 2.3. Reverse transcription reaction mixture.

Component	Quantity
RNA	2µg
10X RT Buffer	2µl
25X dNTP Mix	0.8µl
10X Random Primers	2µl
Reverse Transcriptase	1µl
Nuclease Free Water	Made up to 10µl
Total Per Reaction	10µl

2.4.3 Quantitative Real-Time PCR (qRT-PCR)

Relative quantification of mRNA was done using qRT-PCR measurement of cDNA carried out on a StepOnePlus™ using SYBR® Select Master Mix. Standards were generated from dilutions (4X, 16X, 64X and 256X) of a pool of control samples. Samples for analysis were diluted 15X. Each reaction was carried out in 20 µl of sample mixture as indicated in (Table 2.4) in a Microamp® 96 well reaction plate (Applied Biosystems) with a PCR program as indicated in (Table 2.5).

Table 2.4. qRT-PCR reaction mixture.

Reaction Reagent	Volume
Sample and standards	2µl

SYBR Green Master Mix	10 μ l
Forward and Reverse primers (10 μ M)	2 μ l each
Nuclease free water	4 μ l

Table 2.5. qRT-PCR running parameters.

Stage	Time (seconds)	Temperature ($^{\circ}$ C)
Holding	120	95
Cycling (40X cycles)	15	95
	60	60
Melt Curve	15	95
	60	60
	15	95

Each sample was processed in triplicate, and the average cycle threshold was calculated. Relative gene expression was normalized to the glyceraldehyde-3-phosphate dehydrogenase gene (*GAPDH*) that had a similar amplification efficiency as that of the target genes. Primers for human and mouse *GAPDH*, *PCSK9*, *SREBP2*, *Surf4*, *ApoB*, *HMGCR*, *SREBP1c*, *FASN*, *PPAR- α* and *CPT-1A* were designed by PrimerQuest Real-Time PCR Design Tool, synthesized by IDT, Inc., and listed in the **Table 2.6**.

Table 2.6. Primers for qRT-PCR.

Target	Forward	Reverse
Human GAPDH	5'-GGTGTGAACCATGAGAAGTATGA-3'	5'-GAGTCCTTCCACGATACCAAAG-3'
Human PCSK9	5'-CACAGAGTGGGACATCACAG-3'	5'-TTTGGCAGAGAAGTGGATCAG-3'
Human SREBP2	5'-TTCCTGTGCCTCTCCTTTAAC-3'	5'-TCATCCAGTCAAACCAGCC-3'
Human HMGCR	5'-ACAGATACTTGGGAATGCAGAG-3'	5'-CTGTCGGCGAATAGATACACC-3'
Human Surf4	5'-TCGGGCTCTTTGGAATCATAG-3'	5'-ACATGCTCTTCCCTTCAGAAC-3'
Mouse GAPDH	5'-AACTTTGGCATTGTGGAAGG-3'	5'-GGATGCAGGGATGATGTTCT-3'
Mouse SREBP2	5'-CCCTATTCCATTGACTCTGAGC-3'	5'-CACATAAGAGGATTCGAGAGCG-3'
Mouse Surf4	5'-CAGCGTGAATATATCGACACC-3'	5'-GATTCCAAACAGCCCAAAGC-3'
Mouse HMGCR	5'-GCCCTCAGTTCAAATTCACAG-3'	5'-TTCCACAAGAGCGTCAAGAG-3'
Mouse SREBP1c	5'-ATCGGCGCGGAAGCTGTCGGGGTAGCGTC-3'	5'-ACTGTCTTGGTTGTTGATGAGCTGGAGCAT-3'
Mouse FASN	5'-CCCCTCTGTTAATTGGCTCC-3'	5'-TTGTGGAAGTGCAGGTTAGG-3'
Mouse PPAR- α	5'-CATTCCCTGTTTGTGGCTG-3'	5'-ATCTGGATGGTTGCTCTGC-3'
Mouse CPT1A	5'-AGACAAGAACCCCAACATCC-3'	5'-CAAAGGTGTCAAATGGGAAGG-3'
Mouse ApoB	5'-AGGCTTGTACCCTTCTTTC-3'	5'-GCCTTGTGAGCACCAGTATTA-3'

2.5 Western Blot and Protein Expression Analysis

2.5.1 Protein extraction from cultured cells

Protein extraction from cultured cells was most performed 48 h after transfection. After removing the culture medium, cells were washed once with 2 ml of PBS. After being scraped, the cells were collected in 1 ml of PBS, and then centrifuged (6,000 x g, 4 °C for 6 min). The supernatant was removed. Cells were lysed in lysis buffer A (1% Triton, 150 mM NaCl, 50 mM HEPES, pH 7.4) containing 1 x Complete EDTA-free protease inhibitors for 30 min on ice and vortexed intermittently every 10 min. Cell lysis was spun for 10 min at 20,000 × g at 4 °C, the supernatant was collected as whole cell lysate. Protein concentrations were determined by the BCA protein assay.

2.5.2 Protein extraction from animal tissues

Frozen liver tissue samples stored at -80 °C were thawed, grinded, and weighed in a 2 ml tube, followed by addition of a volume 4 X the tissue weight homogenization buffer (250mM Sucrose, 50mM Tris-HCl, pH7.4, 1mM EDTA, and 1X protease inhibitors) to obtain 20% homogenate as described [148]. Homogenization was involved using a PowerGen 500 Homogenizer (Fischer Scientific). Homogenized tissue was then incubated on ice for 30 min with intermittent vortex every 10 min. The samples were then spun for 10 min at 20,000 × g at 4 °C. The supernatant was collected as tissue homogenate. Protein concentrations were determined by the BCA protein assay.

2.5.3 Protein assay and quantification

Bicinchoninic acid assay (BCA, Thermo Scientific) was used to measure protein concentrations from tissue and cell lysate homogenate, BCA protein assay reagent A and B were mixed 50:1 (BCA solution) to obtain the working BCA solution. Bovine serum albumin (BSA) was used to make

protein standards for the assay at concentrations ranging from 0,2,4,6,8 and 10 mg/ml. 2 µl of standards or samples of tissue and cell lysate was added to a 96 well plate, followed by the addition of 200 µl of the working BCA solution. After that, the plate was then incubated at 37 °C for 30 min. Using a SPECTRA MAX 250 microplate reader, absorbance was read at 562nm.

2.5.4 Immunoblotting

Equivalent amounts of lysate proteins were applied to SDS-PAGE and then transferred to nitrocellulose (GE Healthcare) or PVDF membranes (Millipore) by electroblotting. Immunoblotting was performed using specific antibodies as indicated (Table 2.1). Antibody binding was detected using IRDye® 680 or IRDye® 800-labeled donkey anti-mouse, anti-rabbit, or anti-goat IgG (Li-Cor), followed by imaging on a Licor Odyssey Infrared Imaging System (Li-Cor).

2.6 Immunofluorescence

Confocal microscopy was carried out as described [149-151]. Briefly, Huh7 cells were seeded onto coverslips (1.0×10^5 cells/ml). About 48 h later, cells were fixed and permeabilized with cold methanol for 10 min at -20°C . The cells were then incubated with a goat anti-apoB polyclonal antibody and rabbit anti-Surf4 antibody overnight at 4°C . Antibody binding was detected using Alexa Fluor 647 donkey anti-rabbit IgG and Alexa Fluor 488 donkey anti-goat IgG. Nuclei were stained with 4',6-diamidino-2-phenylindole (Thermo Fisher). After washing, coverslips were mounted on the slides with ProLong Diamond Antifade Mountant (Thermo Fisher). Localizations of apoB and Surf4 were determined using a Leica SP5 laser scanning confocal microscope (filters: 461 nm for 4',6-diamidino-2-phenylindole, 519 nm for Fluor 488, and 633 nm for Fluor 647).

2.7 Immunoprecipitation analysis

When the confluency reached about 80%, cells in two 100 mm dishes were lysed in 1,000 μ l of lysis buffer A containing 1x cOmplete EDTA-free protease inhibitors. About 50 μ l of cell lysate was saved for Western blot. Equal amounts of total protein were applied to a rabbit anti-Surf4 or preimmunized serum and protein G beads. Immunoprecipitated samples were washed three times with lysis buffer A. The immunoprecipitated proteins were then eluted from the beads by addition of 2x SDS-PAGE sample buffer (100 mM Tris-HCl, pH 6.8%, 4% SDS, 20% glycerol, and 0.04% bromophenol) containing 5% β -mercaptoethanol. Equal amounts of eluted samples and whole cell lysate were applied to SDS-PAGE and immunoblotting.

2.8 Measurement of liver lipids

Folch lipid extraction protocol was used to isolate lipids [152]. Briefly, Liver samples were lysed with a homogenization buffer (50 mM Tris-HCl, 250 mM sucrose and 1 mM EDTA, pH 7.4) using PowerGen 500 Homogenizer (Fischer Scientific). Lipids were extracted from 4 mg of liver homogenate transferred into a glass tube and made up to 1ml with PBS; 4 ml of chloroform-methanol mixture (2:1) was then added and vortexed for 1 min. The glass tube was then spun at 700 x g for 10 min in a centrifuge (Eppendorf, 5810R), the chloroform bottom phase was transferred to a new glass tube using a 9-inch glass Pasteur pipette (Fischer) and dried under nitrogen. Lipids were then dissolved in 1 ml chloroform with 2% Triton X-100 and dried under nitrogen again. The dried samples were then re-dissolved in 1 ml of distilled H₂O and incubated in a 37 °C water bath for 15min with intermittent vortex every 5 min. The levels of TG and total cholesterol in 50 μ l of samples were measured using commercial kit from Wako Diagnostics.

2.9 Plasma lipid and Alanine aminotransferase (ALT)

Blood samples were collected from mice on chow or Western-type diet in the heparin-coated tubes (BD Biosciences). To isolate plasma, the samples were then centrifuged at 3,000 x g for 20 min at 4 °C. Each isolated plasma sample was applied, in accordance with the manufacturer's instructions, to the ALT enzymatic activity assay kit (Cayman Chemical) to perform ALT measurement, to the TG kit (Wako Diagnostics) to measure plasma triglyceride levels and to the Cholesterol E kit (Wako Diagnostics) to measure plasma total cholesterol levels.

2.9.1 ALT determination

Using ALT enzymatic activity assay kit (Cayman Chemical), ALT was measured. Briefly, 5 µl plasma from each mouse and positive control samples were added into 96 well plates containing 50 µl ALT substrate and 5 µl enzyme cofactor. The plate was covered and incubated at 37 °C for 15 min. The enzymatic reaction was then started as soon as feasible by adding 5 µl of ALT assay initiator. Immediately absorbance was read at 340 nm once every minute for a period of 5 min with a SPECTRA MAX 250 plate reader.

2.9.2 Cholesterol determination

Plasma total cholesterol levels were carried out using Cholesterol E kit (Wako Diagnostics). Briefly, 3 µl of sample from each mouse and standard solutions (0, 6.25, 12.5, 25, 50, 100 and 200 mg/dl) were added into 96 well plates. After, 200 µl colour reagent solution was loaded, and the plate was then incubated for 5 min at 37 °C followed by absorbance reading with a SPECTRA MAX 250 plate reader at 600 nm.

Plasma HDL and non-HDL were separated using the HDL and LDL/VLDL Cholesterol Assay Kit (Cell Biolabs). Briefly, 10 µl of plasma and 10 µl of the 2X Precipitation Reagent were mixed, incubated for 10 min at room temperature, and then centrifuged at 2,000 x g for 20 min. The

supernatant containing HDL particles was transferred to a new tube. 10 μ l of PBS was used to dissolve the pellet. Cholesterol content in each fraction was measured using the Cholesterol E kit (Wako Diagnostics).

Lipoprotein profiles were analyzed by the Lipidomic Core Facility at the University of Alberta. Briefly, 5 μ l of plasma from each mouse in the same experiment group was pooled and 30 μ l in total was subjected to Fast Protein Liquid Chromatography (FPLC).

2.9.3 Triglycerides determination

Triglycerides levels were determined using triglyceride kit (Wako Diagnostics). Briefly, 5 μ l of plasma was loaded to 96 well plates followed by addition of 90 μ l color reagent R1, then the samples were incubated for 5 minutes at 37°C. Blank absorbance was read at 540 nm, and then 5 μ l glycerol standards (0, 0.35, 0.7, 1.4, and 2.8 mM) were added. Next, 30 μ l of color reagent R2 was added into the mixture and incubated for 5 minutes at 37°C. Absorbance was then read with a SPECTRA MAX 250 plate reader at 540 nm and plasma concentrations were extrapolated from standard curve.

2.10 ELISA Measurement of plasma PCSK9

The mouse PCSK9 ELISA kit (abcam) was used to measure plasma PCSK9 levels (1:4 diluted in the reagent diluent) according to manufacturer's protocol. An assay plate coated with the capture antibody was added with about 50 μ l of standards or diluted samples and 100 μ l of HRP-labeled detection antibody and then blocked in reagent diluent. A reagent detergent wash was performed five times on the plate following the 1 h incubation at 37°C. Each well was then incubated at 37°C for 15 minutes with substrates A and B. The stop solution of 50 μ l was added to terminate the reaction. The absorbance was measured using a SpectraMax i3x plate reader at a wavelength of 450 nm.

2.11 ApoB and TG secretion

The cells were washed twice with DMEM without FBS and then incubated in DMEM containing 0.4 mM oleic acid complexed to 0.5% FA-free BSA (Sigma) for 4 h. The cells were then washed twice in DMEM without FBS and incubated in DMEM without oleic acid and FBS for 16 h. Culture medium and cells were collected separately, and whole cell lysate was prepared. Equal amounts of total proteins in culture medium or whole cell lysate were applied to immunoblotting.

TG secretion was measured as described [83]. Mice were fasted for 10 h and then injected with poloxamer-407 dissolved in saline (100 mg/kg body weight) intraperitoneally. Approximately 100 μ l of blood sample was collected before and 0.5, 1, 2, and 4 h post injection. Plasma TG was measured using a commercial colorimetric kit (Wako Diagnostics).

2.12 Histochemistry

Fresh liver tissues were embedded in optimal cutting temperature compound, cut into 8 μ m thick cryostat sections, and then mounted on slides. The sections were fixed in 10% neutral buffered formalin for 10 min. The fixed sections were soaked in 60% isopropanol for 20 s, stained with Oil Red O for 15 min, rinsed twice in 60% isopropanol, and then soaked in hematoxylin to stain nuclei. Afterward, the sections were sealed with gelatin. All slices were imaged using an OMAX M837ZL-C140U3 microscope.

For H&E staining, liver tissues were fixed in neutral buffered formalin and dehydrated through a series of increasing concentrations of ethanol (70, 95, and 100%) at room temperature. The samples were then embedded in paraffin, cut into 8 μ m thick sections, and mounted on slides. The sections were subsequently deparaffinized, rehydrated, and then washed in 1 X PBS three times. The slides were then soaked in the hematoxylin for 3–5 s and differentiated in 1% ethanol hydrochloride for 1–2 s, followed by an immediate wash with running water for 10–20 s. After soaking in 0.5% eosin

stain for 5 s and washing with water, the slides were dehydrated by immersion in ethanol solutions of different concentrations sequentially, cleared in xylene, and then sealed with neutral gum for microscopic observation.

2.13 Adeno-associated virus preparation

Adeno-associated virus (AAV) containing scrambled shRNA or shRNA against mouse Surf4 was prepared using the AAV-DJ/8 Helper Free Expression System according to the manufacturer's instruction (Cell Biolabs, Inc.; VPK-410-DJ-8). shRNAs against mouse Surf4 and scrambled shRNA were designed by BLOCK-iT™ RNAi Designer and synthesized by IDT with a 9-nucleotide hairpin loop sequence (5'-TTCAAGAGA-3') in the middle, a 5'-BamHI restriction site overhang on the top strand, and a 5'-EcoRI restriction site overhang on the bottom strand (Table 2.7). shRNA was then cloned into the BamHI/EcoRI sites of pAAV-U6-GFP. AAV was packaged and amplified in QBI 293A cells and then purified using Optiprep (Sigma) density-gradient ultracentrifugation as described [153]. AAV particles were collected from the 40% density step, diluted in PBS, concentrated with Amicon Ultra-15 Centrifugal Filter Unit (Millipore; 100K NMWL), and titered using quantitative real-time PCR.

Table 2.7. shRNAs for AAV preparation.

Target	Sequences
Scramble	5'-GTATGCAGCGGTATCGTGTTG-3'
Surf4	5'-GGGACTTGAAGTTTCTCATGA-3'

2.14 Atherosclerotic analysis

Male *Ldlr*^{-/-} or *apoE*^{-/-} mice (10–14 weeks of age) were randomly divided into two groups and injected with AAV-U6-scrambled (Control group) or Surf4 shRNA via retro-orbital injection (2.0

$\times 10^{10}$ gc/mouse). Mice were then fed the Western-Type Diet for up to 14 weeks. Mice were fasted for 10 h and then euthanized. Aortas and hearts were collected immediately and fixed in 4 % paraformaldehyde. Serial sections (10 μ m thick) throughout the three aortic valves of each mouse heart were cut with cryo-sectioning. Heart sections and the whole aorta from the aortic root to the iliac bifurcation were then stained with Oil Red-O as described in our previous study [154]. Images were taken using an OMAX M837ZL-C140U3 microscope. The atherosclerotic burden was quantified by measuring the surface area of Oil Red O positive lesions on the cross-sectional area of the aorta sinus and the whole aorta. Lesion area was quantified with OMAX ToupView and expressed as the percentage of the total area.

2.15 Statistical analysis

All statistical analyses were carried out by GraphPad Prism, version 9.0 (GraphPad Software). The significant differences between groups were determined via Student's t-test. All data met normal distribution criteria, and variance between groups that was analyzed by F-test showed no significant difference ($P > 0.05$). Values of all data, unless otherwise indicated, were depicted as mean \pm SD. The significance was defined as * $P < 0.05$, ** $P < 0.01$, *** $P < 0.001$, and **** $P < 0.0001$. All experiments, unless indicated, were repeated at least three times.

Chapter 3 Manuscript I

SURF4 is not required for endogenous PCSK9 secretion from hepatocytes

(*Biochimica et Biophysica Acta- Molecular and Cell Biology of Lipids*. 2020 Feb; 1865(2): 158555.

PART OF *Journal of Lipid Research*. 2021 Jun; 62: 100091. doi: 10.1016/j.jlr.2021.100091.)

All experiments were conducted and analyzed by Yishi Shen in Zhang's Lab except

Fig 3.1 (Hong-mei Gu-Zhang Lab)

Fig 3.4A (Shijun Deng-Zhang Lab)

SURF4 is not required for endogenous PCSK9 secretion from hepatocytes

Yishi Shen^{a#}, Binxiang Wang^{b#}, Shijun Deng^{a#}, Lei Zhai^{b#}, Hong-mei Gu^a, Adekunle Alabi^a,
Xiaodan Xia^a, Yongfang Zhao^b, Xiaole Chang^b, Shucun Qin^{b*}, Da-wei Zhang^{a*}

^aGroup on the Molecular and Cell Biology of Lipids and Department of Pediatrics, Faculty of Medicine and Dentistry, University of Alberta, Edmonton, Alberta, Canada. ^bInstitute of Atherosclerosis in Shandong First Medical University (Shandong Academy of Medical Sciences), Taian, China

Running title: SURF4 and PCSK9 secretion and expression

Keywords: PCSK9; SURF4; Protein secretion; siRNA knockdown; Lipid metabolism

3.1 Introduction

PCSK9 promotes degradation of LDLR and plays a central role in homeostatic control of plasma LDL-C levels [48, 49, 155-158]. The half-life of circulating PCSK9 is only approximately 5 min [159]. Thus, a possible target in blocking PCSK9-promoted LDLR degradation is the machinery that assists in PCSK9 secretion. However, the molecular mechanism of PCSK9 secretion is currently unknown. Recently, Chen et al. reported that the COPII adaptor protein Sec24A facilitates the ER-to-Golgi transport of PCSK9 [61]. However, PCSK9 is located in the lumen of the ER and unable to directly interact with Sec24A that is located in the cytosol. Cargo receptor, Erv29, preferentially sorts soluble proteins into COPII complex and its recognition of cargos appears not to involve in carbohydrate recognition [160]. SURF4, the human homolog of Erv29, is a polytopic transmembrane protein containing 8 putative transmembrane domains with a lumen-exposed N-terminus that recognizes cargoes and a cytosolic C-terminus that may interact with Sec24 [102]. Considering that PCSK9 is a soluble glycosylated protein but glycosylation is not necessary for its secretion [161], we proposed that SURF4 linked PCSK9 to the COPII coat proteins and mediated its secretion. When we tested our hypothesis, Emmer et al. reported that SURF4 facilitated overexpressed PCSK9 secretion in HEK293T cells [131]. Given that plasma PCSK9 is mainly secreted from the liver and circulating PCSK9 preferentially promotes hepatic LDLR degradation [159, 162], we assessed the role of SURF4 in PCSK9 secretion in human hepatoma-derived cells, Huh7 and HepG2. Our findings revealed that knockdown of *SURF4* increased expression and secretion of PCSK9, indicating a negligible role of SURF4 in PCSK9 secretion in cultured human hepatocytes. We also knocked down hepatic *Surf4* in wild-type (C57BL6/J) mice, however we found that, in contrast to the results from cultured cells, deficiency of hepatic Surf4 had no effect on PCSK9 expression and secretion *in vivo*. Taken together, these findings indicate

that SURF4 is not required for endogenous PCSK9 secretion from hepatocytes.

3.2 Results

3.2.1 Detection of SURF4

We purchased three commercially available anti-SURF4 antibodies. To validate them, we overexpressed DYKDDDDK-tagged SURF4 (GenScript®, OHu05244) in HEK293 cells and then applied whole cell lysate to immunoblotting. As shown in Figure 3.1A, an anti-DYKDDDDK antibody but not the three commercial anti-SURF4 antibodies could detect an extra band of ~25 kDa in SURF4-overexpressed sample (lane 2 vs 1), indicating that these antibodies did not perform very well in our experiments. Thus, we generated one custom-made rabbit polyclonal anti-SURF4 antibody, 1195Sa. This antibody was produced and purified by GenScript® using a peptide that is completely conserved among different species including human, mouse, and rat (Fig 3.1B). We validated its specificity using whole cell lysate derived from HEK293 cells transfected with empty pcDNA3.1 or pcDNA3.1 containing *SURF4* cDNA with an N-terminal hemagglutinin (HA) tag. As shown in Figure 3.1C, a protein band at approximate 25 kDa could be detected by both 1195Sa and an anti-HA antibody only in SURF4-overexpressed sample. 1195Sa also detected a lower band that was absent in the anti-HA antibody blot. This might be a degraded SURF4 that lost the N-terminal HA tag. We also tested if 1195Sa could immunoprecipitate SURF4. Equal amount of whole cell lysate isolated from HepG2 cells was incubated with 1195Sa, pre-immune serum (Pre), or purified rabbit IgG (R-IgG) and protein-G beads. The immunoprecipitated proteins were eluted and subjected to immunoblotting. As shown in Figure 3.1D, 1195Sa, but not pre-immune serum, nor purified rabbit IgG pulled down SURF4 from whole cell lysate (Lane 3 vs 1 or 2). Actin was not detected in all three immunoprecipitated samples. These results demonstrated the specificity of 1195Sa for SURF4. Thus, it was used in the experiments described below.

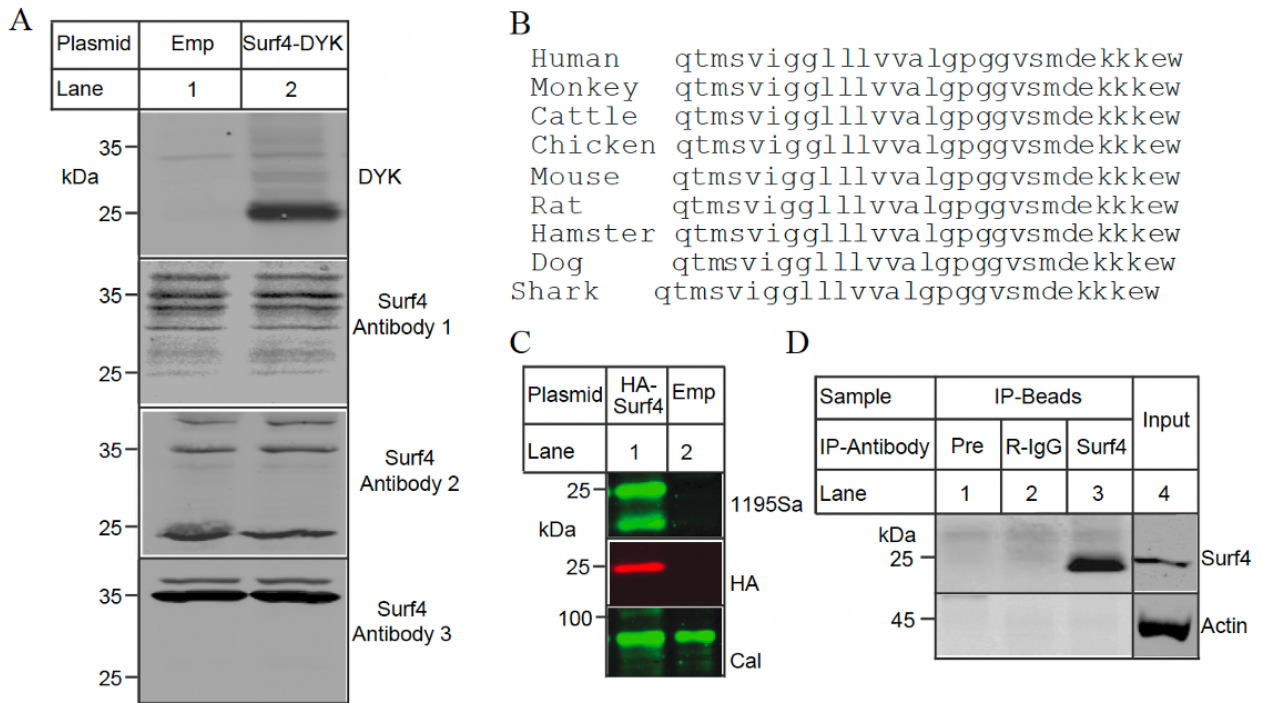


Figure 3.1. Detection of SURF4. (A) Expression of DYKDDDDK-tagged SURF4. HEK293 cells were transfected with empty pCDNA3.1 (Emp) or SURF4 with a C-terminal DYKDDDDK tag (Surf4-DYK) using PEI. 48 h after transfection, cells were harvested and whole cell lysate was isolated. Same amount of total proteins was then subjected to SDS-PAGE and immunoblotting with antibodies indicated. Anti-DYKDDDDK antibody (DYK, 1:1000), Surf4 antibody 1 (1:500, abcam, ab150327), Surf4 antibody 2 (1:500, abcam, ab192611), Surf4 antibody 3 (1:500, Abnova, H00006836-M01). (B) Alignment of partial SURF4 sequence. The alignment was performed using ClustalW2. Human SURF4 (NP 14935.1), Monkey (NP 001181722.1), Cattle (NP 001095979.1), Chicken (NP 989686.1), Mouse (NP 035642.1), Rat (NP 001029040.1) Hamster (XP 003511779.2), Dog (XP 022279343.1), Shark (XP 007901057.1). (C) Expression of HA-tagged SURF4 in HEK293 cells. HEK293 cells were transfected with empty pCDNA3.1 (Emp) or SURF4 with an N-terminal HA tag (HA-Surf4) using PEI. 48 h after transfection, whole cell lysate was prepared. Same amount of total proteins was subjected to SDS-PAGE and immunoblotting with antibodies indicated. A rabbit anti-HA antibody (HA, 1:5000), a rabbit anti-SURF4 antibody (1195Sa, 1:1000), and a mouse anti calnexin antibody (Cal, 1:1000). (D)

Immunoprecipitation of SURF4. Same amount of whole cell lysate isolated from HepG2 cells was incubated with 1195Sa (Surf4), pre-immune serum (Pre), or purified rabbit IgG (R-IgG) and protein-G beads overnight at 4 °C. After washing, the bound proteins were eluted from the beads. The immunoprecipitated proteins (IP-Beads) and whole cell lysate (Input) were then subjected to immunoblotting with a mouse anti-actin antibody (Actin) and IRDye800CW-labeled 1195Sa (Surf4). Anti-actin antibody binding was detected using IRDye®680-labeled Donkey anti-mouse IgG (Li-Cor). The signals of IRDye800CW-labeled 1195Sa and IRDye®680-labeled Donkey anti-mouse IgG were detected on a Licor Odyssey Infrared Imaging System (Li-Cor).

3.2.2 Knockdown of *SURF4* increased PCSK9 expression and secretion in cultured hepatoma cells

We knocked down expression of *SURF4* in HepG2 cells to define if *SURF4* affected PCSK9 secretion. Two *SURF4* siRNAs that target different regions of *SURF4* efficiently reduced protein levels of *SURF4* in HepG2 cells (Fig. 3.2A). Surprisingly, knockdown of *SURF4* significantly increased PCSK9 abundance in both whole lysate (Fig. 3.2A) and culture medium (Fig. 3.2B). To confirm these findings, we knocked down *SURF4* expression in another human hepatoma-derived cell line, Huh7 cells, and observed similar phenotypes. The levels of cellular PCSK9 in whole cell lysate and secreted PCSK9 in culture medium were all significantly increased in *SURF4* siRNA-transfected cells compared to scrambled siRNA-transfected cells (Fig. 3.2C and 3.2D). Further, we treated cells with lovastatin to increase *PCSK9* expression in Huh7 cells transfected with Scrambled or *SURF4* siRNA. Consistently, knockdown of *SURF4* increased levels of PCSK9 detected in both whole cell lysate and culture medium (Fig. 3.2E). Taken together, these findings indicate that *SURF4* is not essential for endogenous PCSK9 secretion, instead it somehow regulates *PCSK9* expression in cultured human hepatocytes.

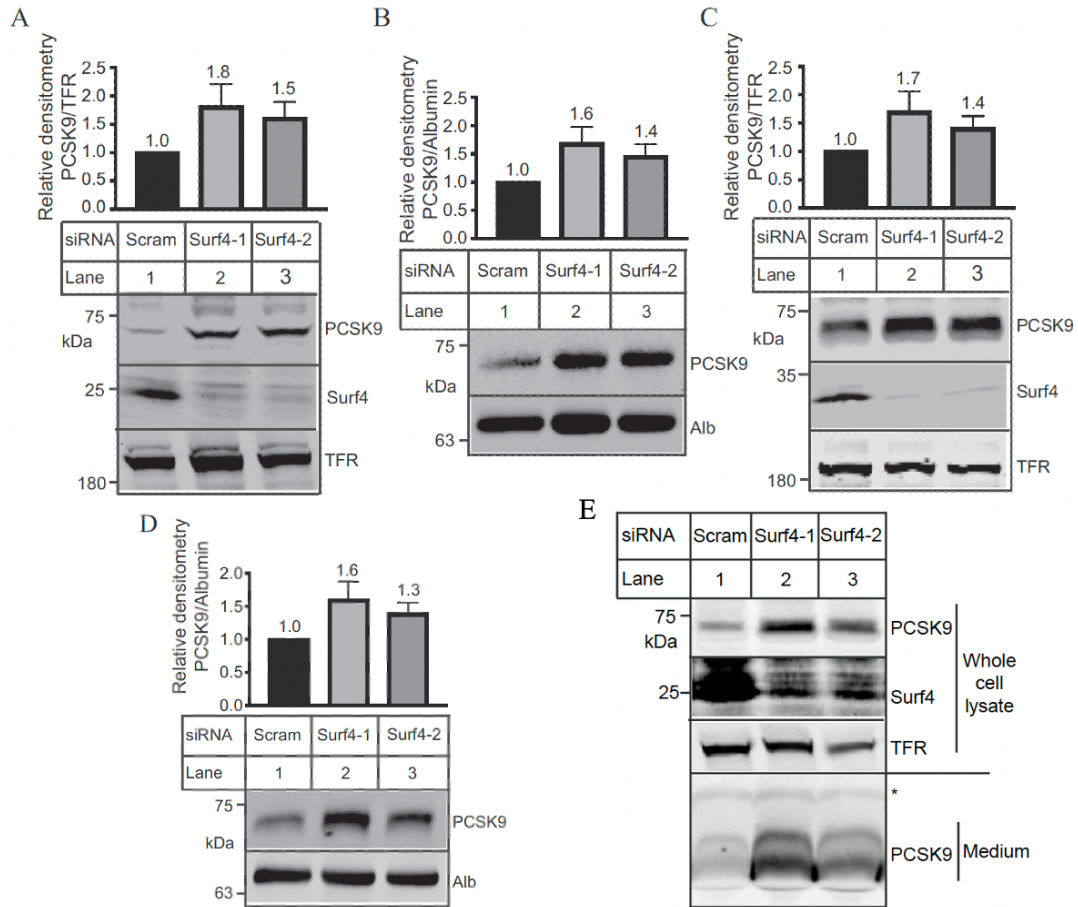


Figure 3.2. Effect of *SURF4* knockdown on PCSK9 secretion. (A) Whole cell lysate and (B) Culture medium. Knockdown of *SURF4* in HepG2 cells. HepG2 cells were transfected with Scrambled or one of the two different *SURF4* siRNA (Surf4-1, Surf4-2). 48 h after, cells were incubated with DMEM without FBS for 24 h. Culture medium was then collected. Cells were harvested for the preparation of whole cell lysate. Same amount of whole cell lysate (A) or culture medium (B) were subjected to immunoblotting with a mouse anti-PCSK9 antibody, 15A6, a rabbit anti-*SURF4* antibody, 1195Sa, a mouse anti-transferrin receptor antibody (TFR), or a goat anti-albumin antibody. The numbers above each bar refer to the ratio of the relative densitometry of PCSK9 in *SURF4* knockdown cells to that of PCSK9 in scrambled siRNA-transfected cells that was defined as 1. The densitometry was determined using a Li-Cor Odyssey Infrared Imaging

System. The relative densitometry was the ratio of the densitometry of PCSK9 to that of transferrin receptor (TFR) in the whole cell lysate (A) or that of albumin in culture medium (B) in the same sample. (C) whole cell lysate and (D) culture medium. Knockdown of *SURF4* in Huh7 cells. The experiment was performed as described above except that Huh 7 cells were used. (E) **Statin-treated cells.** Huh7 cells were transfected with scrambled or one of the two different *SURF4* siRNAs. 48 h later, the cells were treated with lovastatin (10 μ M) and mevalonate (250 μ M) for 24 h. Same amount of whole cell lysate and culture medium was subjected to immunoblotting with a mouse anti-PCSK9 antibody, 15A6, a rabbit anti-SURF4 antibody, and a mouse anti-transferrin receptor (TFR) antibody.

3.2.3 SURF4 does not directly associate with PCSK9

Next, we sought to dissect how SURF4 affected PCSK9 expression. It has been reported that SURF4 interacted with PCSK9 overexpressed in HEK293T cells [131]. Thus, we performed co-immunoprecipitation to determine if endogenous SURF4 interacted with endogenous PCSK9 in HepG2 cells. Considering that the association between cargo receptors and its substrates is normally weak and transient, we incubated cells with deoxyglucose and sodium azide to prevent cargo dissociation as described in [105] and then supplied cells with dithiobis succinimidyl propionate (DSP). Same amount of whole cell lysate was then subjected to 1195Sa and 15A6 to pull down SURF4 and PCSK9, respectively. As shown in Figure 3.3A, the anti-PCSK9 antibody pulled down PCSK9. However, we did not observe SURF4 in the PCSK9 immunoprecipitated sample (lane 2). Similarly, SURF4 was immunoprecipitated by its specific antibody. PCSK9 did not co-immunoprecipitated with SURF4 (lane 3). On the other hand, apoB was pulled down for the whole cell lysates together with SURF4 in the same condition (Fig. 3.3B, lane 3), consistent with a previous report that SURF4 interacted with apoB [123]. These findings indicate that PCSK9 might not be directly associated with SURF4.

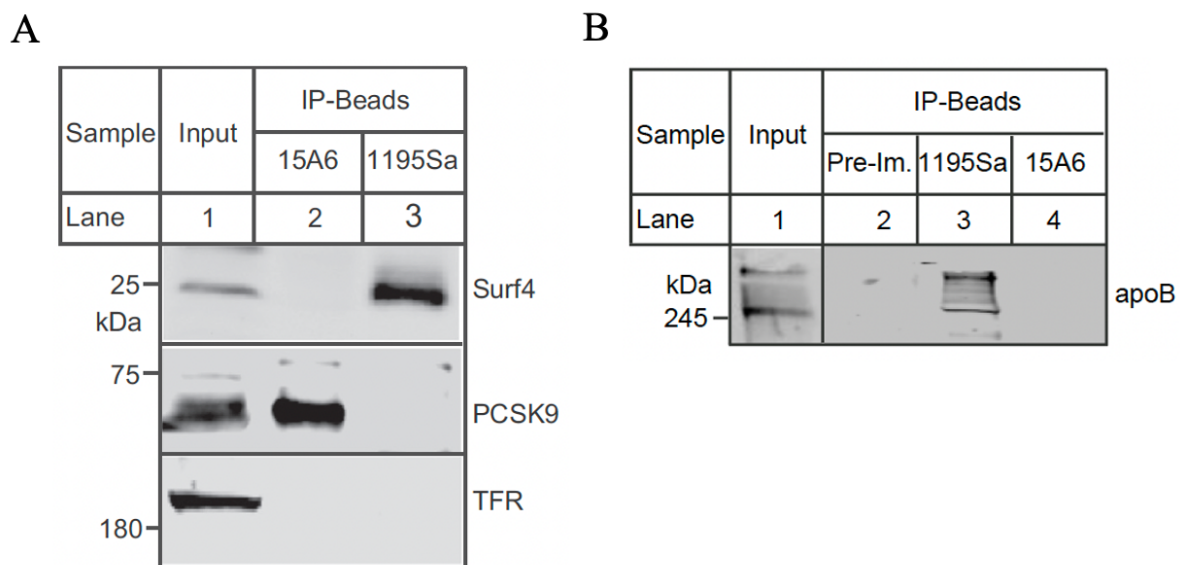


Figure 3.3. Immunoprecipitation of SURF4. (A) Same amount of whole cell lysate isolated from HepG2 cells was incubated with 15A6 or 1195Sa and protein-G beads overnight at 4 °C. Whole cell lysate (Input) and immunoprecipitated proteins (IP-Beads) eluted from the beads were then subjected to immunoblotting with a mouse anti-TFR, IRDye800CW-labeled 1195Sa (Surf4), or IRDye800CW-labeled 13D3 (PCSK9). Anti-transferrin antibody binding was detected using IRDye®680-labeled Donkey anti-mouse IgG (Li-Cor). The signals were detected on a Licor Odyssey Infrared Imaging System (Li-Cor). (B) Same amount of whole cell lysate isolated from HepG2 cells was incubated with 1195Sa, pre-immune serum (Pre-Im.), or 15A6 and protein-G beads overnight at 4 °C. After washing, the bound proteins were eluted from the beads. The immunoprecipitated proteins (IP-Beads) and whole cell lysate (Input) were then subjected to immunoblotting with a goat anti-apoB, followed by IRDye680-labeled donkey anti-goat IgG. The signals were detected on a Licor Odyssey Infrared Imaging System.

3.2.4 Knockdown of *SURF4* increased *SREBP2* transcriptional activity

We then performed qRT-PCR to define mRNA levels of *PCSK9* as well as *SREBP2* and its target *HMGCR* since expression of *PCSK9* is transcriptionally regulated by *SREBP2*. As shown in Figure 3.4A, mRNA levels of *PCSK9*, *SREBP2*, *HMGCR* were all increased in cells transfected with *SURF4* siRNA. These findings suggest that knockdown of *SURF4* expression increases the transcriptional activity of *SREBP2*, leading to enhanced transcription of *PCSK9*. We further determined how *SURF4*, a cargo receptor, regulated transcriptional activity of *SREBP2*. It has been reported that ER stress can enhance SREBPs processing and increase their transcriptional activity [163]. Was it possible that knockdown of *SURF4* induced ER stress and consequently affected SREBPs processing? To test this hypothesis, we detected expression of ER stress marker, *GRP78*, in HepG2 cells treated with thapsigargin or *SURF4* siRNAs. As shown in Figure 3.4B, tunicamycin and thapsigargin markedly increased expression of *GRP78* in HepG2 cells, while knockdown of *SURF4* had no significant effect. Similarly, tunicamycin and thapsigargin but not *SURF4* knockdown dramatically increased *GRP78* expression in Huh7 cells (Fig 3.4C). Thus, knockdown of *SURF4* did not markedly induce ER stress.

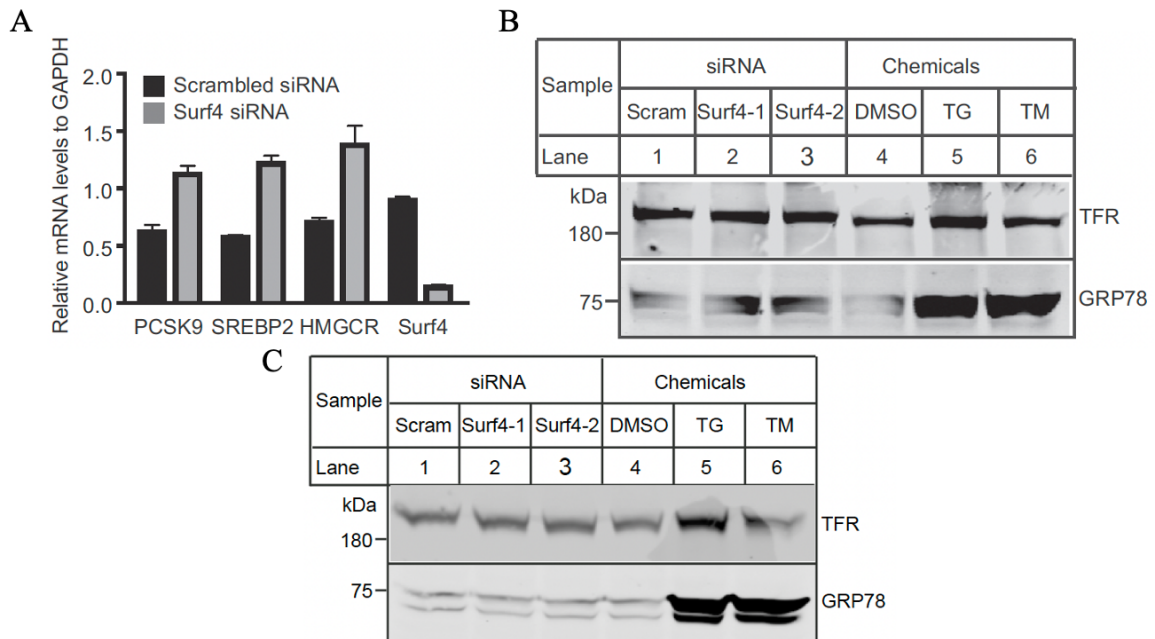


Figure 3.4. Effect of *SURF4* knockdown on *SREBP2* transcriptional activity. (A) qRT-PCR. Total RNAs were extracted from HepG2 cells transfected with either Scrambled or *SURF4* siRNA for 72 h. qRT-PCR was performed on StepOnePlus™ using SYBR® Select Master Mix. **(B) & (C) Examination of ER stress.** HepG2 cells (B) or Huh7 cells (C) were transfected with Scrambled siRNA or one of the two different *SURF4* siRNAs for 72 h, or treated with DMSO alone, thapsigargin (TG, 25 μ M), or tunicamycin (TM, 0.5 μ g/ml) for 24 h. Whole cell lysate was prepared and subjected to immunoblotting with antibodies indicated, a monoclonal mouse anti-TFR (1:2000) and a rabbit anti-GRP78 antibody (1:1000). Similar results were obtained from at least three different experiments.

3.2.5 Knockdown of hepatic *Surf4* has no effect on PCSK9 expression and secretion *in vivo*

To confirm the findings from cultured cells, we knocked down *Surf4* expression in the wild-type (WT) and *Pcsk9*^{-/-} mice using AAV-shRNA. AAV-*Surf4* shRNA significantly reduced mRNA levels of *Surf4* in the liver of both the WT and *Pcsk9*^{-/-} mice (Fig. 3.5A). Silencing of *Surf4* had no significant effect on the levels of plasma PCSK9 (Fig. 3.5B) and liver PCSK9 (Fig. 3.5C) in the WT mice, while PCSK9 was virtually undetectable in *Pcsk9*^{-/-} mice. Thus, unlike the results found in cultured cells [131], the loss of hepatic SURF4 did not affect the levels of PCSK9 in mouse liver and plasma, suggesting that *Surf4* is not required for hepatic PCSK9 secretion.

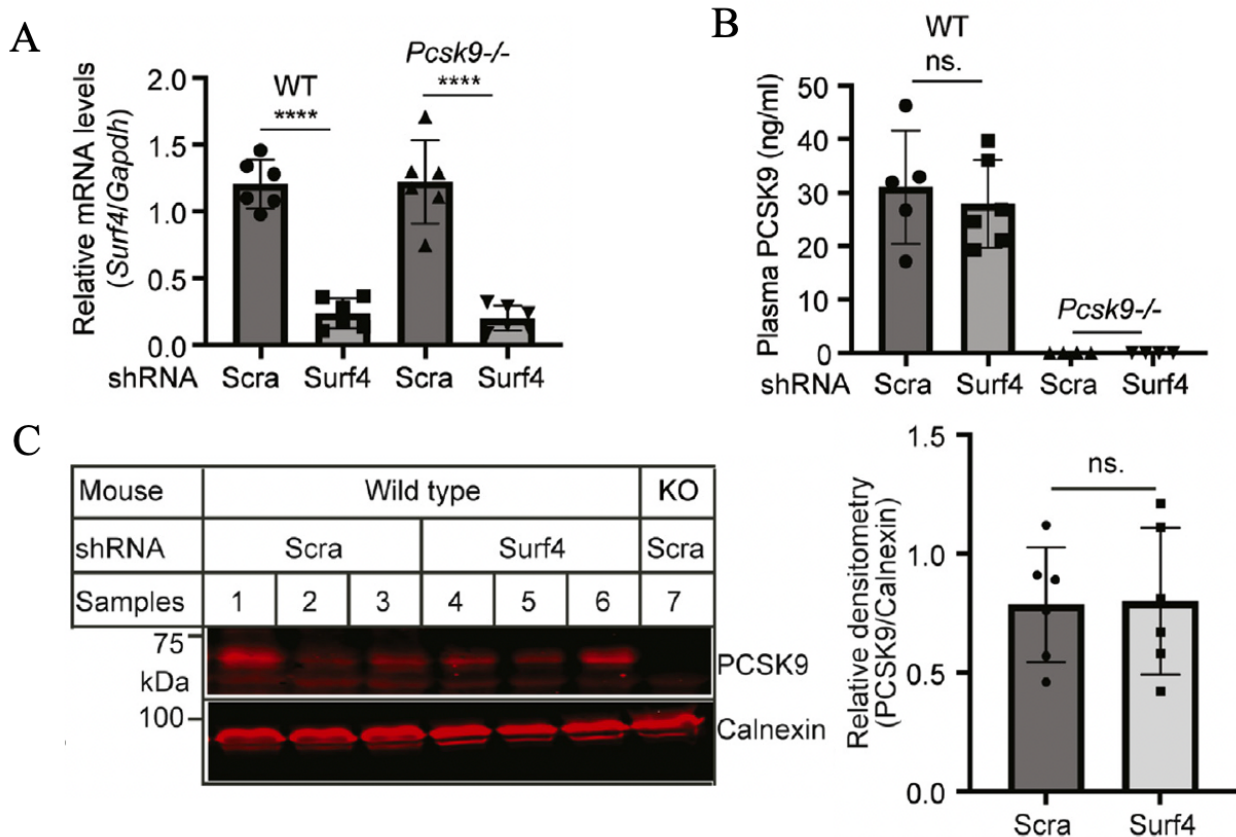


Figure 3.5. The effect of hepatic knockdown of *Surf4* on PCSK9 secretion *in vivo*. The WT and *Pcsk9*^{-/-} (KO) mice (n = 6) were injected with AAV-scrambled (Scra) or *Surf4* shRNA and then fed the Western-type diet for 4 weeks. The relative mRNA levels were the ratio of *Surf4* mRNA

levels to that of *Gapdh* (A). Plasma PCSK9 was measured with an ELISA Kit (R&D Systems) (B). Liver homogenate was applied to immunoblotting to detect PCSK9. The relative densitometry was the ratio of the densitometry of PCSK9 to that of calnexin (C). Student's t-test was used to determine the significant differences between groups. Values of all data were mean \pm SD. The significance was defined as *P < 0.05, **P < 0.01, ***P < 0.001, and ****P < 0.0001. P > 0.05. ns, no significant difference.

3.3 Discussion

We initially proposed that cargo receptor SURF4 might mediate PCSK9 secretion. However, our data revealed that knockdown of *SURF4* expression in culture human hepatocytes increased endogenous PCSK9 expression and secretion. These findings indicate a negligible role of SURF4 in endogenous PCSK9 secretion in human hepatocytes. This is different from a recent report that knockout of *SURF4* increased secretion of PCSK9 overexpressed in HEK293T cells [131]. It is of note that there are several differences between the two studies. First, we used hepatocytes that express and secrete PCSK9, while Emmer et al. employed HEK293 cells that normally do not express PCSK9. Second, we investigated the effects of SURF4 on the expression and secretion of endogenous PCSK9, while Emmer et al. overexpressed GFP-tagged PCSK9 in HEK293 cells under the control of the CMV promoter that strongly and constitutively drives the expression of genes. Third, we used siRNA to transiently reduce SURF4 expression, while Emmer et al. stably knocked out *SURF4* in HEK293 cells via the CRISPER-Cas9 technique. In the Emmer's study, knockout of SURF4 partially reduced secretion of PCSK9 overexpressed in HEK293 cells. Our findings demonstrate that SURF4 is not essential or required for PCSK9 secretion in hepatocytes. However, we cannot exclude the possibility that SURF4 might contribute to PCSK9 secretion when the protein was overexpressed in cultured hepatocytes.

We found that knockdown of *SURF4* expression increased *PCSK9* transcription *in vitro*. PCSK9 is regulated by SREBP2 at the transcriptional level. ER stress increases processing of SREBPs and its transcriptional activity [163]. However, knockdown of *SURF4* did not markedly induce ER stress, which is consistent with the recent report that stable knockout of *SURF4* in HEK293 cells did not increase ER stress [131]. We also sought to determine if *SURF4*, as an ER protein, could associate with SREBP2 and suppress transport of SREBP2 to the Golgi for

processing. We immunoprecipitated SURF4 from whole cell lysate in the presence of a chemical cross linker DSP but failed to observe coimmunoprecipitation of SREBP2 with Surf4 (Data not shown). Thus, how exactly SURF4 regulates transcriptional activity of SREBP2 is unclear. Experiments are ongoing in the lab to investigate the underlying mechanism.

In addition, hepatic *Surf4* silencing did not alter the levels of liver PCSK9 and plasma PCSK9, which is partly consistent with our observation in cultured cells that SURF4 is not required for PCSK9 secretion from hepatocyte. However, we did not observe an increase in *PCSK9* expression in *Surf4* knockdown mice. It is possible that Huh7 and HepG2 cells are human hepatoma-derived cell lines, which have undergone numerous changes and may not represent physiological hepatocytes. In addition, hepatic SURF4 may function differently between human and mouse hepatocytes. Further studies using mouse hepatoma-derived cell lines, such as Hep1c1c7 and Hepa1-6 cells, may shed a light on this possibility. Further studies are needed to investigate the underlying mechanism for this inconsistent. Nevertheless, these findings demonstrate that hepatic SURF4 is not required for endogenous PCSK9 secretion from hepatocytes.

Chapter 4 Manuscript II

Atherosclerosis-associated hepatic secretion of VLDL is dependent on cargo receptor protein SURF4

(Journal of Lipid Research. 2021 Jun; 62: 100091. doi: 10.1016/j.jlr.2021.100091.)

All experiments were conducted and analyzed by Yishi Shen in Zhang's Lab except

Fig 4.1, 4.2 and 4.4 (Bingxiang Wang, Lei Zhai, Yongfa Zhao, Xiaole Chang, Sijie Xing, Boyan Liu, Shucun Qin-Institute of Atherosclerosis in Shandong First Medical University, China)

Fig 4.6G, 4.6H and 4.6I (Xiaodan Xia and **Yishi Shen-Zhang Lab**)

Atherosclerosis-associated hepatic secretion of VLDL is dependent on cargo receptor protein SURF4

Bingxiang Wang^{1#}, Yishi Shen^{3#}, Lei Zhai^{1#}, Xiaodan Xia^{2#}, Hong-mei Gu³, Maggie Wang³, Yongfang Zhao¹, Xiaole Chang¹, Adekunle Alabi³, Sijie Xing³, Shijun Deng³, Boyan Liu¹, Guiqing Wang², Shucun Qin^{1*}, Da-wei Zhang^{3*}

¹ Institute of Atherosclerosis and College of Basic Medical Sciences in Shandong First Medical University (Shandong Academy of Medical Sciences), Taian, China. ² Department of Orthopedics, The Sixth Affiliated Hospital of Guangzhou Medical University, Qingyuan People's Hospital, Qingyuan, China. ³ Department of Pediatrics and Group on the Molecular and Cell Biology of Lipids, Faculty of Medicine and Dentistry, University of Alberta, Edmonton, Alberta, Canada.

#Equal contribution.

Short title: SURF4, and PCSK9 and VLDL secretion

Abbreviations: AAV, adeno-associated virus; Acad1, Acyl-CoA Dehydrogenase Medium Chain; ALT, alanine aminotransferase; ASCVD, atherosclerotic cardiovascular disease; BFA, brefeldin A; COPII, coat protein complex II; CPT, Carnitine Palmitoyltransferase; DsiRNA, Dicer-Substrate siRNA; FFA, free fatty acid; FH, familial hypercholesterolemia; FPLC, fast-performance liquid chromatography; GalNAc, N-acetylgalactosamine; HMG-CoAR, HMG-CoA Reductase; LDLR, LDL receptor; MTP, microsomal triglyceride transfer protein; PCSK9, proprotein convertase subtilisin kexin-like 9; Surf4, Surfeit 4; TANGO1, transport and Golgi organization 1; TALI, TANGO1-like protein; TC, total cholesterol; TG, triglyceride; VTV, VLDL transport vesicle; WT, wild-type.

Abstract

Plasma LDL is produced from catabolism of VLDL and is cleared from circulation mainly via the hepatic LDLR. VLDL is exclusively secreted by hepatocytes, however, the mechanism regulating its secretion is not completely understood. SURF4 is a cargo receptor localized in the ER membrane. It recruits cargos into COPII vesicles to facilitate their secretion. Here, we investigated the role of SURF4 in VLDL secretion. We generated *Surf4* hepatocyte-specific knockout (*Surf4*^{LKO}) mice, and found that knockout of *Surf4* significantly reduced plasma levels of cholesterol, TG and lipid-binding protein apoB. In cultured human hepatocytes, SURF4 co-immunoprecipitated and co-localized with apoB100, and *SURF4* silencing reduced secretion of apoB100. Furthermore, knockdown of *Surf4* in *Ldlr*^{-/-} mice significantly reduced TG secretion, plasma levels of apoB and non-HDL cholesterol, and the development of atherosclerosis. However, *Surf4*^{LKO} mice and *Surf4* knockdown in *Ldlr*^{-/-} mice displayed similar levels of liver lipids and plasma ALT activity as control mice, indicating that inhibition of *Surf4* does not cause notable liver damage. Expression of SCD1 was also reduced in the liver of these mice, suggesting a reduction in *de novo* lipogenesis. In summary, hepatic deficiency of *Surf4* reduced VLDL secretion and the development of atherosclerosis, but did not cause hepatic lipid accumulation or liver damage.

Key words: apolipoproteins, LDL, lipid metabolism, lipoprotein metabolism, liver, triglyceride, stearyl-CoA-1, apoB100, LDLR, triglyceride

4.1 Introduction

VLDL is a TG-enriched lipoprotein mainly generated and secreted from the liver. TG in VLDL is hydrolyzed by LPL, leading to the formation of IDL that can be further metabolized to LDL [9, 164]. Plasma LDL-C levels are positively correlated with the risk of ASCVD, one of the leading causes of morbidity and mortality worldwide. Also, emerging evidence indicates that elevated levels of remnant cholesterol, such as VLDL and IDL, are associated with an increased risk of ASVCD [165]. It has also been reported that dysregulation of VLDL secretion occurs under many pathophysiological conditions. For example, insulin resistance and obesity can cause VLDL overproduction, increasing the risk for ASVCD [166]. Furthermore, patients with homozygous FH harboring LDLR null mutations or with autosomal recessive hypercholesterolemia cannot be effectively treated by current available lipid-lowering drugs, such as statins and PCSK9 inhibitors [167]. Inhibition of VLDL secretion can markedly reduce plasma levels of cholesterol and the development of atherosclerosis [84, 135, 168-170]. However, the biggest challenge is that current strategies to inhibit VLDL secretion usually lead to hepatic TG accumulation and subsequent fatty liver and liver steatosis as VLDL secretion is the primary route of TG export from the liver [135, 168, 169, 171]. Thus, deciphering the molecular mechanism of VLDL secretion not only advances our understanding of the regulation of lipid metabolism but is also essential for the identification of novel therapeutic targets with minimal side effects.

Newly synthesized apoB100 is cotranslationally lipidated in the lumen of the ER of hepatocytes by MTP. Unlipidated apoB100 is rapidly degraded via the proteasome-dependent and independent pathways [9, 172]. After assembly in the ER lumen, VLDL is transported to the Golgi apparatus through specific VTV as VLDL is too large to utilize the classical COPII vesicles [9, 16]. Recently, Santos et al. reported that TANGO1 and TALI protein were required for the formation

of VTV and VLDL secretion in HepG2 cells [16]. TANGO1 was also required for the export of other bulky molecules, such as collagens, via bringing them to the ER exit site [16, 20-22]. Both TANGO1 and TALI contain an N-terminal luminal SH3-like domain that is required for secretion of bulky cargos [16]. However, how does the SH3-like domain recognize various kinds of bulky cargos such as collagens and VLDL? It has been reported that the SH3-like domain of TANGO1 does not directly interact with collagens. Instead, heat shock protein (HSP) 47 binds to collagens and the SH3-like domain in TANGO1, bridging the interaction between collagens and TANGO1 [22]. It is currently unknown whether such a protein is required for sorting VLDL into VTV. However, understanding this process can provide critical information for the development of novel LDL production-based therapies.

SURF4 is ubiquitously expressed and localized in the ER membrane. It consists of 8 putative transmembrane domains, a C-terminal cytosolic domain that associates with SEC24 in COPII, and a N-terminal cytosolic domain. SURF4 acts as a cargo receptor to recruit substrates into COPII vesicles, facilitating their secretion [102, 107, 123]. To further determine the role of hepatic SURF4 in VLDL secretion, we generated *Surf4* hepatocyte-specific knockout (*Surf4*^{LKO}) mice and found that a lack of hepatic *Surf4* significantly reduced VLDL secretion. Furthermore, knockdown of *Surf4* drastically reduced the development of atherosclerosis in *Ldlr*^{-/-} mice but did not cause hepatic lipid accumulation or notable liver damage.

4.2 Results

4.2.1 Generation of *Surf4*^{LKO} mice

To study the role of SURF4 in VLDL secretion, we generated *Surf4*^{LKO} mice as VLDL is mainly secreted from hepatocytes [173]. Exon 2 of the *Surf4* gene was flanked by the loxP sites via CRISPR-Cas9 (Fig. 4.1A). We then crossed *Surf4*^{Flox} mice with mice expressing Cre recombinase

under the control of the hepatocyte-specific albumin (Alb) promoter to delete functional *Surf4* specifically in hepatocytes. The Cre-mediated recombination removed the entire exon 2, which deleted amino acid residues from Phe¹⁷ to Leu⁷⁸ and caused a frameshift at Thr⁷⁹. This shift introduced six amino acid residues (LAVFWC) after Gln¹⁶, followed by a stop codon (Fig. 4.1A). SURF4 protein was essentially undetectable in hepatocytes of *Surf4*^{LKO} mice (Fig. 4.1B). Genotyping also showed that the *Surf4* gene was undetectable in the liver of *Surf4*^{LKO} mice but was detected in the other tissues of *Surf4*^{LKO} mice (Fig. 4.1C). *Surf4*^{LKO} and *Surf4*^{Flox} mice displayed similar body weight, and fat and lean mass (Fig. 4.1D to F).

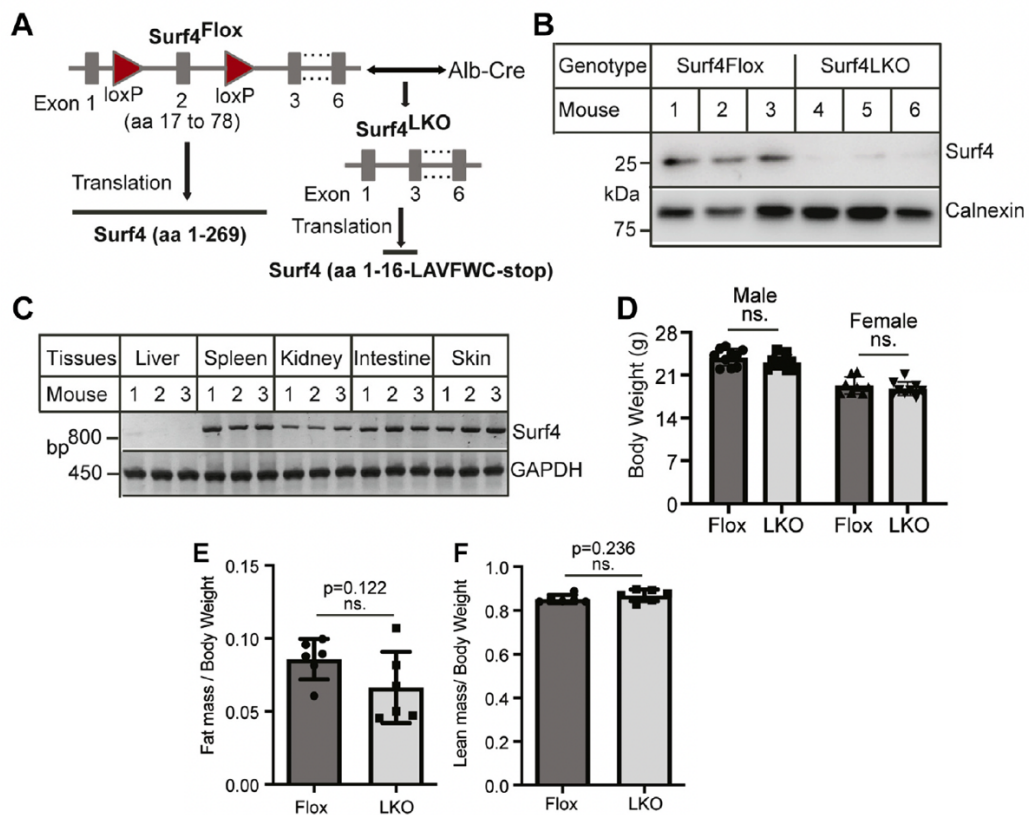


Figure 4.1. Generation of *Surf4*^{LKO} mice. A: Schematic of *Surf4*^{LKO} mice generation. *Surf4*^{Flox} mice were mated with Alb-Cre mice to generate heterozygous *Surf4*^{LKO} mice, which were then bred to produce homozygous *Surf4*^{LKO} mice. B: Immunoblotting. Whole cell lysate of primary

hepatocytes isolated from *Surf4*^{Flox} and *Surf4*^{LKO} mice (n = 3) was applied to immunoblotting with antibodies indicated. C: Genotyping. DNA from different tissues of *Surf4*^{LKO} mice (n = 3) was used to detect the LoxP-flanked exon 2 of *Surf4*. One of the primers was located within exon 2 between the two LoxP sites. The PCR product was amplified only in the WT or floxed *Surf4* gene but not in *Surf4* gene knockout of exon 2. D–F: Body weight and fat and lean mass. About 14-week-old male and female *Surf4*^{FLOX} and *Surf4*^{LKO} mice on a regular chow diet were fasted for 10 h and then weighed (D, 10 mice per group). Fat (E) and lean mass (F) were measured using NMR (six mice per group).

4.2.2 Impact of lacking hepatic SURF4 on plasma lipid levels.

We then measured plasma lipid levels and found that the WT, *Surf4*^{Flox} and heterozygous *Surf4*^{LKO} mice showed similar levels of plasma TG, TC, HDL-C, and non-HDL-C (Figs. 4.2A to D). Conversely, both male and female homozygous *Surf4*^{LKO} mice exhibited a significant reduction in plasma levels of TC, HDL-C, non-HDL-C, and TG compared to *Surf4*^{Flox} mice (Figs. 4.2E to H). FPLC data showed that cholesterol and TG levels were reduced in all fractions, including VLDL, IDL/LDL, and HDL (Figs. 4.2I and J). Therefore, hepatic SURF4 played a vital role in regulating plasma cholesterol and TG levels in mice.

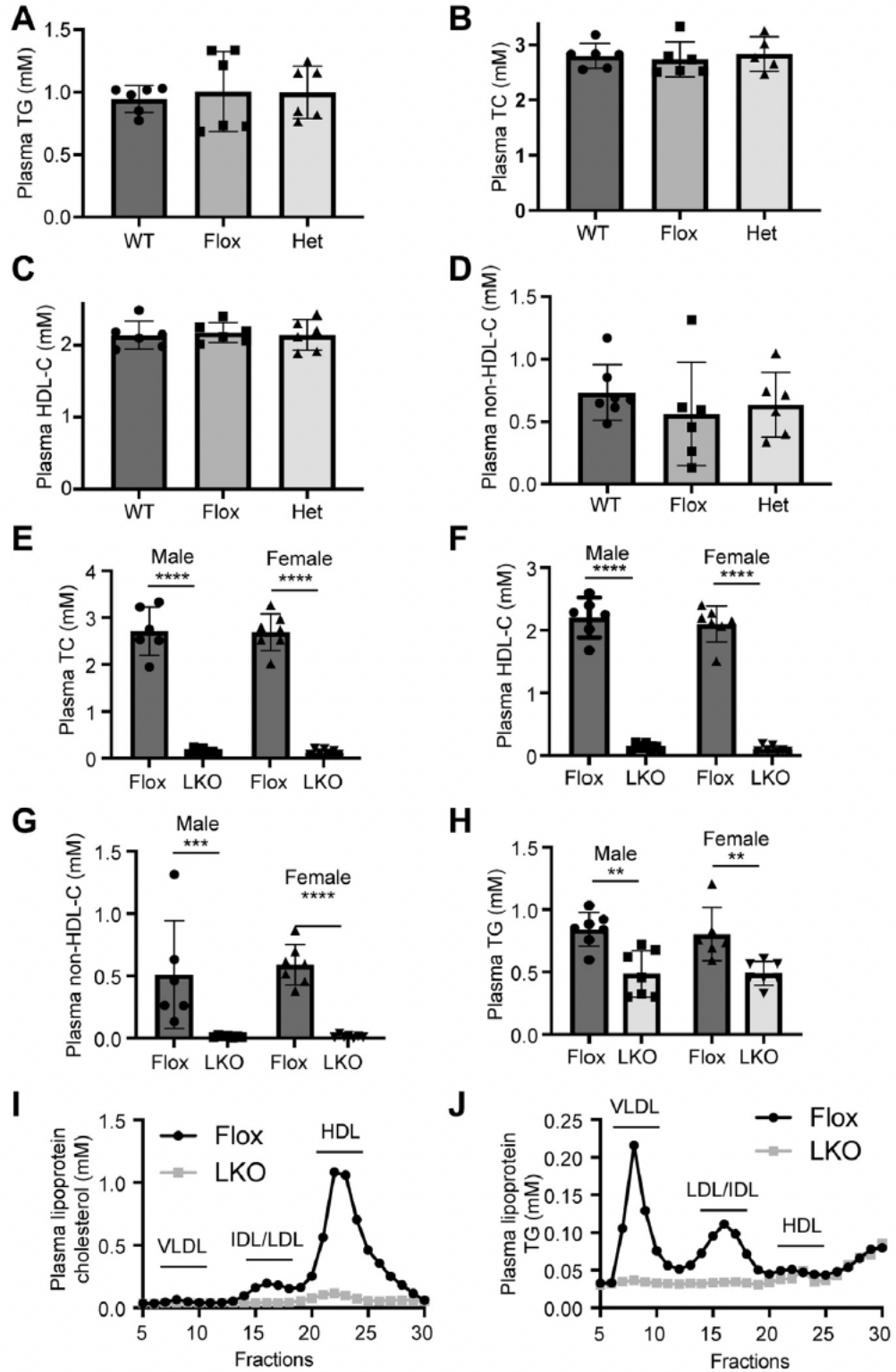


Figure 4.2. Impact of lacking hepatic SURF4 on plasma lipid levels. A–H: Plasma lipid levels.

About 10–14-week-old mice (WT, *Surf4*^{Flox} [Flox], heterozygous *Surf4*^{LKO} [Het], and homozygous

Surf4^{LKO} [LKO]) on a regular chow diet were fasted for 10 h. Lipids in fasting plasma were measured using their specific enzymatic kits ($n \geq 6$). Non-HDL-C was calculated by subtracting HDL-C from TC. I and J: Lipid profile. About 100 μ l of plasma from each mouse in the same group ($n = 6$) was pooled, applied to fast protein liquid chromatography, and then eluted at 1 ml/fraction. Cholesterol and TG in each fraction were measured using their specific kits. Student's t-test was used to determine the significant differences between groups. Values of all data were mean \pm SD. The significance was defined as *P < 0.05, **P < 0.01, ***P < 0.001, and ****P < 0.0001. ns, no significant difference.

4.2.3 Effects of SURF4 on apoB secretion.

Next, we dissected how SURF4 affected plasma lipid levels. Fasting plasma TG is mainly contributed by VLDL, a TG-rich lipoprotein produced mainly by the liver. SURF4 is a cargo receptor located in the ERES [123]. Was it possible that SURF4 directly mediated apoB and/or apoA-I secretion regulating plasma levels of LDL-C and HDL-C? To test this hypothesis, we knocked down the expression of *SURF4* in human hepatoma-derived cell lines, Huh7 and HepG2 that express and secrete both apoB and apoA-I. Two *SURF4* siRNAs efficiently reduced *SURF4* expression in whole cell lysate (Fig. 4.3A top, lanes 2 and 3 vs. 1; Fig. 4.3B and C). The levels of apoB100 and apoA-I in whole cell lysate were comparable in the control and *SURF4* knockdown cells. Conversely, knockdown of *SURF4* reduced the levels of apoB100 but not apoA-I or albumin in culture medium (Fig. 4.3A bottom, lanes 2 and 3 vs. 1; Fig. 4.3B and C). The finding on apoA-I was different from the results of *Surf4*^{LKO} mice, which showed a marked reduction in plasma levels of apoA-I. One possible explanation was that the expression of SURF4 was reduced about 60% in both Huh7 and HepG2 cells (Fig. 4.3B and C), while *Surf4* was essentially undetectable in hepatocytes of *Surf4*^{LKO} mice (Fig. 4.1B). The remaining SURF4 in the knockdown cells might be sufficient to mediate apoA-I secretion. We then examined if SURF4 interacted with apoB100 using co-immunoprecipitation. As shown in Fig. 4D, an anti-SURF4 antibody (1195Sa) but not the pre-immune serum (Pre) effectively pulled down SURF4 from whole cell lysate isolated from Huh7 (lane 2 vs. 3) and HepG2 cells (lane 3 vs. 2). apoB 100 was present only in the SURF4-IP sample, whereas TFR was undetectable in all immunoprecipitated samples, suggesting an interaction between SURF4 and apoB100. This finding was consistent with a previous report that SURF4 interacted with apoB and facilitated its secretion in HepG2 cells [123]. To further confirm this finding, we performed confocal microscopy in Huh7 cells using the anti-SURF4 polyclonal

antibody, 1195Sa, that could specifically detect SURF4 [147]. We observed that apoB and SURF4 exhibited a similar distribution pattern, residing primarily in the perinuclear region (Fig. 4.3E and F), where the two proteins were partially colocalized as shown in the merged panel (Fig. 4.3G, yellow). Therefore, SURF4 appeared to associate with apoB. Taken together, these findings suggest that the lack of hepatic SURF4 may impair VLDL secretion.

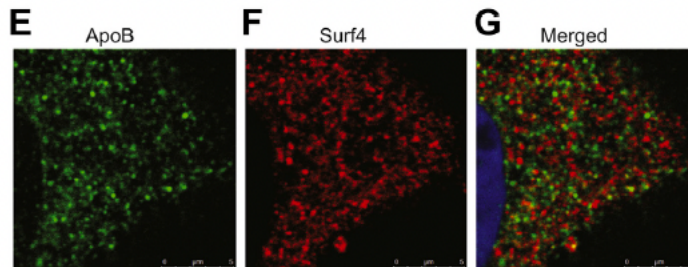
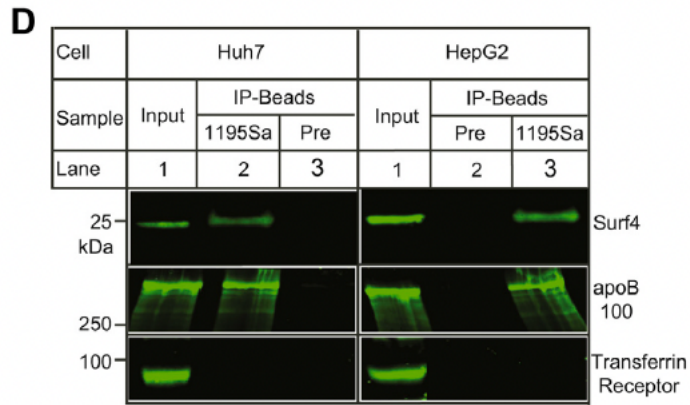
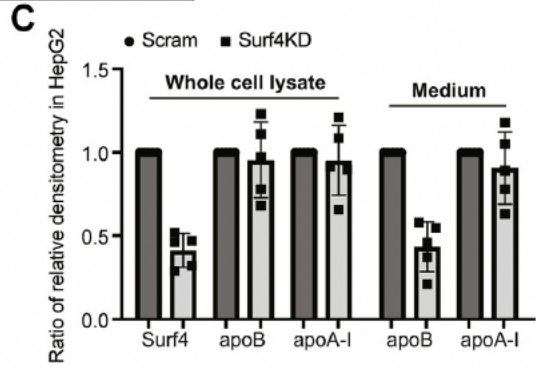
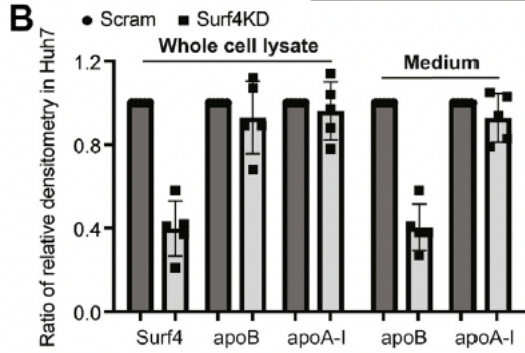
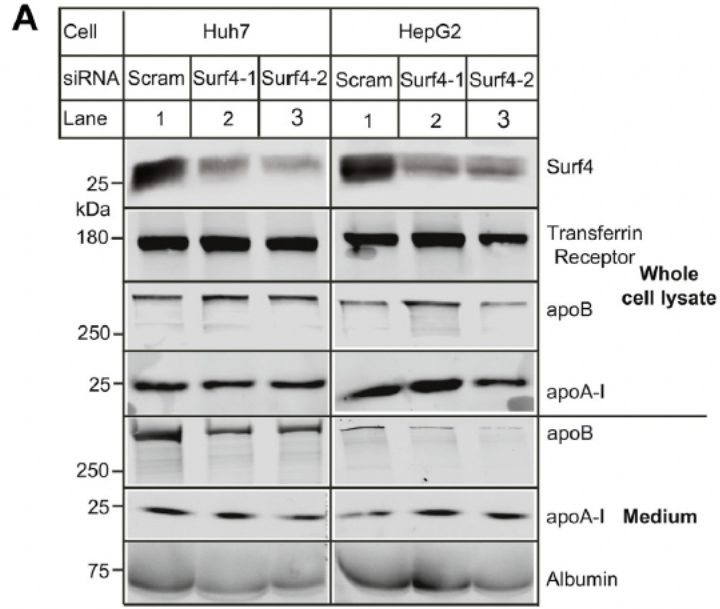


Figure 4.3. The effect of *SURF4* knockdown on the level of apoB and apoA-I in cultured cells.

A–C: Knockdown of *SURF4*. Huh7 and HepG2 cells were transfected with scrambled (Scram.) or one of the two *SURF4* siRNAs (Surf4-1 and Surf4-2). About 36 h after transfection, the cells were incubated with oleic acid for 4 h, washed, and then incubated in DMEM without FBS and oleic acid for 16 h. Whole cell lysate was prepared. Same amount of total proteins in whole cell lysate (top) and culture medium (bottom) was applied to Western blot using antibodies indicated. Similar results were obtained from at least five experiments. The relative densitometry was the ratio of the densitometry of target to that of TFR in whole cell lysate or albumin in medium in the same condition. The ratio of the relative densitometry was the ratio of the relative densitometry of the target in *SURF4* knockdown cells to that of the same target in the control cells transfected with scrambled siRNA. The relative densitometry of the target in the control cells was defined as 1. D: Coimmunoprecipitation. The same amount of whole cell lysate from Huh7 or HepG2 was incubated with the preimmunized serum (Pre) or a rabbit anti-SURF4 antibody (1195Sa) and protein-G agarose. Whole cell lysate (input) and immunoprecipitated proteins (IP-Beads) were applied to Western blot with antibodies indicated. Similar results were obtained from at least three more experiments. E–G: Confocal microscopy. Huh7 cells were fixed, permeabilized, and then incubated with a goat anti-apoB (abcam) and a rabbit anti-SURF4 antibody, followed by confocal microscopy; apoB (green), SURF4 (red), and DAPI (blue). An x–y optical section of the cells illustrates the cellular distribution of proteins (magnification: 325X). Representative images were shown.

4.2.4 Effects of *Surf4* deficiency on hepatic lipids

Our next experiments were to investigate whether impaired VLDL secretion caused lipid accumulation in the liver of *Surf4*^{LKO} mice. Both *Surf4*^{Flox} and *Surf4*^{LKO} mice showed similar hepatic TG and TC levels (Fig. 4.4A to B). Consistently, knockout of hepatic *Surf4* did not significantly alter liver weight or plasma ALT activity (Figs. 4.4C and D). Additionally, Oil Red O and H&E staining of liver sections and histological scores of lipid droplets, inflammation infiltration and ballooning were comparable in *Surf4*^{LKO} and *Surf4*^{Flox} mice (Figs. 4.4E and F). Thus, lacking hepatic *Surf4* did not cause hepatic lipid accumulation or significant liver damage.

We then examined protein levels of the key players involved in lipid metabolism in the liver. As shown in Figure 6A, the protein levels of SCD1, CPT1a and FASN were significantly decreased (Fig. 4.4G). Plasma levels of ketone body, β -hydroxybutyrate, in *Surf4*^{LKO} mice were reduced (Fig. 4.4H). Fatty acid oxidation was also significantly reduced in primary hepatocytes isolated from *Surf4*^{LKO} mice (Fig. 4.4I). Taken together, these findings indicated that fatty acid oxidation was reduced in the liver of *Surf4*^{LKO} mice and suggested that lacking hepatic *Surf4* might reduce *de novo* lipogenesis.

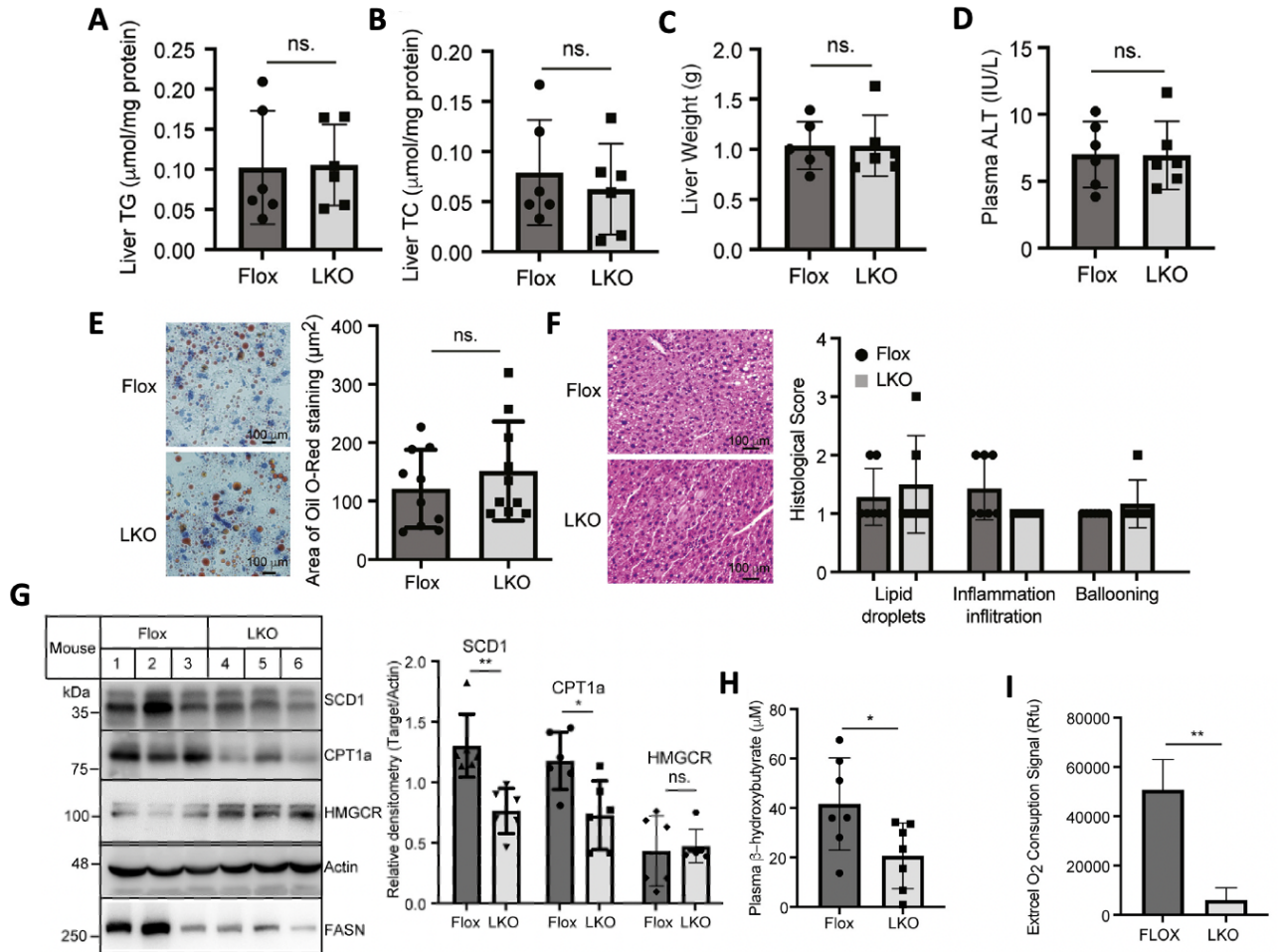


Figure 4.4. Effect of hepatic *Surf4* silencing on liver lipids and gene expression. About 12–14-week-old male *Surf4*^{Flox} and *Surf4*^{LKO} mice on a regular chow diet were fasted for 10 h before euthanasia. A and B: Liver lipids. Lipids were extracted from liver homogenate and then subjected to measurement of TG (A) and TC (B) using their specific enzymatic kits (n = 6). C: Weight of a whole liver (n = 6). D: Plasma ALT. ALT was measured according to the manufacturer's instruction (n = 6). E and F: Oil Red O (E) and H&E staining (F) of liver sections. The images were quantified using ImageJ (E) (10 mice per group). The slides of H&E staining were assessed for lipid droplets, inflammation infiltration, and ballooning blindly (F) (n \geq 6). G: Western blot of liver homogenate with antibodies indicated. The relative densitometry was the ratio of the densitometry of the protein indicated to that of actin (n = 6). Representative images were shown. H: Plasma ketone bodies were

measured using a kit (n = 7). I: FA oxidation. Primary hepatocytes isolated from *Surf4*^{Flox} or *Surf4*^{LKO} mice were subjected to measurement of FA oxidation using a commercial kit from abcam. Representative figures were shown. Student's t-test was used to determine the significant differences between groups. Values of all data were mean ± SD. The significance was defined as *P < 0.05, **P < 0.01, ***P < 0.001, and ****P < 0.0001. ns, no significant difference.

4.2.5 Effects of SURF4 on the development of atherosclerosis

Next, we investigated the effect of lacking hepatic *Surf4* on the development of atherosclerosis in *Ldlr*^{-/-} mice. Male *Ldlr*^{-/-} mice were injected with AAV-Scrambled or *Surf4* shRNA and then fed the Western-type diet for fourteen weeks. As shown in Figure 4.5A, AAV-*Surf4* shRNA efficiently reduced *Surf4* mRNA levels by approximately 61% but did not affect the mRNA level of *apoB* in mouse liver. *Surf4* silencing markedly reduced TG secretion (Fig. 4.5B) and plasma levels of apoB100 and apoB48, but not apoA-I. (Fig. 4.5C). On the other hand, the levels of apoB100, apoB48 and apoA-I were comparable in liver homogenate of the control and *Surf4* knockdown mice (Fig. 4.5D). Plasma levels of TG, TC, non-HDL-C, but not HDL-C were significantly reduced in *Surf4* knockdown mice (Figs. 4.5E to H). Consistently, FPLC data showed that cholesterol levels were dramatically reduced in both VLDL and LDL fractions, but not HDL of *Surf4* knockdown mice (Fig. 4.5I). *Surf4* silencing also reduced plasma TG levels in both VLDL and LDL fractions (Fig. 4.5J). We then examined if *Surf4* knockdown caused liver damage in *Ldlr*^{-/-} mice. As shown in Figures 4.6A to E, the levels of liver TG and TC, plasma ALT activity, liver and body weight were comparable in the control and *Surf4* knockdown mice. Western blot analysis revealed that knockdown of *Surf4* reduced the protein levels of SCD1 but not HMGCR or CPT1a (Fig. 4.6F). Thus, knockdown of *Surf4* in *Ldlr*^{-/-} mice significantly reduced plasma levels of cholesterol and TG but did not cause hepatic lipid accumulation or significant liver damage.

Next, we examined the effect of *Surf4* silencing on the development of atherosclerosis and found that *Ldlr*^{-/-} mice injected with AAV-scrambled shRNA formed plaques in the aortic arch, which were virtually eliminated in *Surf4* knockdown mice (Figs. 4.6G and H). Oil-red O staining of the aorta consistently showed a significant reduction in lesion area in the aorta of *Surf4* knockdown mice (Fig. 4.6I; 9.4% in the control and 1% in the *Surf4* knockdown group, p<0.0001).

Average atherosclerotic lesion areas in the aortic sinus were also dramatically reduced in mice injected with AAV-*Surf4* shRNA (0.4683 mm² and 0.02594 mm² in AAV-Scrambled and *Surf4* shRNA injected mice, respectively, p=0.0089) (Fig. 4.6J). Thus, knockdown of *Surf4* markedly reduced the development of atherosclerosis in *Ldlr*^{-/-} mice.

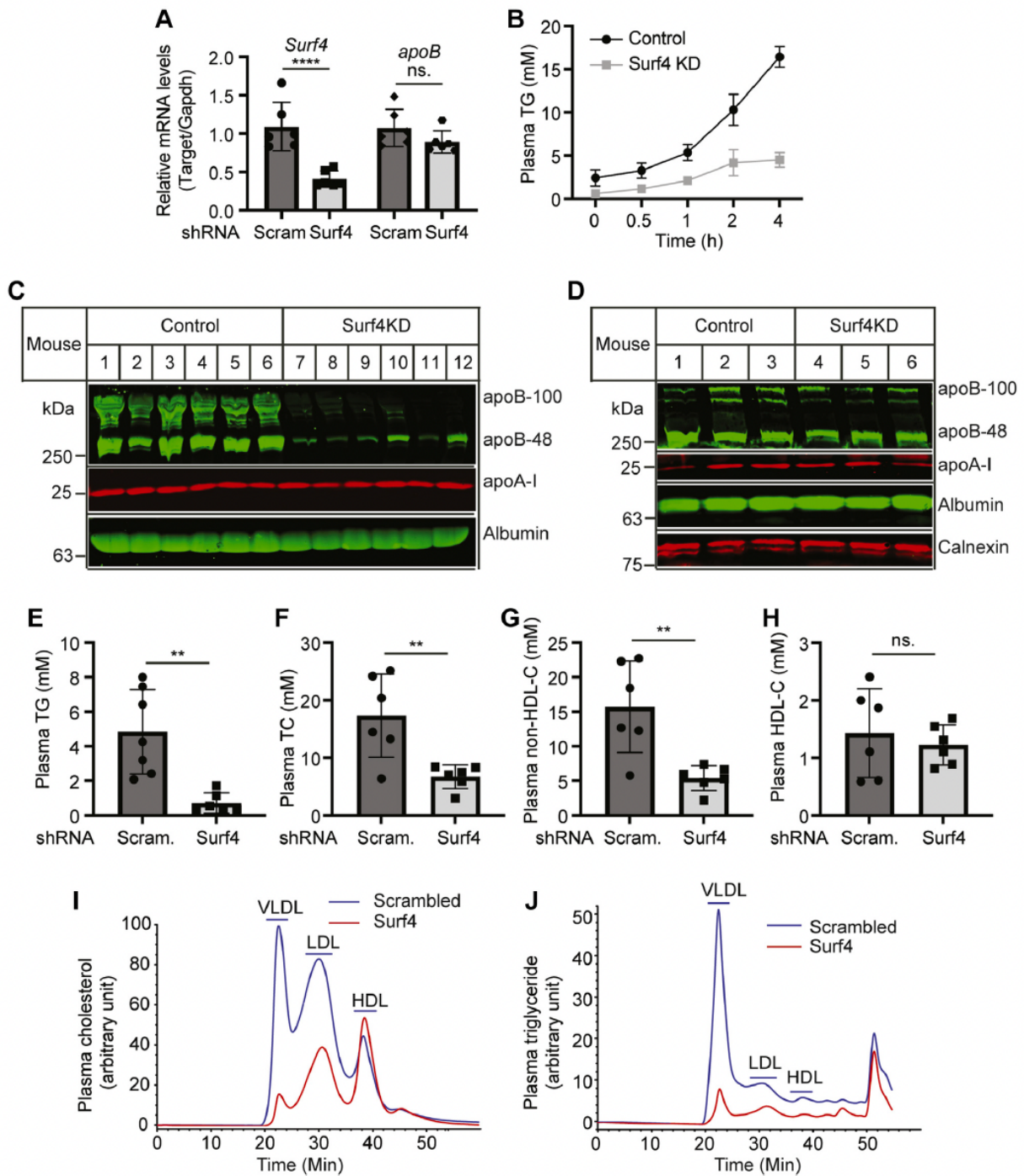


Figure 4.5. The effect of *Surf4* knockdown on plasma lipid levels and the expression of apoB and apoA-I in *Ldlr*^{-/-} mice. About 8–10-week-old male *Ldlr*^{-/-} mice were injected with AAV-scrambled (Scram.) or *Surf4* shRNA and then fed the Western-type diet for 14 weeks. A: Quantitative real-time PCR. The relative mRNA levels were the ratio of the mRNA levels of the

target gene to that of *Gapdh* (n = 6). B: TG secretion. Blood was collected from mice before and 0.5, 1, 2, and 4 h after P-407 injection. Plasma TG was measured using a kit (Wako Diagnostics) (n = 4). C and D: Immunoblotting of the same amount of plasma (C) or liver homogenate (D) with antibodies indicated (n = 6). Representative images were shown. E–H: Plasma lipids were measured using kits (Wako Diagnostics) (n = 6). I and J: Lipid profile. About 5 μ l of plasma from each mouse in the same group (n = 6) was pooled and applied to fast protein liquid chromatography analysis of cholesterol (I) and TG (J). Student's t-test was used to determine the significant differences between groups. Values of all data were mean \pm SD. The significance was defined as *P < 0.05, **P < 0.01, ***P < 0.001, and ****P < 0.0001. P > 0.05, no significant difference (ns).

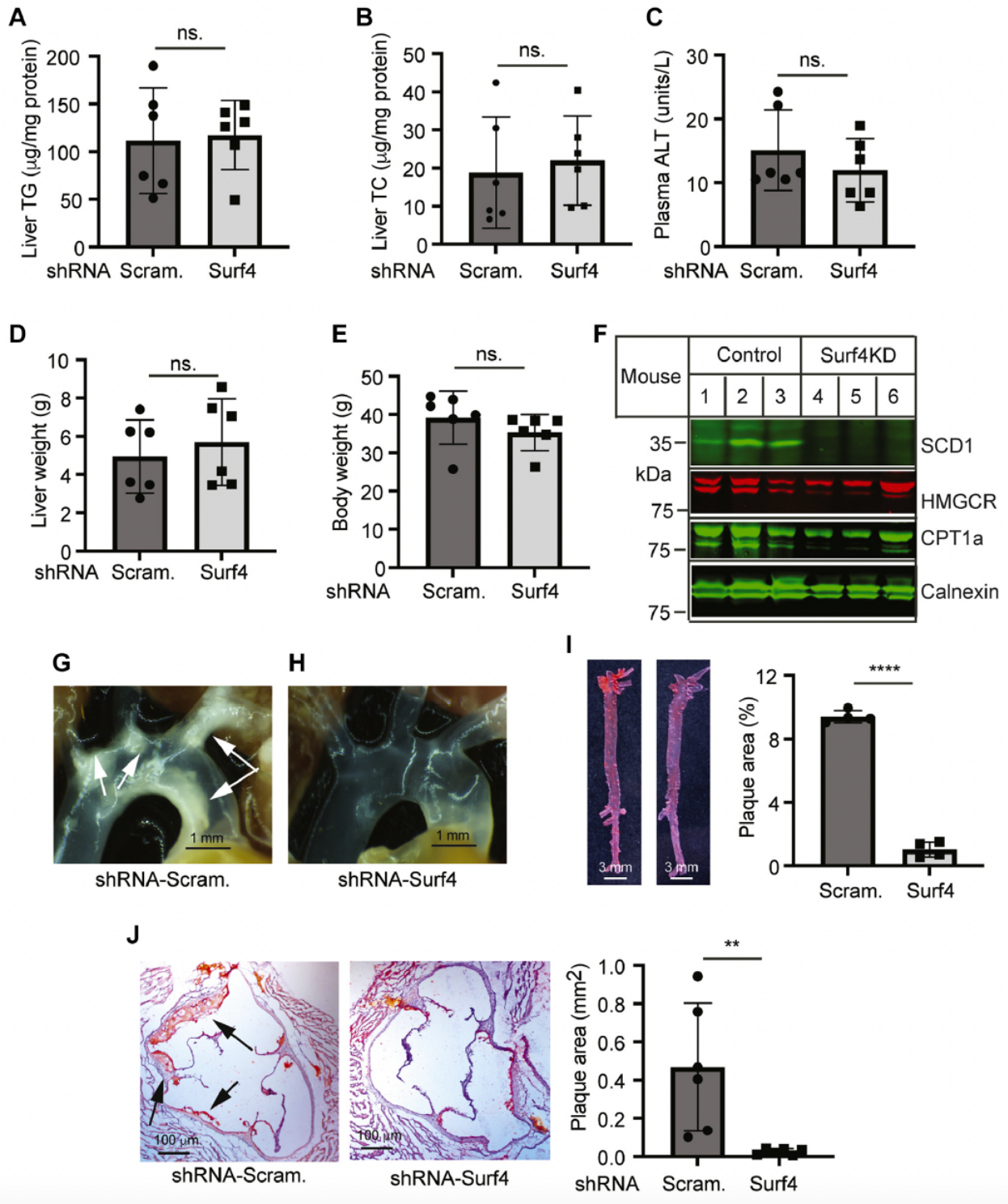


Figure 4.6. The effect of *Surf4* knockdown on the levels of liver lipids and the development of atherosclerosis in *Ldlr*^{-/-} mice. Mice were treated as described in the legend to Fig. 4.5. A and B: Liver lipids were extracted from mouse livers for the measurement of TG (A) and TC (B) using

enzymatic kits (Wako Diagnostics) (six mice per group). C: Plasma ALT measured with a kit (Cayman Chemical Company). D and E: Liver and body weight of mice (six mice per group). F: Immunoblotting of the same amount of liver homogenate from the control and *Surf4* knockdown mice (six mice per group) with antibodies indicated. Representative images were shown. G–H: Representative images of aortic arches. Similar results were observed in five more mice in each group. I and J: Oil Red O staining of the aorta (I, four mice per group) and heart sections (J, six mice per group). Magnification, 40X. Atherosclerotic lesions in the aorta and aortic sinus were quantified using OMAX ToupView. Representative figures were shown. Student's t-test was used to determine the significant differences between groups. Values of all data were mean \pm SD. The significance was defined as *P < 0.05, **P < 0.01, ***P < 0.001, and ****P < 0.0001. P > 0.05, no significant difference (ns).

4.3 Discussion

VLDL, a TG-enriched lipoprotein mainly produced in and secreted from the liver, is catabolized to LDL in the circulatory system. Inhibition of VLDL secretion can significantly reduce plasma levels of LDL-C and alleviate the development of atherosclerosis. VLDL is transported from the ER to the Golgi apparatus through VTV [9]. However, how VLDL is recruited from the ER lumen to VTV is unclear. Our findings indicate that SURF4 may recruit VLDL from the ER lumen to VTV for the subsequent delivery to the Golgi apparatus. However, SURF4 was not required for PCSK9 secretion *in vivo*.

When this work was being prepared for publication, Wang et al. reported that a variance in *Surf4*, rs3758348, was significantly associated with reduced plasma levels of TC and LDL-C in humans [133]. Consequently, they reported that knockout of hepatic *Surf4* using CRISPR-Cas9 significantly reduced plasma levels of cholesterol and TG and reduced the development of atherosclerosis in a mouse model of hypercholesterolemia induced by overexpressing PCSK9. We and Wang et al. both found that plasma ALT levels were comparable in the control and *Surf4* silencing mice. However, there were several differences between our findings and theirs. First, we found that the lack of hepatic *Surf4* did not cause TG and cholesterol accumulation in the liver. We confirmed these findings using various methods: oil-red O staining and measurement of liver lipids using enzymatic kits. Conversely, Wang et al. reported that knockdown of *Surf4* in their mouse model significantly increased liver TG and cholesterol levels. They also knocked down *Surf4* expression by administering AAV-TBG-Cre to *Surf4*^{Flox} mice and reported that liver TG but not cholesterol levels were increased in the *Surf4* knockdown mice. Second, Wang et al. reported that plasma cholesterol levels were reduced in heterozygous *Surf4* liver knockout mice. However, we observed that haplodeficiency of hepatic *Surf4* did not significantly affect plasma levels of

cholesterol and TG. Our findings were consistent with a recent report that plasma cholesterol and TG levels were comparable in heterozygous *Surf4* global knockout mice and the WT mice [134]. It is possible that the levels of SURF4 expressed from one copy of the *Surf4* gene is enough to mediate VLDL secretion. Third, Wang et al. claimed that SURF4 mediated secretion of lipoproteins apoA-I and apoB. We also observed that plasma levels of HDL were significantly reduced in *Surf4*^{LKO} mice. However, knockdown of *SURF4* in cultured human hepatocytes did not affect apoA-I secretion. Plasma apoA-I and HDL cholesterol levels were also comparable in the control and *Surf4* knockdown *Ldlr*^{-/-} mice. The reasons for these differences were unclear. Different approaches were used in the two studies to silence *Surf4* expression in mouse liver. We bred *Surf4*^{Flox} mice with Alb-Cre mice to delete functional *Surf4* specifically in hepatocytes. *Surf4* was knocked out perinatally. Wang et al. administered Cre-dependent spCas9 knock-in (KI) mice with AAV-*Surf4* gRNAs to knock down *Surf4* expression in the liver of adult mice. It is also possible that the knockdown efficiency of *Surf4* might be different in the two studies, causing the different phenotypes.

The reduction in fasting plasma levels of LDL-C and apoB100 was most likely caused by impaired VLDL secretion. The exact mechanism by which plasma HDL-C levels were reduced is unclear. In *Surf4*^{LKO} mice, plasma HDL-C (Fig. 2F) were significantly reduced. These findings were consistent with the report from Wang et al. [133] and indicated that SURF4 might also mediate apoA-I secretion. However, knockdown of *SURF4* in Huh7 and HepG2 cells did not significantly affect the level of apoA-I in whole cell lysate and culture medium (Fig. 4A, B and C). Similarly, knockdown of *Surf4* expression in *Ldlr*^{-/-} mice did not significantly affect the level of apoA-I in plasma (Fig. 7C) and liver homogenate (Fig. 7D). Knockdown of *Surf4* in *Ldlr*^{-/-} mice also did not affect plasma levels of HDL-C even though non-HDL cholesterol levels were markedly reduced

(Fig. 7G, H and I). One main difference between *Surf4*^{LKO} mice and the knockdown experiments was that hepatic SURF4 was essentially undetectable in *Surf4*^{LKO} mice (Fig. 1B), while the expression of *Surf4* was only partially reduced in cultured cells and *Ldlr*^{-/-} mice (Fig. 4A, B and C and Fig. 7A). Similarly, the *Surf4* variant, rs3758348 that reduced *Surf4* expression, significantly reduced plasma TC and LDL-C but not HDL-C levels in humans [133]. Thus, the remaining SURF4 in the knockdown experiments might still be able to facilitate secretion of apoA-I effectively.

Hepatic TG homeostasis is regulated by *de novo* lipogenesis, fatty acid uptake, fatty acid oxidation and VLDL secretion. Inhibition of apoB and MTP impaired VLDL production and increased hepatic TG, leading to liver steatosis [169, 174-176]. On the other hand, Conlon et al. reported that knockdown of apoB for 6 weeks did not cause liver steatosis even though a mild lipid accumulation was observed at 3 weeks after apoB knockdown [170]. Similarly, our findings showed that VLDL secretion was impaired and fatty acid oxidation was reduced in *Surf4*^{LKO} mice, and yet we did not observe significant hepatic TG accumulation or notable liver damage. It has been reported that *de novo* lipogenesis was a key contributor to fatty liver and was increased significantly in subjects with non-alcoholic fatty liver disease [177]. The levels of SCD1, a rate-limiting enzyme in converting saturated FAs to monounsaturated FAs in *de novo* lipogenesis, was significantly reduced in the liver of *Surf4*^{LKO} mice and *Surf4* knockdown *Ldlr*^{-/-} mice. This finding indicated a reduction in *de novo* lipogenesis, which might partially explain why liver TG levels were not increased in *Surf4*^{LKO} mice. It also explained the reduction in the expression of *PPAR-α* target genes and plasma levels of ketone bodies because *de novo* lipogenesis provides endogenous ligands for activating *PPAR-α* transcriptional activity to upregulate expression of genes involved in fatty acid β-oxidation [178]. Of note, *de novo* lipogenesis is an important contributor to fatty liver in hyperinsulinemia and insulin resistance, but not to hepatic TG levels under normal

physiological conditions [179]. Conlon et al. reported that knockdown of apoB100 in mice caused accumulation of lipid droplets in the ER lumen of hepatocytes, which triggered ER autophagy, effectively removing TG accumulated in mouse hepatocytes [170]. Furthermore, it has been reported that apoB accumulated in the ER lumen of hepatocytes increased autophagy, leading to resolution [180]. The levels of plasma apoB were markedly reduced in *Surf4*^{LKO} mice (Fig. 3B), however, we did not observe a significant increase in hepatic apoB levels (Fig. 3E). Therefore, autophagy may play a role in clearing apoB and TG retained in the liver of *Surf4*^{LKO} mice. The lack of hepatic *Surf4* might also affect metabolic rate, and hepatic fatty acid uptake and phospholipid metabolism. Experiments are undergoing to investigate these possibilities.

In summary, we provided evidence for the physiological role of Surf4, which mediates VLDL secretion. Inhibition of hepatic Surf4 reduced VLDL secretion and the development of atherosclerosis. These findings were consistent with the recent report from the Chen group [133]. Wang et al. also reported that SURF4 interacted with SAR1B to facilitate the transport of VLDL from the ER to the Golgi [133]. Therefore, secretion of VLDL appears to require the formation of VLDL transport vesicles with the help of COPII, TANGO1, SAR1B, KLH12, and SURF4 as indicated by Ginsberg et al. [10]. Interestingly, inhibition of hepatic *Surf4* did not cause hepatic lipid accumulation or notable liver damage in mice fed a regular chow diet or *Ldlr*^{-/-} mice fed the Western-type diet, even when VLDL secretion was impaired. Furthermore, despite that HDL was significantly reduced in *Surf4*^{LKO} mice, knockdown of *SURF4* expression in cultured human hepatocytes and *Ldlr*^{-/-} mice had no significant effect on apoA-I secretion and plasma HDL-C levels. Thus, our findings indicate that SURF4-based therapy can potentially lower plasma LDL-C levels by inhibiting VLDL secretion and subsequent LDL production, thereby reducing the risk of atherosclerosis for patients who are intolerant to or cannot be effectively managed by existing

therapies.

Chapter 5 Manuscript III

The role of hepatic *Surf4* in lipoprotein metabolism and the development of atherosclerosis in *apoE*^{-/-} mice

(Biochimica et Biophysica Acta- Molecular and Cell Biology of Lipids. 2022 July; 1867(10): 159196.)

All experiments were conducted and analyzed by Yishi Shen in Zhang's Lab

**The role of hepatic *Surf4* in lipoprotein metabolism and the development of atherosclerosis
in *apoE*^{-/-} mice**

Yishi Shen^a, Hong-mei Gu^a, Lei Zhai^b, Binxiang Wang^b, Shucun Qin^{b*}, Da-wei Zhang^{a*}

^aGroup on the Molecular and Cell Biology of Lipids and Department of Pediatrics, Faculty of Medicine and Dentistry, University of Alberta, Edmonton, Alberta, Canada. ^bInstitute of Atherosclerosis in Shandong First Medical University (Shandong Academy of Medical Sciences), Taian, China

Running title: Surf4 and atherosclerosis

Keywords: VLDL secretion, cargo receptor, PCSK9, shRNA knockdown, lipid metabolism, chylomicron remnant, LDL.

Abstract

Elevated plasma levels of LDL-C increase the risk of atherosclerotic cardiovascular disease. Circulating LDL is derived from VLDL metabolism and cleared by LDLR. We have previously demonstrated that cargo receptor SURF4 mediates VLDL secretion. Inhibition of hepatic *Surf4* impairs VLDL secretion, significantly reduces plasma LDL-C levels, and markedly mitigates the development of atherosclerosis in *Ldlr*^{-/-} mice. Here, we investigated the role of SURF4 in lipoprotein metabolism and the development of atherosclerosis in another commonly used mouse model of atherosclerosis, apolipoprotein E knockout (*apoE*^{-/-}) mice. Adeno-associated viral shRNA was used to silence *Surf4* expression mainly in the liver of *apoE*^{-/-} mice. In *apoE*^{-/-} mice fed a regular chow diet, knockdown of *Surf4* expression significantly reduced TG secretion and plasma levels of non-HDL cholesterol and TG without causing hepatic lipid accumulation or liver damage. When *Surf4* was knocked down in *apoE*^{-/-} mice fed the Western-type diet, we observed a significant reduction in plasma levels of non-HDL cholesterol, but not TG. Knockdown of *Surf4* did not increase hepatic cholesterol and TG levels or cause liver damage, but significantly diminished atherosclerosis lesions. Therefore, our findings indicate the potential of hepatic SURF4 inhibition as a novel therapeutic strategy to reduce the risk of atherosclerotic cardiovascular disease.

5.1 Introduction

ASCVD is one of the leading causes of mortality worldwide. Elevated plasma LDL-C levels significantly increase the risk of ASCVD [28, 181]. LDLR is primarily responsible for plasma LDL clearance [27]. Mutations in LDLR cause FH, characterized by increased plasma LDL-C levels and risk of premature coronary heart disease [182]. Statins and PCSK9 inhibitors increase hepatic LDLR levels and reduce cardiovascular events [183]. However, these treatments are not effective in controlling plasma LDL-C levels in patients with homozygous FH who carry loss-of-function mutations in LDLR [167].

Circulating LDL concentrations are determined by LDL clearance and production. LDL is produced through metabolism of VLDL, a TG-rich lipoprotein exclusively secreted by hepatocytes. Newly synthesized apoB100 is cotranslationally lipidated by MTP to form nascent VLDL particles, followed by core lipidation via fusion with TG-rich particles in the ER lumen. VLDL particles are subsequently transported to the Golgi apparatus for further modifications and then secretion into the circulation [172, 184]. Inhibition of VLDL secretion can significantly reduce plasma levels of LDL-C and ameliorate the development of atherosclerosis [10, 84, 135, 168, 169]. However, Mipomersen, an antisense oligonucleotide (ASO) targeting apoB100, and Lomitapide, a small inhibitor of MTP, can lead to several side effects, such as liver steatosis [78, 185]. Thus, there is a need to investigate alternative targets that can reduce VLDL secretion without causing severe side effects.

VLDL is too large to fit into the classic COP II vesicle for transport to the Golgi apparatus; instead, it utilizes specific VTV. Several key players have been identified in the formation of VTV, such as TANGO1 and SAR1B [9, 10, 16]. Recently, we and others demonstrated that SURF4, a cargo receptor in the ER membrane, facilitates VLDL secretion from hepatocytes [133, 154].

Furthermore, we found that knockout of hepatic *Surf4* significantly impaired VLDL secretion and reduced plasma TG and cholesterol levels, but did not lead to lipid accumulation in the liver. We also observed that knockdown of hepatic *Surf4* dramatically reduced the development of atherosclerosis without causing notable liver damage in *Ldlr*^{-/-} mice [154].

Ldlr^{-/-} mice are one of the commonly used mouse models of atherosclerosis. Lack of LDLR increases circulating LDL-C levels and promotes the development of atherosclerosis. On the other hand, *apoE*^{-/-} mice have impaired clearance of apoE-containing lipoprotein particles, such as chylomicron and VLDL remnants, which promotes the development of atherosclerosis [186]. apoE also exerts anti-atherogenic effects in a lipoprotein-independent manner [187-189]. It has been reported that the same pathway or targets may have different effects on the development of atherosclerosis in the two mouse models. For example, knockout of hepatic lipase increases and reduces atherosclerotic lesions in *Ldlr*^{-/-} and *apoE*^{-/-} mice, respectively [190-192]. On the other hand, deficiency of SR-BI accelerates the development of atherosclerosis in both *Ldlr*^{-/-} and *apoE*^{-/-} mice [193, 194]. Gene knockdown imitates the effect of drugs that generally modulate but do not completely inhibit activity of their targets, and AAV-shRNA can reduce expression of genes, with long-term high efficacy in a single dose, and is widely used in clinical trials [195, 196]. Therefore, to further determine the potential of hepatic SURF4 inhibition as a lipid-lowering strategy, we used AAV-shRNA to inhibit *Surf4* expression mainly in the liver of *apoE*^{-/-} mice. We found that silencing of hepatic *Surf4* decreased plasma non-HDL cholesterol levels and atherosclerotic lesions in *apoE*^{-/-} mice. However, inhibition of SURF4 did not cause significant hepatic lipid accumulation or notable liver damage.

5.2 Results

5.2.1 Role of hepatic SURF4 in lipoprotein metabolism in *apoE*^{-/-} mice on a regular chow diet

To investigate the role of hepatic SURF4 in lipid metabolism in *apoE*^{-/-} mice, we used AAV DJ8-shRNA to silence *Surf4* primarily in mouse liver since the AAV-DJ8 subtype primarily transduces the liver, with nonhepatic tissues, such as the intestine and kidneys only transduced at very high viral doses and to a much lesser extent [197]. We introduced AAV-scrambled or *Surf4*-shRNA into male and female *apoE*^{-/-} mice and then fed mice with a chow diet for 4 weeks. As shown in Figure 5.1A, body weight was comparable in the two groups. AAV-*Surf4*-shRNA significantly reduced the mRNA level of *Surf4* in the liver (Figure 5.1B), but not in other tissues tested, including the heart, lung, kidneys and intestine (Figure 5.1C). Consequently, SURF4 protein levels in the liver homogenate were significantly reduced in *apoE*^{-/-} mice administered AAV-*Surf4* shRNA (Figures 5.1D and E). We then measured plasma lipid levels and found that compared to control mice, *Surf4*-shRNA injected *apoE*^{-/-} mice exhibited a significant reduction in plasma levels of TG and TC but did not have any significant changes in plasma HDL-C levels (Figures 5.1F to H). Fast protein liquid chromatography (FPLC) analysis of lipoprotein cholesterol revealed that cholesterol levels in the fractions of chylomicron remnants/VLDL and IDL/LDL were all reduced in *Surf4* knockdown mice compared to the control group (Figure 5.1 I). Therefore, inhibition of hepatic *Surf4* reduces plasma non-HDL cholesterol and TG levels in *apoE*^{-/-} mice.

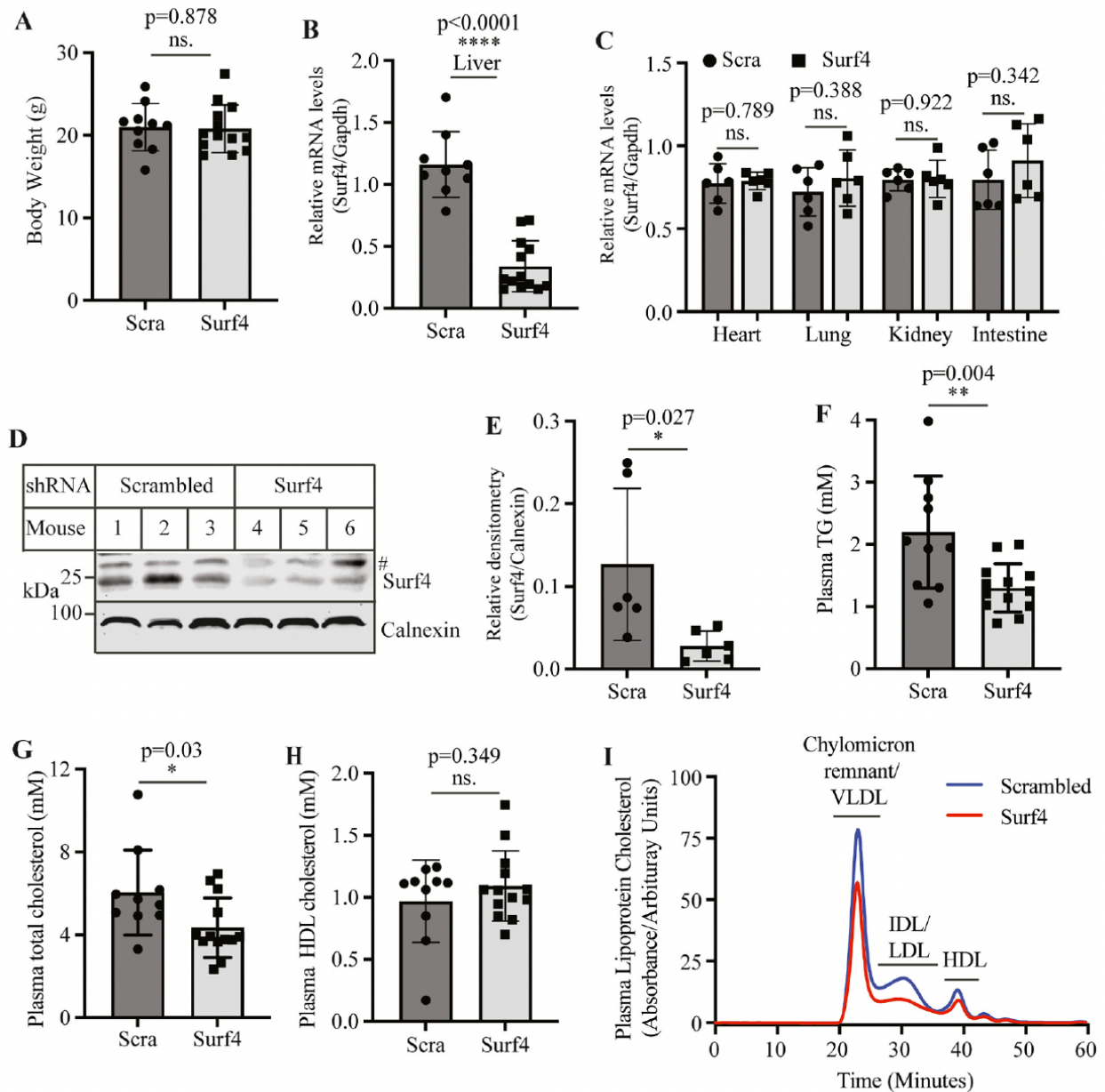


Figure 5.1. Effect of hepatic *Surf4* silencing on plasma lipid levels. *apoE*^{-/-} mice (10-14 weeks old) were injected with AAV-scrambled (Scra, 6 females and 4 males) or *Surf4* shRNA (7 females and 6 males) and then fed the chow diet for 4 weeks. **(A)** Body weight. Mice were fasted for 10 h and then weighed. **(B and C)** qRT-PCR. Total RNAs were isolated from different tissues of mice (males and females) fasted for 10 h and then subjected to qRT-PCR. The relative mRNA levels were the ratio of the mRNA levels of target genes to that of *Gapdh* in the same mouse ($n \geq 6$). **(D)**

and E) Western blot. Equal amount of homogenate prepared from the liver of fasted mice was applied to immunoblotting to detect SURF4. Representative images were shown (D). #, non-specific band. The relative densitometry was the ratio of the densitometry of SURF4 to that of calnexin in the same mouse (E, n=6, 3 males and 3 females in each group). **(F to H)** Plasma lipids. Plasma was isolated from blood samples collected from mice fasted for 10 h. Plasma TG (F), total cholesterol (G) and HDL cholesterol (H) levels were measured using their specific enzymatic kits (n ≥ 10). **(I)** Cholesterol profile of plasma lipoproteins. 5 µl of plasma from each mouse in the same group (n = 6, 3 males and 3 females in each group) was pooled and applied to FPLC analysis of cholesterol. Student's t-test was used to determine the significant difference between two groups. Values of all data were mean ± SD. The significance was defined as *P < 0.05, **P < 0.01, and ****P < 0.0001. P > 0.05, no significant difference (ns).

Next, we investigated whether deficiency of hepatic *Surf4* reduced TG secretion. Mice (both males and females) were fasted for 10 h and then injected with P-407 to inhibit LPL, and then plasma TG levels were measured at various time points. As shown in Figure 5.2A, plasma TG levels in control mice were increased from 4.54 mM (1-h time point) to 7.95 mM (2-h time point) and then 13.52 mM (4-hr time point). However, TG levels were increased much less in *Surf4* knockdown mice, from 3.86 mM (1-h) to 4.83 mM (2-h time point) and 6.9 mM (4-h time point). Furthermore, consistent with our previous findings in *Ldlr*^{-/-} mice [154], plasma apoB100 levels were significantly reduced in *Surf4* knockdown mice (Figures 5.2B and C). Conversely, knockdown of hepatic *Surf4* did not significantly affect plasma levels of apoB48 that can be produced by the liver and the intestine in mice. Purcell-Huynh et al. reported that high-fat feeding increased hepatic production of human apoB48 but not apoB100 in human apoB transgenic mice. The levels of mouse apoB48 were also increased and detected in LDL-sized particles in mice fed a high-fat diet [198]. Therefore, plasma apoB48 in *apoE*^{-/-} mice is probably contributed by intestine-derived chylomicron remnants and hepatic-produced apoB48 particles due to impaired clearance [199]. In addition, plasma apoA-I levels were comparable in the two groups (Figures 5.2B and C), consistent with no significant change in plasma HDL-C levels (Figure 5.1H). Taken together, these findings suggest that deficiency of *Surf4* in the liver of *apoE*^{-/-} mice appears to impair VLDL secretion.

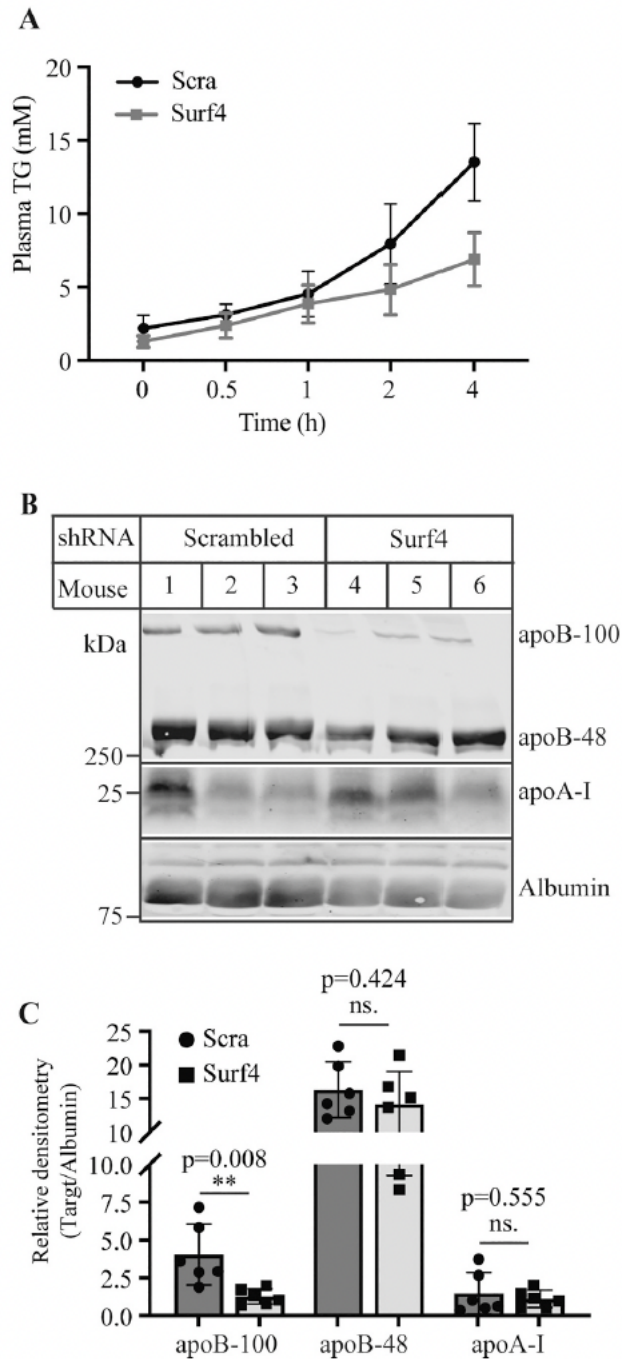


Figure 5.2. Effect of hepatic SURF4 deficiency on TG secretion. *apoE*^{-/-} mice (10-14 weeks old) were injected with AAV-scrambled (Scra) or *Surf4* shRNA, fed the chow diet for 4 weeks, and then fasted for 10 h prior to experiments. **(A)** TG secretion. Blood samples were collected from mice before (0) and 0.5, 1, 2, and 4 h after P-407 injection. Plasma TG levels were measured using a kit

(Wako Diagnostics) (n=6, 3 males and 3 females in each group). **(B and C)** Western blot. Equal amount of plasma from mice injected with AAV-scrambled (Scra) or *Surf4* shRNA was applied to SDS-PAGE (6% for apoB and 10% for apoA-I and Albumin) and immunoblotting. Representative images were shown (B). The relative densitometry was the ratio of the densitometry of the protein indicated to that of Albumin in the same mouse (C, n = 6, 3 males and 3females in each group). Student's t-test was used to determine the significant difference between two groups. Values of all data were mean \pm SD. The significance was defined as **P < 0.01 and P > 0.05, no significance (ns).

5.2.2 Impact of hepatic *Surf4* silencing on the liver in *apoE*^{-/-} mice on a regular chow diet

We then examined whether SURF4 deficiency could lead to significant liver damage. As shown in Figure 5.3A, knockdown of hepatic *Surf4* did not significantly change plasma ALT activity. H&E staining of liver sections was also similar in mice administered AAV-scrambled or *Surf4* shRNA (Figure 5.3B). We then assessed the mRNA levels of genes encoding important factors in lipid metabolism, including *apoB*, *Srebp1c*, *Fasn*, *Srebp2*, *Hmgcr*, *Ppar-α*, and *Cpt1a*. *Srebp1c*, *Srebp2*, and *Ppar-α* are transcriptional factors that upregulate transcription of genes involved in *de novo* lipogenesis, cholesterol biosynthesis, and fatty acid β-oxidation, respectively, and FASN, HMGCR, and CPT1a are rate-limiting enzymes in *de novo* lipogenesis, cholesterol biosynthesis, and fatty acid β-oxidation, respectively. We observed no significant difference in the mRNA levels of these genes and the protein levels of apoB100, apoB48, FASN, HMGCR, and CPT1a in the liver of the control and *Surf4*-knockdown mice (Figures 5.3C to E). TG and TC levels were also comparable in the liver of mice administered AAV-scrambled or *Surf4* shRNA (Figures 5.3F and G). Therefore, deficiency of hepatic SURF4 does not result in hepatic lipid accumulation or notable liver damage in *apoE*^{-/-} mice fed a regular chow diet.

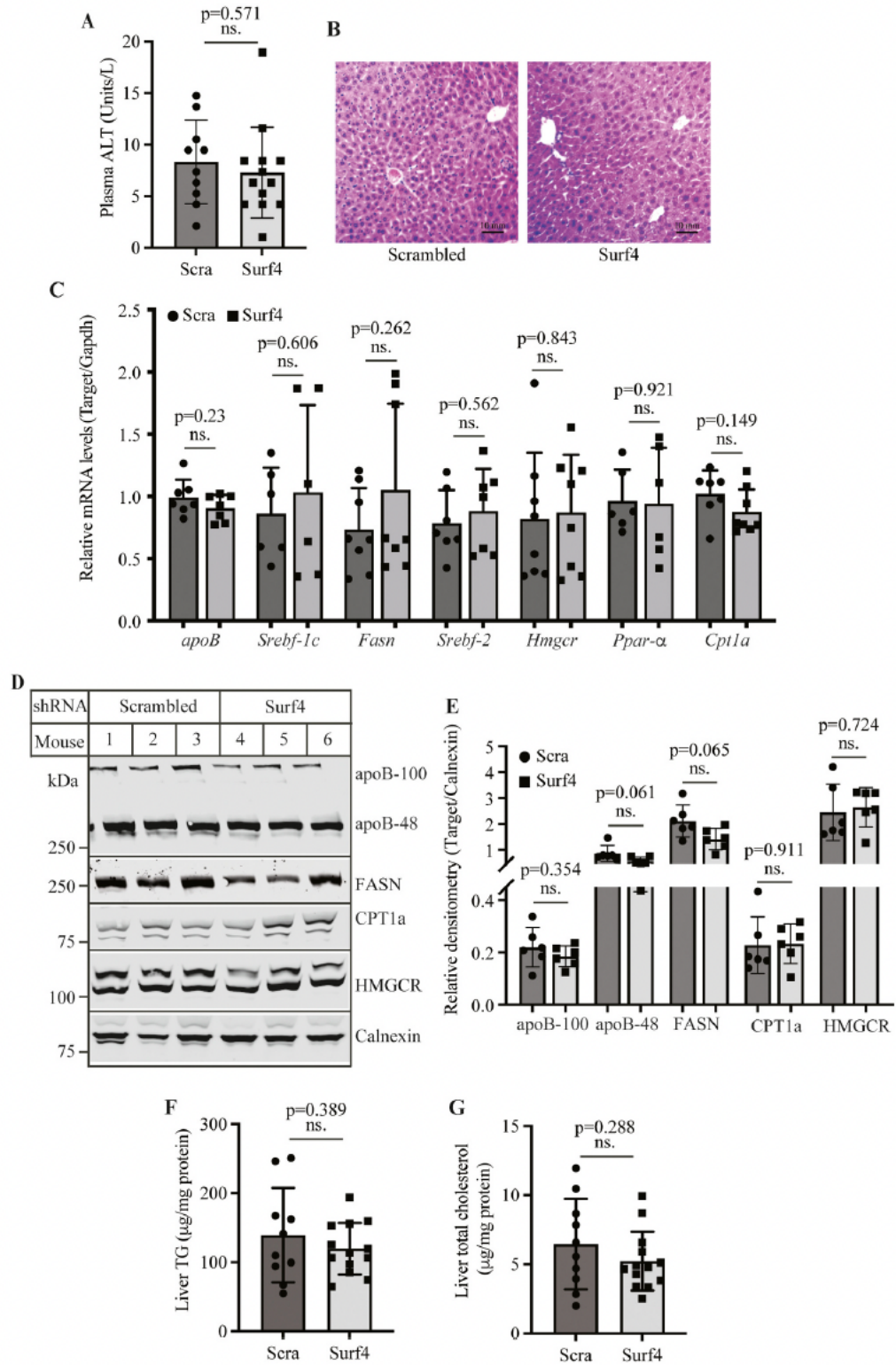


Figure 5.3. Effect of hepatic *Surf4* silencing on the liver. *apoE*^{-/-} mice (10-14 weeks old,) were injected with AAV-scrambled (Scra, 6 females and 4 males) or *Surf4* shRNA (7 females and 6

males), fed the chow diet for 4 weeks, and then fasted for 10 h before euthanasia. **(A)** Plasma ALT. Plasma was isolated from fasting blood samples and subjected to ALT measurement using a commercial kit from Cayman Chemical Company. **(B)** H&E staining of liver sections. Representative figures were shown. Similar results were observed in other samples (n=6, 3 males and 3 females in each group). **(C)** qRT-PCR. Total RNAs were isolated from liver samples for qRT-PCR using SYBR Green Master Mix. The relative mRNA levels were the ratio of the mRNA level of the target to that of *Gapdh* in the same mouse (n=6, 3 males and 3 females in each group). **(D and E)** Western blot. Equal amount of total proteins in liver homogenate was subjected to immunoblotting with antibodies indicated. Representative images were shown (D). The relative densitometry was the ratio of the densitometry of the protein indicated to that of calnexin in the same mouse (E, n = 6, 3 males and 3 females in each group). **(F and G)** Liver lipid levels. Lipids were extracted from mouse livers for the measurement of TG (F) and TC (G) using their specific enzymatic kits (Wako Diagnostics). Student's t-test was used to determine the significant difference between two groups. Values of all data were mean \pm SD. The significance was defined as $P > 0.05$, no significance (ns).

5.2.3 Effects of hepatic SURF4 on the development of atherosclerosis in *apoE*^{-/-} mice

Our subsequent experiments were to determine the effect of hepatic *Surf4* knockdown on the development of atherosclerosis. Male *apoE*^{-/-} mice administered AAV-scrambled or *Surf4* shRNA were fed the Western-type diet for 14 weeks to accelerate the development of atherosclerosis as described [186]. Protein and mRNA levels of SURF4, but not apoB, were significantly reduced in the liver of mice injected with AAV-*Surf4*-shRNA (Figures 5.4A to C). Mice in both groups exhibited comparable body weight (Figure 5.4D). We observed that relative mRNA levels of *Surf4* normalized to *Gapdh* were not statistically different in *apoE*^{-/-} mice fed a regular chow and the Western-type diet (1.161 ± 0.2647 vs 1.06 ± 0.161 , $p = 0.324$; Figures 5.1B and 5.4A). Relative protein levels of SURF4 normalized to calnexin were also comparable in the regular chow and the Western-type diet-fed *apoE*^{-/-} mice (0.1268 ± 0.09192 vs 0.198 ± 0.05259 , $p = 0.131$; Figures 5.1E and 5.4C). These findings suggest that high-fat/high-cholesterol feeding did not significantly affect *Surf4* expression. However, *Surf4* knockdown mice fed the Western-type diet had a less reduction in *Surf4* levels compared to *Surf4* knockdown mice on the chow diet (Figures 5.4C and 5.1E). It was of note that mice were injected with a single dose of AAV-shRNA. SURF4 levels were detected in mice on a regular chow and the Western-type diet 4 and 14 weeks after AAV administration, respectively. The efficiency of AAV-shRNA-mediated knockdown of *Surf4* might decrease over time. Nevertheless, atherosclerotic lesion of the whole aorta from the aortic root to the iliac bifurcation in *Surf4* knockdown mice was reduced by approximately 21% compared with that in control mice, but the difference did not reach statistical significance (16.28% vs 12.78%, $p=0.0519$) (Figures 5.4E and F). On the other hand, atherosclerotic lesion area in the aortic sinus was significantly reduced in mice injected with AAV-*Surf4*-shRNA ($529.8 \pm 173.8 \times 10^3 \mu\text{m}$ vs 384.6

$\pm 102.1 \times 10^3 \mu\text{m}$, $p=0.026$) (Figures 5.4G and H). Taken together, these findings demonstrate that inhibition of hepatic SURF4 reduces the development of atherosclerosis in *apoE*^{-/-} mice.

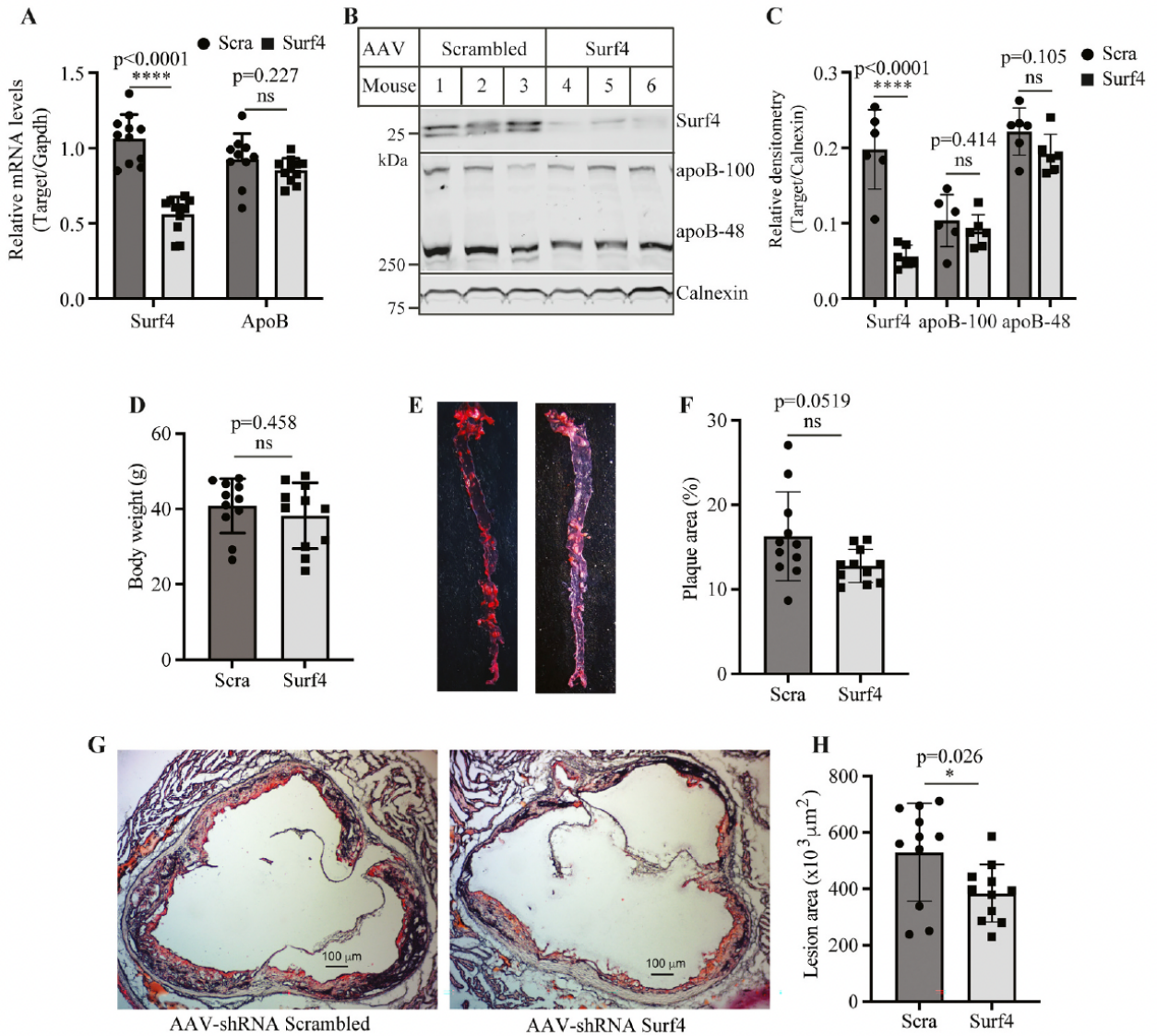


Figure 5.4. Effect of hepatic *Surf4* silencing on the development of atherosclerosis. *apoE*^{-/-} mice (10-14 weeks old, male) were injected with AAV-scrambled (Scra, n=11) or *Surf4* shRNA (n=11), fed the Western-type diet for 14 weeks, and then fasted for 10 h before euthanasia for sample collection. **(A)** qRT-PCR. Total RNAs were extracted from liver samples for qRT-PCR. The relative mRNA levels were the ratio of the mRNA levels of the target gene to that of *Gapdh* in the

same mouse (n=11, male). **(B and C)** Immunoblotting. Equal amount of total proteins in liver homogenate was subjected to Western blot using antibodies indicated. Representative images were shown (B). The relative densitometry was the ratio of the densitometry of the protein indicated to that of calnexin in the same mouse (C, n = 6, male). **(D)** Body weight of mice fasted for 10 h. **(E-H)** Oil Red O staining and quantification data of the whole aorta (E and F) and heart sections (G and H, Magnification, 40X). Representative figures were shown (E and G). Atherosclerotic lesions in the aorta and aortic sinus were quantified using OMAX ToupView and expressed as percentage of the total area (F and H). Student's t-test was used to determine the significant difference between two groups. Values of all data were mean \pm SD. The significance was defined as *P < 0.05, ****P < 0.0001, and P > 0.05, no significant difference (ns).

5.2.4 Effects of hepatic SURF4 on lipoprotein metabolism in *apoE*^{-/-} mice on the Western-type diet

Similar to the findings in *apoE*^{-/-} mice fed a regular chow diet, knockdown of *Surf4* in *apoE*^{-/-} mice fed the Western-type diet reduced TG secretion (Figure 5.5A). Plasma levels of apoB100, but not apoB48 or apoA-I were also significantly reduced in *Surf4* knockdown mice (Figures 5.5B and C). However, plasma TG and HDL-C levels were not markedly changed (Figures 5.5D and E). On the other hand, plasma TC levels were significantly reduced in *Surf4*-knockdown mice (Figure 5.5F). Consistently, FPLC data showed that cholesterol levels were reduced in both the chylomicron remnants/VLDL and IDL/LDL fractions, but not in the HDL fractions (Figure 5.5G). We then assessed the expression of genes important for lipid metabolism in the liver. mRNA levels of *Ppar-α*, *Cpt1a*, *Srebf2*, *Hmgcr*, *Srebf1c*, and *Fasn*, and protein levels of CPT1a, HMGCR, and FASN were all comparable in the control and *Surf4*-knockdown mice (Figures 5.6 A to C). Hepatic TG and TC levels and plasma ALT activity were also not significantly changed in mice injected with AAV-*Surf4* shRNA compared with control mice (Figures 5.6D-F). H&E staining of liver sections was also similar in mice administered AAV-scrambled or *Surf4* shRNA (Figure 5.6G). Therefore, in *apoE*^{-/-} mice fed the Western-type diet, *Surf4* knockdown reduces plasma non-HDL cholesterol levels and the development of atherosclerosis, but does not affect plasma TG and HDL cholesterol levels, nor results in liver TG accumulation or notable liver damage.

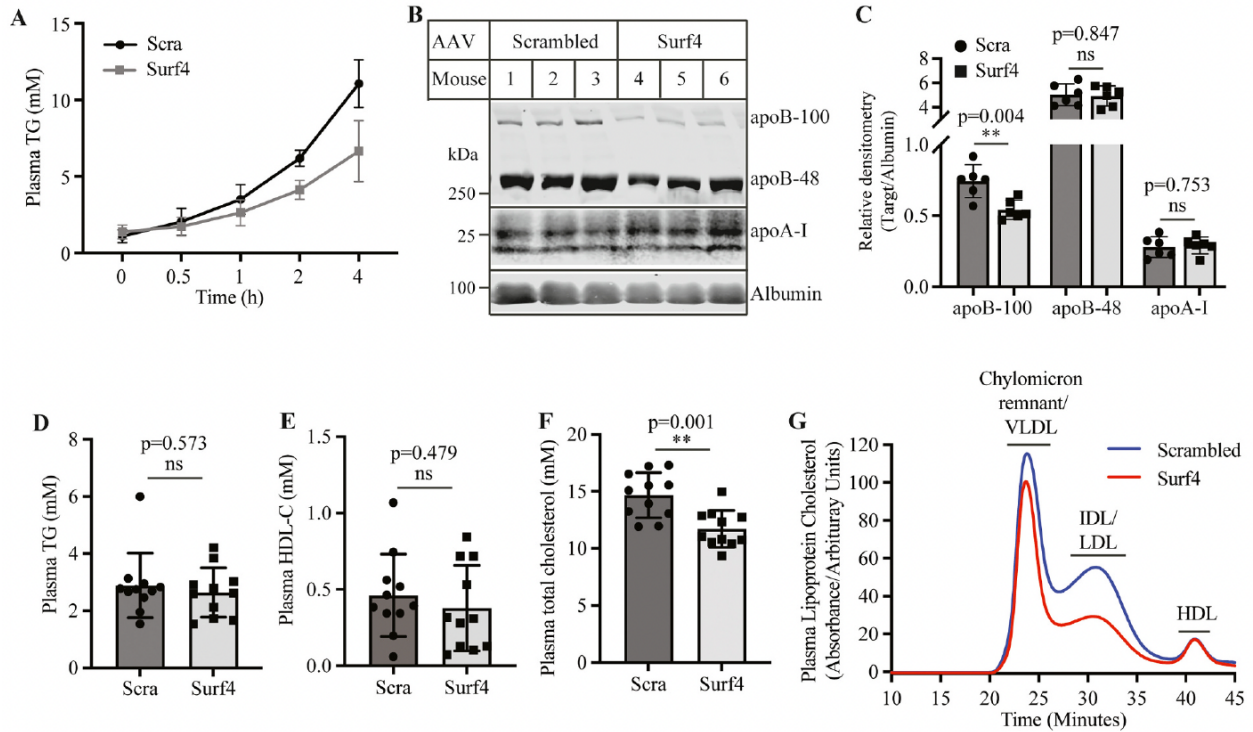


Figure 5.5. Effects of hepatic *Surf4* deficiency on plasma lipids. (A) TG secretion. *apoE*^{-/-} mice (10-14 weeks old, male) were injected with AAV-scrambled (Scra) or *Surf4* shRNA, fed the Western-type diet for 4 weeks, and then fasted for 10 h before P-407 injection. Blood samples were collected from mice before (0) and 0.5, 1, 2, and 4 h after P-407 injection. Plasma TG levels were measured using a kit (Wako Diagnostics) (n=4). (B and C) Immunoblotting. Mice were treated as described in the legend to Figure 4. The same amount of plasma from each mouse was applied to Western blot using antibodies indicated. Representative images were shown (B). The relative densitometry was the ratio of the densitometry of the protein indicated to that of albumin in the same mouse (C, n = 6). (D to F) Plasma lipids. Mice were treated as described in the legend to Figure 4. The levels of TG (D), HDL cholesterol (E), and TC (F) in fasting plasma were measured using their specific kits (n=11, male). (G) Cholesterol profile of plasma lipoproteins. 5 μ l of plasma from each mouse in the same group (n = 6, male) was pooled and applied to FPLC analysis of cholesterol. Student's t-test was used to determine the significant difference between two groups.

Values of all data were mean \pm SD. The significance was defined as **P < 0.01, and P > 0.05 no significance (ns).

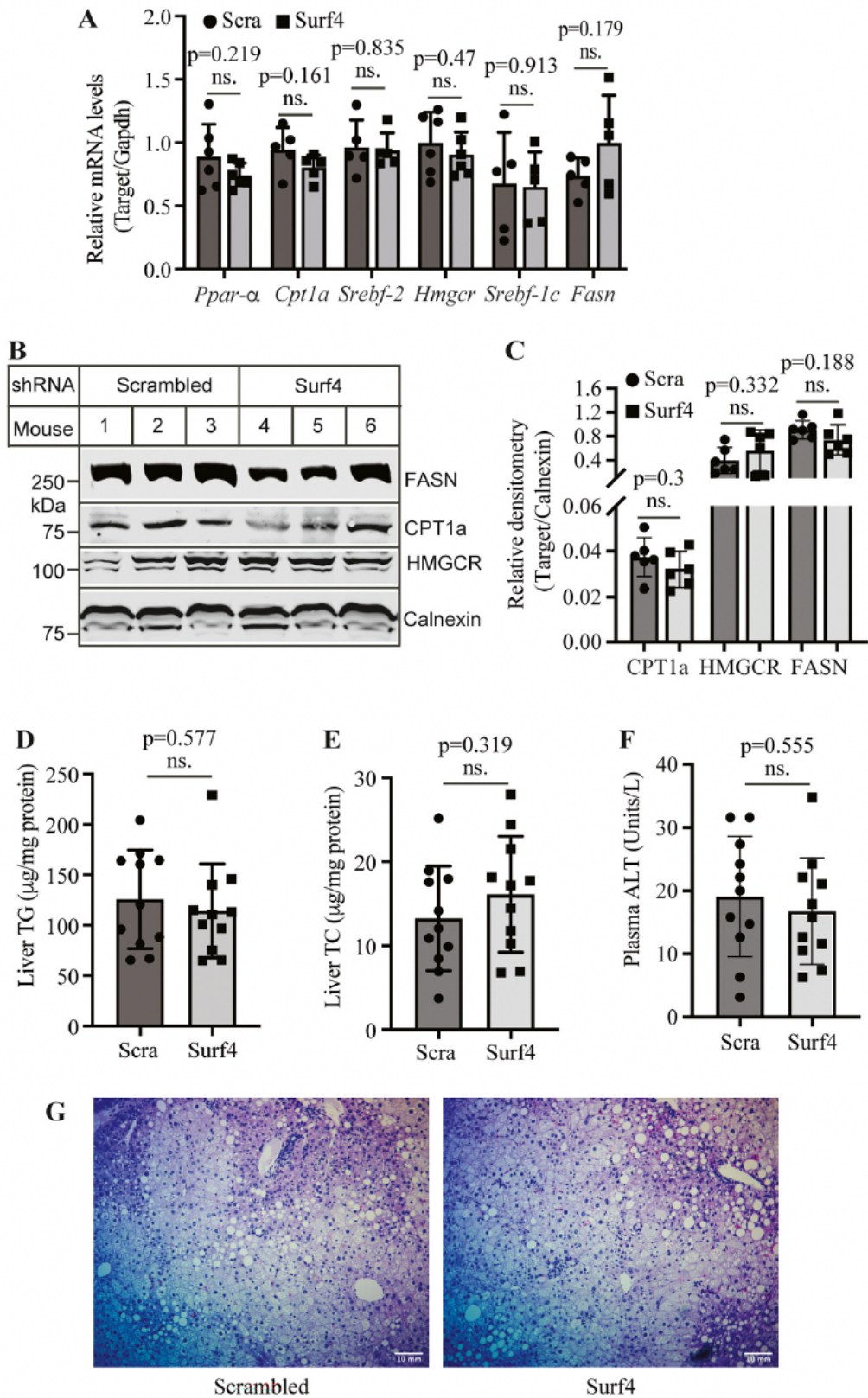


Figure 5.6. Effects of hepatic *Surf4* silencing on liver lipids and gene expression. Mice were

treated as described in the legend to Figure 4. **(A)** qRT-PCR. Total RNAs were extracted from the liver samples for qRT-PCR. The relative mRNA levels were the ratio of the mRNA level of the target to that of *Gapdh* in the same mouse (N=6, male). **(B and C)** Western blot. Equal amount of total proteins in liver homogenate was subjected to immunoblotting with antibodies indicated. Representative images were shown (B). The relative densitometry was the ratio of the densitometry of the protein indicated to that of calnexin in the same mouse (C, n = 6, male). **(D and E)** Liver lipids (n=11, male). Total lipids were extracted from mouse livers for the measurement of TG (D) and TC (E) using enzymatic kits (Wako Diagnostics). **(F)** Plasma ALT. A commercial kit (Cayman Chemical Company) was used to measure fasting plasma ALT levels (n=11, male). **(G)** H&E staining of liver sections. Representative figures were shown. Similar results were observed in other samples (n=3, male). Student's t-test was used to determine the significant difference between two groups. Values of all data were mean \pm SD. The significance was defined as $P > 0.05$, no significance (ns).

5.3 Discussion

Inhibition of VLDL secretion can significantly reduce plasma LDL-C levels and the risk of ASCVD. However, VLDL secretion is one of the main pathways by which hepatocytes remove excessive TG. Therefore, impaired VLDL secretion tends to cause hepatic TG accumulation, leading to liver steatosis. Our previous study showed that inhibition of hepatic *Surf4* markedly reduces plasma cholesterol levels and ameliorates the development of atherosclerosis without causing hepatic TG accumulation in *Ldlr*^{-/-} mice. Here, we investigated the role of hepatic SURF4 in lipoprotein metabolism in *apoE*^{-/-} mice fed a regular chow or the Western-type diet. We observed similar phenotypes except for plasma TG levels in the two conditions. *Surf4* knockdown in the liver significantly reduced plasma levels of TC, non-HDL cholesterol, and apoB100 without significantly affecting plasma HDL-C, apoA-I and apoB48 levels, or hepatic cholesterol and TG levels. However, we found that *Surf4* knockdown significantly reduced plasma TG levels by approximately 40% in *apoE*^{-/-} mice fed a regular chow diet but not in mice on the Western-type diet. In *apoE*^{-/-} mice, the absence of apoE prevents efficient clearance of circulating chylomicron remnants, resulting in elevated plasma TG levels. High fat content in the Western-type diet may mask changes in plasma TG levels caused by impaired VLDL secretion in *Surf4*-knockdown *apoE*^{-/-} mice.

Hepatic *Surf4* deficiency reduces atherosclerotic lesions in *apoE*^{-/-} mice, but to a much lesser extent than in *Ldlr*^{-/-} mice, which have more than 80% reduction in atherosclerotic lesions [154]. In *apoE*^{-/-} mice, we observed only an approximately 20% reduction in atherosclerotic lesions. This could be partly explained by the fact that *Surf4* deficiency resulted in a much less reduction in plasma TC levels in *apoE*^{-/-} mice than in *Ldlr*^{-/-} mice. Plasma TC levels were reduced by approximately 85% and 20% in *Surf4*-knockdown *Ldlr*^{-/-} and *apoE*^{-/-} mice fed the Western-type

diet, respectively [154]. This is probably caused by different lipid metabolism in the two mouse models. Under normal physiological conditions, chylomicron and VLDL remnants are efficiently cleared from the circulation in a LDLR-dependent and independent pathway [200, 201]. However, apoB48 on chylomicron remnant and apoB100 on VLDL or IDL cannot bind to LDLR; instead, apoE on these lipoprotein particles is required for their clearance. The absence of apoE results in accumulation of VLDL and chylomicron remnants in *apoE^{-/-}* mice. Hepatic *Surf4* silencing impairs VLDL secretion, thereby reducing VLDL remnants and LDL in the circulation; however, intestine-derived chylomicron remnants still accumulate in the circulation and are a major contributor to plasma cholesterol levels, especially when mice are fed the high cholesterol/high fat Western-type diet. On the other hand, chylomicron remnants can be effectively cleared via the LRP1 pathway in the absence of LDLR [201]. Therefore, in *Ldlr^{-/-}* mice, LDL (but not chylomicron remnants) is a significant source of plasma cholesterol, and *Surf4* silencing-induced deficiency in VLDL secretion can markedly reduce plasma cholesterol levels.

It is of note that apoE can also suppress atherosclerosis independently of lowering plasma cholesterol levels [187, 189, 202, 203], such as by polarizing macrophages from M1 to M2 [204], inhibiting inflammation via microRNAs [205], suppressing smooth muscle cell proliferation [206], antioxidative activity [202, 207], and promoting cellular cholesterol efflux from macrophages [208]. For example, the expression of low levels of apoE in macrophages or the adrenal glands does not significantly affect plasma lipoprotein cholesterol levels but significantly reduces atherosclerosis in *apoE^{-/-}* mice [203, 209]. Hepatic *Surf4* deficiency cannot compensate for the loss of these multiple anti-atherogenic effects of apoE in *apoE^{-/-}* mice. On the other hand, the development of atherosclerosis in *Ldlr^{-/-}* mice is primarily driven by elevated plasma LDL-C levels. Therefore,

knockdown of *Surf4* in the liver significantly reduces plasma LDL-C levels and thus drastically attenuates atherosclerosis in *Ldlr*^{-/-} mice.

VLDL secretion is one of the main ways for hepatocytes to remove excessive TG under normal physiological conditions. However, silencing of hepatic *Surf4* does not significantly increase TG levels in the liver of both *Ldlr*^{-/-} and *apoE*^{-/-} mice despite impaired VLDL secretion. Deficiency of carboxylesterase 3 also decreases VLDL secretion and does not result in hepatic TG accumulation because of increased fatty acid β -oxidation in the liver of carboxylesterase 3 knockout mice [210]. However, we observed no significant changes in the expression of genes involved in fatty acid β -oxidation in *Surf4*-knockdown *Ldlr*^{-/-} and *apoE*^{-/-} mice. Expression of genes involved in *de novo* lipogenesis was reduced only in *Surf4*-knockdown *Ldlr*^{-/-} mice [154]. These observations suggest that mechanisms other than fatty acid β -oxidation and *de novo* lipogenesis may be responsible for restoring TG homeostasis in the liver of *Surf4*-knockdown mice [199]. Notably, mouse hepatocytes produce both apoB100 and apoB48. The liver of mice expressing only apoB48 was comparable to that of WT mice, suggesting that apoB48 could mediate hepatic TG secretion in the absence of apoB100 [199]. We did not observe a significant change in plasma apoB48 levels in *Surf4* knockdown mice (Figures 2C and 5C). Therefore, hepatic apoB48 might mediate TG secretion and prevent TG accumulation in the liver of *Surf4* knockdown mice. Alternatively, it has been reported that increased autophagy is responsible for the removal of excessive TG in the liver of *ApoB* silenced mice [170]. Experiments are undergoing to elucidate these possibilities.

In summary, our findings demonstrate that inhibition of hepatic *Surf4* can significantly reduce plasma apoB 100 and non-HDL cholesterol levels and mitigate the development of atherosclerosis in *Ldlr*^{-/-} and *apoE*^{-/-} mice [154], the two commonly used mouse models of atherosclerosis. Emerging evidence shows that plasma apoB levels are a more accurate predictor of atherosclerotic

cardiovascular events than plasma LDL-C or non-HDL cholesterol levels. Lowering plasma apoB is significantly associated with reduced risk of cardiovascular disease [211, 212]. Therefore, our findings suggest that hepatic *Surf4* inhibition has the potential as a therapeutic strategy to reduce the risk of ASCVD in patients who cannot be successfully treated with current therapy. A limitation of our studies is that mice, unlike humans, express apoB48 in hepatocytes. Hepatic apoB48 can mediate TG secretion [199]. Whether SURF4 is required for secretion of apoB48-containing lipoprotein particles remains elusive. Therefore, hepatic TG in *Surf4* knockout and knockdown mice could be secreted through apoB48. Further studies are needed to elucidate the role of SURF4 in apoB48 secretion and confirm our findings in other animal models, such as hamsters, which, like humans, do not express apoB48 in the liver.

Chapter 6

Discussion and Future Perspectives

Numerous compelling studies have demonstrated a clear relationship between plasma LDL-C levels and the risk of atherosclerosis formation. Elevated plasma LDL-C levels increase risk of atherosclerosis, on the other hand, lowering plasma LDL-C levels reduces risk of atherosclerosis formation. LDL-C is catabolized from VLDL and cleared by LDL receptor which is post-transcriptionally regulated by PCSK9. However, the secretion of PCSK9 and VLDL from hepatocytes is not fully understood. In this thesis, I determined to explore the role of hepatic Surf4 in mediating PCSK9 and VLDL secretion, by which it regulates plasma lipid levels and the development of atherosclerosis.

6.1 The role of SURF4 in PCSK9 secretion from hepatocytes

6.1.1 SURF4 regulates *PCSK9* expression but is not required for its secretion *in vitro*

Plasma PCSK9 is mainly secreted from the hepatocytes and post-transcriptionally regulates LDLR degradation [37, 183]. However, the exact mechanism which mediates PCSK9 secretion from the hepatocytes is not well understood. It has been reported that SURF4 facilitates secretion of overexpressed PCSK9 from HEK293T cells, while its role in secretion of endogenous PCSK9 from hepatocytes is still not clear [131]. Here, we were the first to demonstrate that SURF4 plays a negligible role in mediating endogenous PCSK9 from cultured hepatocytes. I found that deficiency of SURF4 did not impair endogenous PCSK9 secretion, conversely, loss of SURF4 significantly increased both intracellular and extracellular PCSK9 in Huh7 and HepG2 cells. Furthermore, I found that no direct interaction between SURF4 and PCSK9 could be detected by co-immunoprecipitation, which further exclude its role in mediating PCSK9 secretion from the ER. Considering that PCSK9 is transcriptionally regulated by SREBP2, I then defined mRNA levels of *PCSK9* as well as *SREBP2* and its target *HMGCR*, and found that mRNA levels of *PCSK9*, *SREBP2* and *HMGCR* were all increased in the cells lacking SURF4, suggesting that knockdown of *SURF4*

increased the transcriptional activity of *SREBP2* leading to enhanced transcription of *PCSK9*. As previously reported that ER stress induces enhanced SREBP2 processing, it would be of interest to see if knockdown of *SURF4* induced ER stress, which in turn increased the transcriptional activity of *SREBP2* [213]. However, by determining the expression of GRP78, the marker of ER stress, I found that knockdown of *SURF4* did not induce ER stress, indicating it involved other unknown mechanisms enhancing *SREBP2* transcriptional activity.

6.1.2 Hepatic SURF4 does not affect PCSK9 expression and secretion *in vivo*

In our previous experiments, we have found that deficiency of SURF4 increased PCSK9 expression in cultured human hepatocytes. It would be of interest to investigate the role of hepatic SURF4 in PCSK9 expression and secretion in hepatocytes. In contrast to what we reported in cultured cells, silencing of hepatic *Surf4* did not affect the levels of plasma PCSK9. Similarly, knockdown of hepatic *Surf4* has no effect on liver PCSK9 levels. Taken together, these findings indicate that, unlike the results found in cultured cells, loss of hepatic SURF4 did not affect the levels of plasma PCSK9 and liver PCSK9, suggesting that hepatic SURF4 is not required for hepatic PCSK9 secretion *in vivo*.

6.1.3 Conclusion

In summary, Chapter 3 has demonstrated that SURF4 regulates *PCSK9* expression, which is via regulating the transcriptional activity of *SREBP2*, but is not required for PCSK9 secretion from cultured human hepatocytes. Furthermore, we also demonstrated that hepatic SURF4 does not regulate liver *PCSK9* expression and secretion *in vivo*. Taken together, these findings indicate that hepatic SURF4 is not essential for PCSK9 secretion from hepatocytes.

6.2 The role of hepatic SURF4 in lipoprotein metabolism and the development of atherosclerosis in *Ldlr*^{-/-} mice and *apoE*^{-/-} mice

6.2.1 The role of hepatic SURF4 in lipoprotein metabolism and the development of atherosclerosis in *Ldlr*^{-/-} mice

Plasma levels of LDL-C have been proven to positively correlated with the development of atherosclerosis in numerous studies [1, 2]. We have demonstrated that hepatic SURF4 mediates VLDL secretion and loss of hepatic SURF4 dramatically reduced plasma LDL-C and apoB100 levels. I also demonstrated that SURF4 interacts and associates with apoB100 by co-immunoprecipitation and confocal microscopy. Knockdown of *SURF4* reduced apoB100 secretion from Huh7 and HepG2 cells. These findings indicate that SURF4 may interacts with apoB100 and mediates VLDL secretion from hepatocytes. I then knocked down hepatic *Surf4* expression in *Ldlr*^{-/-} mice and fed the mice with Western-type diet for 14 weeks to induce atherosclerosis formation. I found that deficiency of hepatic *Surf4* dramatically reduced VLDL secretion and plasma levels of LDL-C, TG, and non-HDL-C in *Ldlr*^{-/-} mice. Furthermore, I found that lacking hepatic *Surf4* did not result in obvious hepatic lipid accumulation or impaired liver function. Next, I examined the effect of lacking hepatic *Surf4* on the development of atherosclerosis and found that *Surf4* knockdown *Ldlr*^{-/-} mice showed a significant reduction in atherosclerotic lesion area compared with control *Ldlr*^{-/-} mice.

6.2.2 The role of hepatic SURF4 in lipoprotein metabolism and the development of atherosclerosis in *apoE*^{-/-} mice

apoE^{-/-} mouse is another commonly used animal model for studying atherosclerosis, which has impaired clearance of apoE-containing lipoprotein particles, such as chylomicron and VLDL remnant [186]. It has been reported that the same target may have different effects on the development of atherosclerosis in *apoE*^{-/-} and *Ldlr*^{-/-} mice. For instance, knockout hepatic lipase

increases and reduces atherosclerotic plaques in *Ldlr*^{-/-} and *apoE*^{-/-} mice, respectively [190-192]. On the other hand, deficiency of SR-BI accelerates the development of atherosclerosis in both *Ldlr*^{-/-} and *apoE*^{-/-} mice [193, 194]. Therefore, to further determine the potential of hepatic *Surf4* inhibition as an effective lipid-lowering strategy, it is necessary to apply *apoE*^{-/-} mouse model into our study.

To determine the role of hepatic SURF4 in lipid metabolism in *apoE*^{-/-} mice, I knocked down *Surf4* expression in *apoE*^{-/-} mice using AAV-shRNA. As expected, compared to control *apoE*^{-/-} mice, *Surf4* knockdown *apoE*^{-/-} mice fed a regular chow diet exhibited a significant reduction in plasma levels of TG, TC, but not HDL-C. I also found that secretion of apoB100 and VLDL from hepatocytes was dramatically impaired in *Surf4* knockdown mice. However, liver TG, TC, and plasma ALT levels were all comparable between control and *Surf4* knockdown *apoE*^{-/-} mice. Thus, these findings suggest that deficiency of hepatic SURF4 impairs VLDL secretion and subsequent lower plasma lipid levels in *apoE*^{-/-} mice, but did not lead to obvious hepatic lipid accumulation or impaired liver function in the mice.

I then fed the mice with Western-type diet for 14 weeks to assess *Surf4* knockdown on the development of atherosclerosis. I found that, similar with the findings in *apoE*^{-/-} mice fed a regular chow diet, knockdown of hepatic *Surf4* in *apoE*^{-/-} mice fed with Western-type diet reduced TG secretion from liver. Further, hepatic *Surf4* silencing reduced plasma TC, but not TG and HDL-C levels. Hepatic lipid levels and liver function were not significantly altered in *Surf4* knockdown *apoE*^{-/-} mice. Both mRNA and protein levels of key players in hepatic lipid metabolism, such as FASN, HMGCR and CPT1a, were also comparable between control and *Surf4* knockdown *apoE*^{-/-} mice. Therefore, hepatic *Surf4* knockdown reduces non-HDL-C levels, but does not affect plasma levels of TG and HDL-C, nor induces hepatic lipid accumulation or liver damage in *apoE*^{-/-} mice.

fed the Western-type diet. I also found that deficiency of hepatic SURF4 significantly reduced atherosclerotic lesions in *apoE*^{-/-} mice.

6.2.3 Conclusion

In Chapters 4 and 5, we applied both *Ldlr*^{-/-} and *apoE*^{-/-} mice to investigate the role of hepatic SURF4 in regulating lipid metabolism and the development of atherosclerosis. I confirmed that inhibition of hepatic SURF4 can significantly reduce plasma apoB100 and non-HDL-C levels lead to reduced risk of atherosclerosis without causing significant hepatic lipid accumulation or impaired liver function in both commonly used mouse models of atherosclerosis. Taken together, these findings suggest that inhibition of hepatic SURF4 could be a potential therapeutic target for lowering plasma cholesterol levels and the risk of atherosclerotic cardiovascular disease in patients who cannot benefit from current therapies.

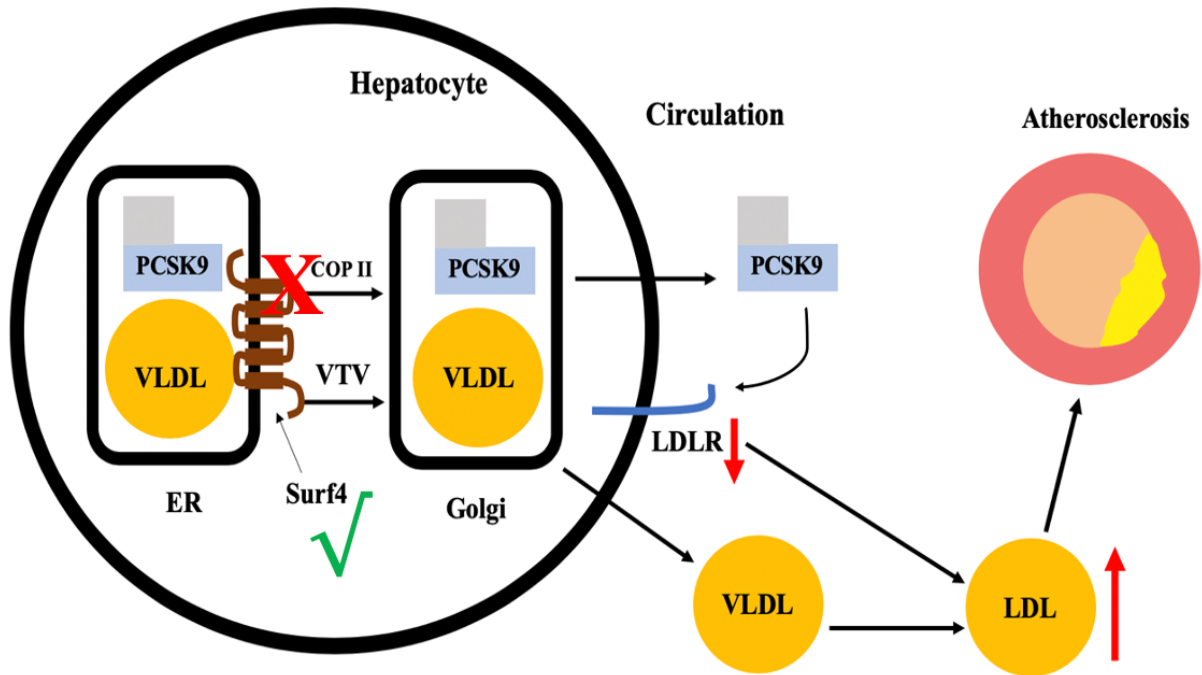


Figure 6.1. Final model of proposed role of hepatic SURF4 in mediating lipoprotein metabolism and the development of atherosclerosis. SURF4 interacts with apoB100 and facilitates VLDL transportation from the ER to the Golgi apparatus, regulating plasma lipid levels and the formation of atherosclerosis. However, Surf4 plays a negligible role in mediating PCSK9 secretion from hepatocytes.

6.3 Future Direction

6.3.1 To investigate the mechanism by which hepatic lipid homeostasis is maintained in *Surf4* knockdown mice

In Chapter 4 & 5, we found that knockdown of hepatic *Surf4* reduced VLDL secretion but did not result in hepatic cholesterol and TG accumulation. VLDL is one of the main ways for the liver to get rid of excessive endogenous TG. Thus, it would be of interest to investigate how hepatic lipid homeostasis is maintained in *Surf4* knockdown mice. I proposed following studies to determine the mechanisms involved in hepatic lipid homeostasis. *De novo* lipogenesis will be assessed by determining the transcriptional activity of several key genes, such as *SREBP-1c*, *DAGT1*, *DGAT2*, etc. Fatty acid uptake, fatty acid oxidation, and direct fatty acid secretion will also be examined by determining their specific markers respectively. Deficiency of SURF4 may trap VLDL particles in the ER lumen, which can trigger ER stress and autophagy to eliminate excessive VLDLs in the lumen. To test this possibility, I will determine both GRP78 and LC3-II by qRT-PCR and immunoblotting. These results will unmask the mechanisms by which hepatic lipid homeostasis is maintained.

6.3.2 To investigate the role of SURF4 in chylomicron secretion in intestine

VLDLs are synthesized by the hepatocytes for delivering endogenous lipids to peripheral tissues, and chylomicrons are the large TG-rich lipoproteins, which are produced from dietary lipids in enterocytes and deliver exogenous lipids to cardiac, skeletal muscle tissue, etc. Functionally, they share some similarities, and their transportation from the ER to the Golgi also shares some similarities, such as they both require TANGO1 and SAR1B for their specialized transport vesicles formation. Our previous results showed that knockdown of *Surf4* in the liver of *Ldlr*^{-/-} mice reduced plasma levels of both apoB100 and apoB48, indicating that SURF4 may interact with apoB48 and

facilitate its secretion as well. Considering that apoB48 is the essential structure protein of chylomicron, I hypothesize that deficiency of intestinal SURF4 will reduce chylomicron secretion, leading to reduced plasma lipid levels and risk of atherosclerosis subsequently. To test this hypothesis, I have designed following experiments. Caco-2 cells derived from human colorectal adenocarcinoma will be used to generate *SURF4* knockout (*SURF4*^{-/-}) stable cell line by utilizing clustered regularly interspaced short palindromic repeats (CRISPR-Cas9) technique. Both secreted and intracellular apoB48 will be determined by immunoblotting. If impaired apoB secretion was observed, I will also perform SURF4 reconstitute experiments by reintroducing wild type SURF4 into *SURF4*^{-/-} cells and determine whether it can rescue apoB secretion in the cells. Further, *Surf4* intestine specific knockout (*Surf4*^{IKO}) mice will be generated to assess the effects of deficiency of intestinal *Surf4* on lipid metabolism *in vivo*. In addition, we will also generate *apoE* and intestinal *Surf4* specific double knockout mice (*apoE*^{-/-}/*Surf4*^{IKO}) and fed the mice with Western-type diet to assess the effects of intestinal *Surf4* on the development of atherosclerosis. I speculate that deficiency of intestinal *Surf4* will impair chylomicron secretion from enterocytes, and, as a result, reduce plasma lipid levels, especially TG levels, and the risk of atherosclerosis.

6.3.3 To investigate the role of SURF4 in collagen secretion

It has been reported that TANGO1 interacts with apoB100 and mediates VLDL particles transportation out of the ER. Another bulky cargo, collagen, also needs the assistant of TANGO1 to be transported from the ER to the Golgi. Considering there are some similarities existing between VLDL and collagen, such as they are both bulky cargoes which cannot utilize classic COPII vesicles, and *SURF4* is ubiquitous expressed, it is reasonable to expect that SURF4 may facilitate secretion of collagen out of the ER as well. Further studies are required to investigate whether inhibition of

SURF4 in different cells can impair collagen secretion and prevent related diseases, such as inhibiting collagen secretion from hepatic stellate cells and ameliorate liver fibrosis etc.

Reference

1. Boren, J., et al., *Low-density lipoproteins cause atherosclerotic cardiovascular disease: pathophysiological, genetic, and therapeutic insights: a consensus statement from the European Atherosclerosis Society Consensus Panel*. Eur Heart J, 2020. **41**(24): p. 2313-2330.
2. Ference, B.A., et al., *Low-density lipoproteins cause atherosclerotic cardiovascular disease. 1. Evidence from genetic, epidemiologic, and clinical studies. A consensus statement from the European Atherosclerosis Society Consensus Panel*. Eur Heart J, 2017. **38**(32): p. 2459-2472.
3. Libby, P., *The changing landscape of atherosclerosis*. Nature, 2021. **592**(7855): p. 524-533.
4. Libby, P., et al., *Atherosclerosis*. Nat Rev Dis Primers, 2019. **5**(1): p. 56.
5. Thayse, K., et al., *VCAM-1 Target in Non-Invasive Imaging for the Detection of Atherosclerotic Plaques*. Biology (Basel), 2020. **9**(11).
6. Alves-Bezerra, M. and D.E. Cohen, *Triglyceride Metabolism in the Liver*. Compr Physiol, 2017. **8**(1): p. 1-8.
7. Hirano, K., et al., *Targeted disruption of the mouse apobec-1 gene abolishes apolipoprotein B mRNA editing and eliminates apolipoprotein B48*. J Biol Chem, 1996. **271**(17): p. 9887-90.
8. Nakamuta, M., et al., *Complete phenotypic characterization of apobec-1 knockout mice with a wild-type genetic background and a human apolipoprotein B transgenic background, and restoration of apolipoprotein B mRNA editing by somatic gene transfer of Apobec-1*. J Biol Chem, 1996. **271**(42): p. 25981-8.
9. Tiwari, S. and S.A. Siddiqi, *Intracellular trafficking and secretion of VLDL*. Arterioscler Thromb Vasc Biol, 2012. **32**(5): p. 1079-86.
10. Ginsberg, H.N., *ApoB SURFs a Ride from the ER to the Golgi*. Cell Metab, 2021. **33**(2): p. 231-233.
11. Sundaram, M., et al., *Expression of apolipoprotein C-III in McA-RH7777 cells enhances VLDL assembly and secretion under lipid-rich conditions*. J Lipid Res, 2010. **51**(1): p. 150-61.
12. Cohn, J.S., et al., *Rate of production of plasma and very-low-density lipoprotein (VLDL) apolipoprotein C-III is strongly related to the concentration and level of production of VLDL triglyceride in male subjects with different body weights and levels of insulin sensitivity*. J Clin Endocrinol Metab, 2004. **89**(8): p. 3949-55.
13. Shelness, G.S. and J.A. Sellers, *Very-low-density lipoprotein assembly and secretion*. Curr Opin Lipidol, 2001. **12**(2): p. 151-7.
14. Barlowe, C. and A. Helenius, *Cargo Capture and Bulk Flow in the Early Secretory Pathway*. Annu Rev Cell Dev Biol, 2016. **32**: p. 197-222.
15. Stagg, S.M., et al., *Structure of the Sec13/31 COPII coat cage*. Nature, 2006. **439**(7073): p. 234-8.
16. Santos, A.J., et al., *TANGO1 and Mia2/cTAGE5 (TALI) cooperate to export bulky pre-chylomicrons/VLDLs from the endoplasmic reticulum*. J Cell Biol, 2016. **213**(3): p. 343-54.
17. Tiwari, S., et al., *Silencing of Small Valosin-containing Protein-interacting Protein (SVIP) Reduces Very Low Density Lipoprotein (VLDL) Secretion from Rat Hepatocytes by Disrupting Its Endoplasmic Reticulum (ER)-to-Golgi Trafficking*. J Biol Chem, 2016. **291**(24): p. 12514-12526.

18. Butkinaree, C., et al., *A regulator of secretory vesicle size, Kelch-like protein 12, facilitates the secretion of apolipoprotein B100 and very-low-density lipoproteins--brief report.* Arterioscler Thromb Vasc Biol, 2014. **34**(2): p. 251-4.
19. Bai, J., et al., *A retrospective study of NENs and miR-224 promotes apoptosis of BON-1 cells by targeting PCSK9 inhibition.* Oncotarget, 2017. **8**(4): p. 6929-6939.
20. Rios-Barrera, L.D., et al., *Dual function for Tango1 in secretion of bulky cargo and in ER-Golgi morphology.* Proc Natl Acad Sci U S A, 2017. **114**(48): p. E10389-E10398.
21. Raote, I., et al., *TANGO1 builds a machine for collagen export by recruiting and spatially organizing COPII, tethers and membranes.* Elife, 2018. **7**: p. e32723.
22. Ishikawa, Y., et al., *Intracellular mechanisms of molecular recognition and sorting for transport of large extracellular matrix molecules.* Proc Natl Acad Sci U S A, 2016. **113**(41): p. E6036-E6044.
23. Pan, X., et al., *Isolation and characterization of renal erythropoietin-producing cells from genetically produced anemia mice.* PLoS One, 2011. **6**(10): p. e25839.
24. Aller, S.G., et al., *Structure of P-glycoprotein reveals a molecular basis for poly-specific drug binding.* Science, 2009. **323**(5922): p. 1718-22.
25. Hidalgo, B., et al., *Epigenome-Wide Association Study of Fasting Measures of Glucose, Insulin, and HOMA-IR in the Genetics of Lipid Lowering Drugs and Diet Network Study.* Diabetes, 2014. **63**(2): p. 801-7.
26. Dallinga-Thie, G.M., et al., *The metabolism of triglyceride-rich lipoproteins revisited: new players, new insight.* Atherosclerosis, 2010. **211**(1): p. 1-8.
27. Goldstein, J.L. and M.S. Brown, *The LDL receptor.* Arterioscler Thromb Vasc Biol, 2009. **29**(4): p. 431-8.
28. Goldstein, J.L. and M.S. Brown, *A century of cholesterol and coronaries: from plaques to genes to statins.* Cell, 2015. **161**(1): p. 161-72.
29. Go, G.W. and A. Mani, *Low-density lipoprotein receptor (LDLR) family orchestrates cholesterol homeostasis.* Yale J Biol Med, 2012. **85**(1): p. 19-28.
30. Garuti, R., et al., *The modular adaptor protein autosomal recessive hypercholesterolemia (ARH) promotes low density lipoprotein receptor clustering into clathrin-coated pits.* J Biol Chem, 2005. **280**(49): p. 40996-1004.
31. McMahon, H.T. and E. Boucrot, *Molecular mechanism and physiological functions of clathrin-mediated endocytosis.* Nat Rev Mol Cell Biol, 2011. **12**(8): p. 517-33.
32. Goldstein, J.L., et al., *Receptor-mediated endocytosis: concepts emerging from the LDL receptor system.* Annu Rev Cell Biol, 1985. **1**: p. 1-39.
33. Chadwick, A.C. and K. Musunuru, *Treatment of Dyslipidemia Using CRISPR/Cas9 Genome Editing.* Curr Atheroscler Rep, 2017. **19**(7): p. 32.
34. Goldstein, J.L., R.A. DeBose-Boyd, and M.S. Brown, *Protein sensors for membrane sterols.* Cell, 2006. **124**(1): p. 35-46.
35. Brown, M.S. and J.L. Goldstein, *Cholesterol feedback: from Schoenheimer's bottle to Scap's MELADL.* J Lipid Res, 2009. **50 Suppl**: p. S15-27.
36. Horton, J.D., J.L. Goldstein, and M.S. Brown, *SREBPs: activators of the complete program of cholesterol and fatty acid synthesis in the liver.* J Clin Invest, 2002. **109**(9): p. 1125-31.
37. Gu, H.M. and D.W. Zhang, *Hypercholesterolemia, low density lipoprotein receptor and proprotein convertase subtilisin/kexin-type 9.* J Biomed Res, 2015. **29**(5): p. 356-61.
38. Seidah, N.G., et al., *The activation and physiological functions of the proprotein convertases.* Int J Biochem Cell Biol, 2008. **40**(6-7): p. 1111-25.

39. Zhou, A., et al., *Proteolytic processing in the secretory pathway*. J Biol Chem, 1999. **274**(30): p. 20745-8.
40. Seidah, N.G., *The PCSK9 discovery, an inactive protease with varied functions in hypercholesterolemia, viral infections, and cancer*. J Lipid Res, 2021. **62**: p. 100130.
41. Horton, J.D., J.C. Cohen, and H.H. Hobbs, *PCSK9: a convertase that coordinates LDL catabolism*. J Lipid Res, 2009. **50 Suppl**: p. S172-7.
42. Abifadel, M., et al., *Mutations in PCSK9 cause autosomal dominant hypercholesterolemia*. Nat Genet, 2003. **34**(2): p. 154-6.
43. Cohen, J.C., et al., *Sequence variations in PCSK9, low LDL, and protection against coronary heart disease*. N Engl J Med, 2006. **354**(12): p. 1264-72.
44. Naoumova, R.P., et al., *Severe hypercholesterolemia in four British families with the D374Y mutation in the PCSK9 gene: long-term follow-up and treatment response*. Arterioscler Thromb Vasc Biol, 2005. **25**(12): p. 2654-60.
45. Timms, K.M., et al., *A mutation in PCSK9 causing autosomal-dominant hypercholesterolemia in a Utah pedigree*. Hum Genet, 2004. **114**(4): p. 349-53.
46. Leren, T.P., *Mutations in the PCSK9 gene in Norwegian subjects with autosomal dominant hypercholesterolemia*. Clin Genet, 2004. **65**(5): p. 419-22.
47. van der Graaf, A., et al., *Molecular basis of autosomal dominant hypercholesterolemia: assessment in a large cohort of hypercholesterolemic children*. Circulation, 2011. **123**(11): p. 1167-73.
48. Lagace, T.A., et al., *Secreted PCSK9 decreases the number of LDL receptors in hepatocytes and in livers of parabiotic mice*. J Clin Invest, 2006. **116**(11): p. 2995-3005.
49. Zhang, D.W., et al., *Binding of proprotein convertase subtilisin/kexin type 9 to epidermal growth factor-like repeat A of low density lipoprotein receptor decreases receptor recycling and increases degradation*. J Biol Chem, 2007. **282**(25): p. 18602-12.
50. Rashid, S., et al., *Decreased plasma cholesterol and hypersensitivity to statins in mice lacking Pcsk9*. Proc Natl Acad Sci U S A, 2005. **102**(15): p. 5374-9.
51. Qian, Y.W., et al., *Secreted PCSK9 downregulates low density lipoprotein receptor through receptor-mediated endocytosis*. J Lipid Res, 2007. **48**(7): p. 1488-98.
52. Leren, T.P., *Sorting an LDL receptor with bound PCSK9 to intracellular degradation*. Atherosclerosis, 2014. **237**(1): p. 76-81.
53. Poirier, S., et al., *GRP94 Regulates Circulating Cholesterol Levels through Blockade of PCSK9-Induced LDLR Degradation*. Cell Rep, 2015. **13**(10): p. 2064-71.
54. Lambert, G., et al., *The PCSK9 decade*. J Lipid Res, 2012. **53**(12): p. 2515-24.
55. Sobati, S., et al., *PCSK9: A Key Target for the Treatment of Cardiovascular Disease (CVD)*. Adv Pharm Bull, 2020. **10**(4): p. 502-511.
56. Shapiro, M.D., H. Tavori, and S. Fazio, *PCSK9: From Basic Science Discoveries to Clinical Trials*. Circ Res, 2018. **122**(10): p. 1420-1438.
57. Barale, C., et al., *PCSK9 Biology and Its Role in Atherothrombosis*. Int J Mol Sci, 2021. **22**(11).
58. Bayona, A., et al., *Loss-of-function mutation of PCSK9 as a protective factor in the clinical expression of familial hypercholesterolemia: A case report*. Medicine (Baltimore), 2020. **99**(34): p. e21754.
59. Lebeau, P., et al., *Loss-of-function PCSK9 mutants evade the unfolded protein response sensor GRP78 and fail to induce endoplasmic reticulum stress when retained*. J Biol Chem, 2018. **293**(19): p. 7329-7343.

60. Deng, S.J., et al., *The role of the C-terminal domain of PCSK9 and SEC24 isoforms in PCSK9 secretion*. *Biochim Biophys Acta Mol Cell Biol Lipids*, 2020. **1865**(6): p. 158660.
61. Chen, X.W., et al., *SEC24A deficiency lowers plasma cholesterol through reduced PCSK9 secretion*. *Elife*, 2013. **2**: p. e00444.
62. Chatterjee, S., A.J. Choi, and G. Frankel, *A systematic review of Sec24 cargo interactome*. *Traffic*, 2021. **22**(12): p. 412-424.
63. Harrington, R.A., *Statins-Almost 30 Years of Use in the United States and Still Not Quite There*. *JAMA Cardiol*, 2017. **2**(1): p. 66.
64. Stancu, C. and A. Sima, *Statins: mechanism of action and effects*. *J Cell Mol Med*, 2001. **5**(4): p. 378-87.
65. Silverman, M.G., et al., *Association Between Lowering LDL-C and Cardiovascular Risk Reduction Among Different Therapeutic Interventions: A Systematic Review and Meta-analysis*. *JAMA*, 2016. **316**(12): p. 1289-97.
66. Pearson, G.J., et al., *2021 Canadian Cardiovascular Society Guidelines for the Management of Dyslipidemia for the Prevention of Cardiovascular Disease in Adults*. *Can J Cardiol*, 2021. **37**(8): p. 1129-1150.
67. Toth, P.P., et al., *Management of Statin Intolerance in 2018: Still More Questions Than Answers*. *Am J Cardiovasc Drugs*, 2018. **18**(3): p. 157-173.
68. Ward, N.C., G.F. Watts, and R.H. Eckel, *Statin Toxicity*. *Circ Res*, 2019. **124**(2): p. 328-350.
69. Sabatine, M.S., et al., *Evolocumab and Clinical Outcomes in Patients with Cardiovascular Disease*. *N Engl J Med*, 2017. **376**(18): p. 1713-1722.
70. Weintraub, W.S. and S.S. Gidding, *PCSK9 Inhibitors: A Technology Worth Paying For?* *Pharmacoeconomics*, 2016. **34**(3): p. 217-20.
71. Raal, F.J., et al., *Inclisiran for the Treatment of Heterozygous Familial Hypercholesterolemia*. *N Engl J Med*, 2020. **382**(16): p. 1520-1530.
72. Ray, K.K., et al., *Two Phase 3 Trials of Inclisiran in Patients with Elevated LDL Cholesterol*. *N Engl J Med*, 2020. **382**(16): p. 1507-1519.
73. Meng, Z. and M. Lu, *RNA Interference-Induced Innate Immunity, Off-Target Effect, or Immune Adjuvant?* *Front Immunol*, 2017. **8**: p. 331.
74. Wright, R.S., et al., *Pooled Patient-Level Analysis of Inclisiran Trials in Patients With Familial Hypercholesterolemia or Atherosclerosis*. *J Am Coll Cardiol*, 2021. **77**(9): p. 1182-1193.
75. Akdim, F., et al., *Effect of mipomersen, an apolipoprotein B synthesis inhibitor, on low-density lipoprotein cholesterol in patients with familial hypercholesterolemia*. *Am J Cardiol*, 2010. **105**(10): p. 1413-9.
76. Panta, R., K. Dahal, and S. Kunwar, *Efficacy and safety of mipomersen in treatment of dyslipidemia: a meta-analysis of randomized controlled trials*. *J Clin Lipidol*, 2015. **9**(2): p. 217-25.
77. Santos, R.D., et al., *Long-term efficacy and safety of mipomersen in patients with familial hypercholesterolaemia: 2-year interim results of an open-label extension*. *Eur Heart J*, 2015. **36**(9): p. 566-75.
78. Blom, D.J., et al., *Lomitapide and Mipomersen-Inhibiting Microsomal Triglyceride Transfer Protein (MTP) and apoB100 Synthesis*. *Curr Atheroscler Rep*, 2019. **21**(12): p. 48.
79. Fogacci, F., et al., *Efficacy and Safety of Mipomersen: A Systematic Review and Meta-Analysis of Randomized Clinical Trials*. *Drugs*, 2019. **79**(7): p. 751-766.

80. Newberry, E.P., et al., *Liver-Specific Deletion of Mouse Tm6sf2 Promotes Steatosis, Fibrosis, and Hepatocellular Cancer*. Hepatology, 2021. **74**(3): p. 1203-1219.
81. Smagris, E., et al., *Inactivation of Tm6sf2, a Gene Defective in Fatty Liver Disease, Impairs Lipidation but Not Secretion of Very Low Density Lipoproteins*. J Biol Chem, 2016. **291**(20): p. 10659-76.
82. Luo, F., et al., *Hepatic TM6SF2 Is Required for Lipidation of VLDL in a Pre-Golgi Compartment in Mice and Rats*. Cell Mol Gastroenterol Hepatol, 2022. **13**(3): p. 879-899.
83. Lian, J., et al., *Liver specific inactivation of carboxylesterase 3/triacylglycerol hydrolase decreases blood lipids without causing severe steatosis in mice*. Hepatology, 2012. **56**(6): p. 2154-62.
84. Lian, J., et al., *Ces3/TGH deficiency improves dyslipidemia and reduces atherosclerosis in Ldlr(-/-) mice*. Circ Res, 2012. **111**(8): p. 982-90.
85. Jacobs, R.L., et al., *Targeted deletion of hepatic CTP:phosphocholine cytidyltransferase alpha in mice decreases plasma high density and very low density lipoproteins*. J Biol Chem, 2004. **279**(45): p. 47402-10.
86. Jacobs, R.L., et al., *Hepatic CTP:phosphocholine cytidyltransferase-alpha is a critical predictor of plasma high density lipoprotein and very low density lipoprotein*. J Biol Chem, 2008. **283**(4): p. 2147-55.
87. Noga, A.A., Y. Zhao, and D.E. Vance, *An unexpected requirement for phosphatidylethanolamine N-methyltransferase in the secretion of very low density lipoproteins*. J Biol Chem, 2002. **277**(44): p. 42358-65.
88. Zhao, Y., et al., *Lack of phosphatidylethanolamine N-methyltransferase alters plasma VLDL phospholipids and attenuates atherosclerosis in mice*. Arterioscler Thromb Vasc Biol, 2009. **29**(9): p. 1349-55.
89. Li, Z. and D.E. Vance, *Phosphatidylcholine and choline homeostasis*. J Lipid Res, 2008. **49**(6): p. 1187-94.
90. Williams, T. and M. Fried, *A mouse locus at which transcription from both DNA strands produces mRNAs complementary at their 3' ends*. Nature, 1986. **322**(6076): p. 275-9.
91. Williams, T., et al., *The mouse surfeit locus contains a very tight cluster of four "housekeeping" genes that is conserved through evolution*. Proc Natl Acad Sci U S A, 1988. **85**(10): p. 3527-30.
92. Huxley, C. and M. Fried, *The mouse surfeit locus contains a cluster of six genes associated with four CpG-rich islands in 32 kilobases of genomic DNA*. Mol Cell Biol, 1990. **10**(2): p. 605-14.
93. Mashkevich, G., et al., *SHY1, the yeast homolog of the mammalian SURF-1 gene, encodes a mitochondrial protein required for respiration*. J Biol Chem, 1997. **272**(22): p. 14356-64.
94. Da-Re, C., et al., *Leigh syndrome in Drosophila melanogaster: morphological and biochemical characterization of Surf1 post-transcriptional silencing*. J Biol Chem, 2014. **289**(42): p. 29235-46.
95. Giallongo, A., J. Yon, and M. Fried, *Ribosomal protein L7a is encoded by a gene (Surf-3) within the tightly clustered mouse surfeit locus*. Mol Cell Biol, 1989. **9**(1): p. 224-31.
96. Xu, F.G., Q.Y. Ma, and Z. Wang, *Blockade of hedgehog signaling pathway as a therapeutic strategy for pancreatic cancer*. Cancer Lett, 2009. **283**(2): p. 119-24.
97. Song, C., et al., *A de novo variant in MMP13 identified in a patient with dominant metaphyseal anadysplasia*. Eur J Med Genet, 2019. **62**(11): p. 103575.

98. Garson, K., T. Duhig, and M. Fried, *Tissue-specific processing of the Surf-5 and Surf-4 mRNAs*. *Gene Expr*, 1996. **6**(4): p. 209-18.
99. Garson, K., et al., *Surf5: a gene in the tightly clustered mouse surfait locus is highly conserved and transcribed divergently from the rpL7A (Surf3) gene*. *Genomics*, 1995. **30**(2): p. 163-70.
100. Angiolillo, A., et al., *The human homologue of the mouse Surf5 gene encodes multiple alternatively spliced transcripts*. *Gene*, 2002. **284**(1-2): p. 169-78.
101. Moraleva, A., et al., *Involvement of the specific nucleolar protein SURF6 in regulation of proliferation and ribosome biogenesis in mouse NIH/3T3 fibroblasts*. *Cell Cycle*, 2017. **16**(20): p. 1979-1991.
102. Reeves, J.E. and M. Fried, *The surf-4 gene encodes a novel 30 kDa integral membrane protein*. *Mol Membr Biol*, 1995. **12**(2): p. 201-8.
103. Caldwell, S.R., K.J. Hill, and A.A. Cooper, *Degradation of endoplasmic reticulum (ER) quality control substrates requires transport between the ER and Golgi*. *J Biol Chem*, 2001. **276**(26): p. 23296-303.
104. Jumper, J., et al., *Highly accurate protein structure prediction with AlphaFold*. *Nature*, 2021. **596**(7873): p. 583-589.
105. Appenzeller, C., et al., *The lectin ERGIC-53 is a cargo transport receptor for glycoproteins*. *Nat Cell Biol*, 1999. **1**(6): p. 330-4.
106. Mitrovic, S., et al., *The cargo receptors Surf4, endoplasmic reticulum-Golgi intermediate compartment (ERGIC)-53, and p25 are required to maintain the architecture of ERGIC and Golgi*. *Mol Biol Cell*, 2008. **19**(5): p. 1976-90.
107. Yin, Y., et al., *Surf4 (Erv29p) binds amino-terminal tripeptide motifs of soluble cargo proteins with different affinities, enabling prioritization of their exit from the endoplasmic reticulum*. *PLoS Biol*, 2018. **16**(8): p. e2005140.
108. Vitale, A. and J. Denecke, *The endoplasmic reticulum-gateway of the secretory pathway*. *Plant Cell*, 1999. **11**(4): p. 615-28.
109. Lin, Z., et al., *The Endoplasmic Reticulum Cargo Receptor SURF4 Facilitates Efficient Erythropoietin Secretion*. *Mol Cell Biol*, 2020. **40**(23).
110. Ordonez, A., et al., *Cargo receptor-assisted endoplasmic reticulum export of pathogenic alpha1-antitrypsin polymers*. *Cell Rep*, 2021. **35**(7): p. 109144.
111. Saegusa, K., et al., *Cargo receptor Surf4 regulates endoplasmic reticulum export of proinsulin in pancreatic beta-cells*. *Commun Biol*, 2022. **5**(1): p. 458.
112. Jelkmann, W., *Erythropoietin*. *Front Horm Res*, 2016. **47**: p. 115-27.
113. Maxwell, P.H., et al., *Sites of erythropoietin production*. *Kidney Int*, 1997. **51**(2): p. 393-401.
114. Shih, H.M., C.J. Wu, and S.L. Lin, *Physiology and pathophysiology of renal erythropoietin-producing cells*. *J Formos Med Assoc*, 2018. **117**(11): p. 955-963.
115. Newton, S.S. and M. Sathyanesan, *Erythropoietin and Non-Erythropoietic Derivatives in Cognition*. *Front Pharmacol*, 2021. **12**: p. 728725.
116. Gooptu, B., U.I. Ekeowa, and D.A. Lomas, *Mechanisms of emphysema in alpha1-antitrypsin deficiency: molecular and cellular insights*. *Eur Respir J*, 2009. **34**(2): p. 475-88.
117. Wu, Y., et al., *A lag in intracellular degradation of mutant alpha 1-antitrypsin correlates with the liver disease phenotype in homozygous PiZZ alpha 1-antitrypsin deficiency*. *Proc Natl Acad Sci U S A*, 1994. **91**(19): p. 9014-8.

118. Nicholson, A.M., et al., *Prosaposin is a regulator of progranulin levels and oligomerization*. Nat Commun, 2016. **7**: p. 11992.
119. Zhou, X., et al., *Impaired prosaposin lysosomal trafficking in frontotemporal lobar degeneration due to progranulin mutations*. Nat Commun, 2017. **8**: p. 15277.
120. Terryn, J., C.M. Verfaillie, and P. Van Damme, *Tweaking Progranulin Expression: Therapeutic Avenues and Opportunities*. Front Mol Neurosci, 2021. **14**: p. 713031.
121. Chitramuthu, B.P., H.P.J. Bennett, and A. Bateman, *Progranulin: a new avenue towards the understanding and treatment of neurodegenerative disease*. Brain, 2017. **140**(12): p. 3081-3104.
122. Devireddy, S. and S.M. Ferguson, *Efficient progranulin exit from the ER requires its interaction with prosaposin, a Surf4 cargo*. J Cell Biol, 2022. **221**(2).
123. Saegusa, K., et al., *SFT-4/Surf4 control ER export of soluble cargo proteins and participate in ER exit site organization*. J Cell Biol, 2018. **217**(6): p. 2073-2085.
124. Shomron, O., et al., *COPII collar defines the boundary between ER and ER exit site and does not coat cargo containers*. J Cell Biol, 2021. **220**(6).
125. Weigel, A.V., et al., *ER-to-Golgi protein delivery through an interwoven, tubular network extending from ER*. Cell, 2021. **184**(9): p. 2412-2429 e16.
126. Yan, R., et al., *SURF4-induced tubular ERGIC selectively expedites ER-to-Golgi transport*. Dev Cell, 2022. **57**(4): p. 512-525 e8.
127. Jackson, L.P., et al., *Molecular basis for recognition of dilysine trafficking motifs by COPI*. Dev Cell, 2012. **23**(6): p. 1255-62.
128. Mukai, K., et al., *Homeostatic regulation of STING by retrograde membrane traffic to the ER*. Nat Commun, 2021. **12**(1): p. 61.
129. Deng, Z., et al., *A defect in COPI-mediated transport of STING causes immune dysregulation in COPA syndrome*. J Exp Med, 2020. **217**(11).
130. Phuyal, S. and H. Farhan, *Want to leave the ER? We offer vesicles, tubules, and tunnels*. J Cell Biol, 2021. **220**(6).
131. Emmer, B.T., et al., *The cargo receptor SURF4 promotes the efficient cellular secretion of PCSK9*. Elife, 2018. **7**: p. e38839.
132. Wolf, A., et al., *Autocrine effects of PCSK9 on cardiomyocytes*. Basic Res Cardiol, 2020. **115**(6): p. 65.
133. Wang, X., et al., *Receptor-Mediated ER Export of Lipoproteins Controls Lipid Homeostasis in Mice and Humans*. Cell Metab, 2021. **33**(2): p. 350-366 e7.
134. Emmer, B.T., et al., *Murine Surf4 is essential for early embryonic development*. PLoS One, 2020. **15**(1): p. e0227450.
135. Farese, R.V., Jr., et al., *Knockout of the mouse apolipoprotein B gene results in embryonic lethality in homozygotes and protection against diet-induced hypercholesterolemia in heterozygotes*. Proc Natl Acad Sci U S A, 1995. **92**(5): p. 1774-8.
136. Wu, L., et al., *Surf4 facilitates reprogramming by activating the cellular response to endoplasmic reticulum stress*. Cell Prolif, 2021. **54**(11): p. e13133.
137. Wang, S., et al., *Proteome of mouse oocytes at different developmental stages*. Proc Natl Acad Sci U S A, 2010. **107**(41): p. 17639-44.
138. Gao, Y., et al., *Protein Expression Landscape of Mouse Embryos during Pre-implantation Development*. Cell Rep, 2017. **21**(13): p. 3957-3969.
139. Kong, L., et al., *Surfeit 4 Contributes to the Replication of Hepatitis C Virus Using Double-Membrane Vesicles*. J Virol, 2020. **94**(2).

140. Kong, L., et al., *Prolactin Regulatory Element Binding Protein Is Involved in Hepatitis C Virus Replication by Interaction with NS4B*. J Virol, 2016. **90**(6): p. 3093-111.
141. Snijder, E.J., et al., *A unifying structural and functional model of the coronavirus replication organelle: Tracking down RNA synthesis*. PLoS Biol, 2020. **18**(6): p. e3000715.
142. Kim, J., et al., *SURF4 has oncogenic potential in NIH3T3 cells*. Biochem Biophys Res Commun, 2018. **502**(1): p. 43-47.
143. Yue, Y., et al., *SURF4 maintains stem-like properties via BIRC3 in ovarian cancer cells*. J Gynecol Oncol, 2020. **31**(4): p. e46.
144. Frazzi, R., *BIRC3 and BIRC5: multi-faceted inhibitors in cancer*. Cell Biosci, 2021. **11**(1): p. 8.
145. Tang, X., et al., *A SURF4-to-proteoglycan relay mechanism that mediates the sorting and secretion of a tagged variant of sonic hedgehog*. Proc Natl Acad Sci U S A, 2022. **119**(11): p. e2113991119.
146. Wang, W., R. Shiraishi, and D. Kawauchi, *Sonic Hedgehog Signaling in Cerebellar Development and Cancer*. Front Cell Dev Biol, 2022. **10**: p. 864035.
147. Shen, Y., et al., *Surf4 regulates expression of proprotein convertase subtilisin/kexin type 9 (PCSK9) but is not required for PCSK9 secretion in cultured human hepatocytes*. Biochim Biophys Acta Mol Cell Biol Lipids, 2020. **1865**(2): p. 158555.
148. Bahitham, W., et al., *Liver-specific expression of carboxylesterase 1g/esterase-x reduces hepatic steatosis, counteracts dyslipidemia and improves insulin signaling*. Biochim Biophys Acta, 2016. **1861**(5): p. 482-90.
149. Gu, H.M., et al., *Characterization of the role of EGF-A of low-density lipoprotein receptor in PCSK9 binding*. J Lipid Res, 2013. **54**(12): p. 3345-57.
150. Gu, H.M., et al., *Characterization of palmitoylation of ATP binding cassette transporter G1: effect on protein trafficking and function*. Biochim Biophys Acta, 2013. **1831**(6): p. 1067-1078.
151. Gu, H.M., et al., *Identification of an Amino Acid Residue Critical for Plasma Membrane Localization of ATP-Binding Cassette Transporter G1*. Arterioscler Thromb Vasc Biol, 2016. **36**(2): p. 253-255.
152. Folch, J., M. Lees, and G.H. Sloane Stanley, *A simple method for the isolation and purification of total lipides from animal tissues*. J Biol Chem, 1957. **226**(1): p. 497-509.
153. Zolotukhin, S., et al., *Recombinant adeno-associated virus purification using novel methods improves infectious titer and yield*. Gene Ther, 1999. **6**(6): p. 973-85.
154. Wang, B., et al., *Atherosclerosis-associated hepatic secretion of VLDL but not PCSK9 is dependent on cargo receptor protein Surf4*. J Lipid Res, 2021. **62**: p. 100091.
155. Zhang, D.W., et al., *Structural requirements for PCSK9-mediated degradation of the low-density lipoprotein receptor*. Proc Natl Acad Sci U S A, 2008. **105**(35): p. 13045-50.
156. Cameron, J., et al., *Effect of mutations in the PCSK9 gene on the cell surface LDL receptors*. Hum Mol Genet, 2006. **15**(9): p. 1551-8.
157. Benjannet, S., et al., *NARC-1/PCSK9 and its natural mutants: zymogen cleavage and effects on the low density lipoprotein (LDL) receptor and LDL cholesterol*. J Biol Chem, 2004. **279**(47): p. 48865-75.
158. Denis, M., et al., *Gene inactivation of proprotein convertase subtilisin/kexin type 9 reduces atherosclerosis in mice*. Circulation, 2012. **125**(7): p. 894-901.
159. Grefhorst, A., et al., *Plasma PCSK9 preferentially reduces liver LDL receptors in mice*. J Lipid Res, 2008. **49**(6): p. 1303-11.

160. Szul, T. and E. Sztul, *COPII and COPI traffic at the ER-Golgi interface*. Physiology (Bethesda), 2011. **26**(5): p. 348-64.
161. Benjannet, S., et al., *The proprotein convertase (PC) PCSK9 is inactivated by furin and/or PC5/6A: functional consequences of natural mutations and post-translational modifications*. J Biol Chem, 2006. **281**(41): p. 30561-72.
162. Luo, Y., et al., *Function and distribution of circulating human PCSK9 expressed extrahepatically in transgenic mice*. J Lipid Res, 2009. **50**(8): p. 1581-8.
163. Kim, J.Y., et al., *ER Stress Drives Lipogenesis and Steatohepatitis via Caspase-2 Activation of SIP*. Cell, 2018. **175**(1): p. 133-145 e15.
164. Wang, H. and R.H. Eckel, *Lipoprotein lipase: from gene to obesity*. Am J Physiol Endocrinol Metab, 2009. **297**(2): p. E271-88.
165. Sandesara, P.B., et al., *The Forgotten Lipids: Triglycerides, Remnant Cholesterol, and Atherosclerotic Cardiovascular Disease Risk*. Endocr Rev, 2019. **40**(2): p. 537-557.
166. Choi, S.H. and H.N. Ginsberg, *Increased very low density lipoprotein (VLDL) secretion, hepatic steatosis, and insulin resistance*. Trends Endocrinol Metab, 2011. **22**(9): p. 353-63.
167. Watts, G.F., et al., *Familial hypercholesterolaemia: evolving knowledge for designing adaptive models of care*. Nat Rev Cardiol, 2020. **17**: p. 360-377.
168. Huang, L.S., et al., *apo B gene knockout in mice results in embryonic lethality in homozygotes and neural tube defects, male infertility, and reduced HDL cholesterol ester and apo A-I transport rates in heterozygotes*. J Clin Invest, 1995. **96**(5): p. 2152-61.
169. Raabe, M., et al., *Analysis of the role of microsomal triglyceride transfer protein in the liver of tissue-specific knockout mice*. J Clin Invest, 1999. **103**(9): p. 1287-98.
170. Conlon, D.M., et al., *Inhibition of apolipoprotein B synthesis stimulates endoplasmic reticulum autophagy that prevents steatosis*. J Clin Invest, 2016. **126**(10): p. 3852-3867.
171. Shin, J.Y., et al., *Nuclear envelope-localized torsinA-LAP1 complex regulates hepatic VLDL secretion and steatosis*. J Clin Invest, 2019. **130**: p. 4885-4900.
172. Doonan, L.M., E.A. Fisher, and J.L. Brodsky, *Can modulators of apolipoproteinB biogenesis serve as an alternate target for cholesterol-lowering drugs?* Biochim Biophys Acta Mol Cell Biol Lipids, 2018. **1863**(7): p. 762-771.
173. Zaid, A., et al., *Proprotein convertase subtilisin/kexin type 9 (PCSK9): hepatocyte-specific low-density lipoprotein receptor degradation and critical role in mouse liver regeneration*. Hepatology, 2008. **48**(2): p. 646-54.
174. Tadin-Strapps, M., et al., *siRNA-induced liver ApoB knockdown lowers serum LDL-cholesterol in a mouse model with human-like serum lipids*. J Lipid Res, 2011. **52**(6): p. 1084-97.
175. Ason, B., et al., *ApoB siRNA-induced liver steatosis is resistant to clearance by the loss of fatty acid transport protein 5 (Fatp5)*. Lipids, 2011. **46**(11): p. 991-1003.
176. Rozema, D.B., et al., *Dynamic PolyConjugates for targeted in vivo delivery of siRNA to hepatocytes*. Proc Natl Acad Sci U S A, 2007. **104**(32): p. 12982-7.
177. Lambert, J.E., et al., *Increased de novo lipogenesis is a distinct characteristic of individuals with nonalcoholic fatty liver disease*. Gastroenterology, 2014. **146**(3): p. 726-35.
178. Chakravarthy, M.V., et al., *"New" hepatic fat activates PPARalpha to maintain glucose, lipid, and cholesterol homeostasis*. Cell Metab, 2005. **1**(5): p. 309-22.
179. Sanders, F.W. and J.L. Griffin, *De novo lipogenesis in the liver in health and disease: more than just a shunting yard for glucose*. Biol Rev Camb Philos Soc, 2016. **91**(2): p. 452-68.

180. Qiu, W., et al., *Hepatic autophagy mediates endoplasmic reticulum stress-induced degradation of misfolded apolipoprotein B*. *Hepatology*, 2011. **53**(5): p. 1515-25.
181. Ference, B.A., et al., *Impact of Lipids on Cardiovascular Health: JACC Health Promotion Series*. *J Am Coll Cardiol*, 2018. **72**(10): p. 1141-1156.
182. Goldstein, J.L., H.H. Hobbs, and M.S. Brown, *Familial Hypercholesterolemia*, in *The Metabolic & Molecular Bases of Inherited Disease* C.R. Scriver, Editor. 2001, McGraw-Hill: New York. p. 2863-2913.
183. Xia, X.D., et al., *Regulation of PCSK9 Expression and Function: Mechanisms and Therapeutic Implications*. *Front Cardiovasc Med*, 2021. **8**: p. 764038.
184. Hamilton, R.L., et al., *Chylomicron-sized lipid particles are formed in the setting of apolipoprotein B deficiency*. *J Lipid Res*, 1998. **39**(8): p. 1543-57.
185. Rader, D.J. and J.J. Kastelein, *Lomitapide and mipomersen: two first-in-class drugs for reducing low-density lipoprotein cholesterol in patients with homozygous familial hypercholesterolemia*. *Circulation*, 2014. **129**(9): p. 1022-32.
186. Getz, G.S. and C.A. Reardon, *Diet and murine atherosclerosis*. *Arterioscler Thromb Vasc Biol*, 2006. **26**(2): p. 242-9.
187. Raffai, R.L., S.M. Loeb, and K.H. Weisgraber, *Apolipoprotein E promotes the regression of atherosclerosis independently of lowering plasma cholesterol levels*. *Arterioscler Thromb Vasc Biol*, 2005. **25**(2): p. 436-41.
188. Pendse, A.A., et al., *Apolipoprotein E knock-out and knock-in mice: atherosclerosis, metabolic syndrome, and beyond*. *J Lipid Res*, 2009. **50 Suppl**: p. S178-82.
189. Curtiss, L.K. and W.A. Boisvert, *Apolipoprotein E and atherosclerosis*. *Curr Opin Lipidol*, 2000. **11**(3): p. 243-51.
190. Barcat, D., et al., *Combined hyperlipidemia/hyperalphalipoproteinemia associated with premature spontaneous atherosclerosis in mice lacking hepatic lipase and low density lipoprotein receptor*. *Atherosclerosis*, 2006. **188**(2): p. 347-55.
191. Mezdour, H., et al., *Hepatic lipase deficiency increases plasma cholesterol but reduces susceptibility to atherosclerosis in apolipoprotein E-deficient mice*. *J Biol Chem*, 1997. **272**(21): p. 13570-5.
192. Karackattu, S.L., B. Trigatti, and M. Krieger, *Hepatic lipase deficiency delays atherosclerosis, myocardial infarction, and cardiac dysfunction and extends lifespan in SR-BI/apolipoprotein E double knockout mice*. *Arterioscler Thromb Vasc Biol*, 2006. **26**(3): p. 548-54.
193. Trigatti, B., et al., *Influence of the high density lipoprotein receptor SR-BI on reproductive and cardiovascular pathophysiology*. *Proc Natl Acad Sci U S A*, 1999. **96**(16): p. 9322-7.
194. Covey, S.D., et al., *Scavenger receptor class B type I-mediated protection against atherosclerosis in LDL receptor-negative mice involves its expression in bone marrow-derived cells*. *Arterioscler Thromb Vasc Biol*, 2003. **23**(9): p. 1589-94.
195. Koornneef, A., et al., *Apolipoprotein B knockdown by AAV-delivered shRNA lowers plasma cholesterol in mice*. *Mol Ther*, 2011. **19**(4): p. 731-40.
196. Borel, F., M.A. Kay, and C. Mueller, *Recombinant AAV as a platform for translating the therapeutic potential of RNA interference*. *Mol Ther*, 2014. **22**(4): p. 692-701.
197. Grimm, D., et al., *In vitro and in vivo gene therapy vector evolution via multispecies interbreeding and retargeting of adeno-associated viruses*. *J Virol*, 2008. **82**(12): p. 5887-911.

198. Purcell-Huynh, D.A., et al., *Transgenic mice expressing high levels of human apolipoprotein B develop severe atherosclerotic lesions in response to a high-fat diet*. J Clin Invest, 1995. **95**(5): p. 2246-57.
199. Farese, R.V., Jr., et al., *Phenotypic analysis of mice expressing exclusively apolipoprotein B48 or apolipoprotein B100*. Proc Natl Acad Sci U S A, 1996. **93**(13): p. 6393-8.
200. Jones, C., et al., *Disruption of LDL but not VLDL clearance in autosomal recessive hypercholesterolemia*. J Clin Invest, 2007. **117**(1): p. 165-74.
201. Rohlmann, A., et al., *Inducible inactivation of hepatic LRP gene by cre-mediated recombination confirms role of LRP in clearance of chylomicron remnants*. J Clin Invest, 1998. **101**(3): p. 689-95.
202. Tangirala, R.K., et al., *Reduction of isoprostanes and regression of advanced atherosclerosis by apolipoprotein E*. J Biol Chem, 2001. **276**(1): p. 261-6.
203. Thorngate, F.E., et al., *Low levels of extrahepatic nonmacrophage ApoE inhibit atherosclerosis without correcting hypercholesterolemia in ApoE-deficient mice*. Arterioscler Thromb Vasc Biol, 2000. **20**(8): p. 1939-45.
204. Baitsch, D., et al., *Apolipoprotein E induces antiinflammatory phenotype in macrophages*. Arterioscler Thromb Vasc Biol, 2011. **31**(5): p. 1160-8.
205. Li, K., et al., *Apolipoprotein E enhances microRNA-146a in monocytes and macrophages to suppress nuclear factor-kappaB-driven inflammation and atherosclerosis*. Circ Res, 2015. **117**(1): p. e1-e11.
206. Swertfeger, D.K. and D.Y. Hui, *Apolipoprotein E receptor binding versus heparan sulfate proteoglycan binding in its regulation of smooth muscle cell migration and proliferation*. J Biol Chem, 2001. **276**(27): p. 25043-8.
207. Miyata, M. and J.D. Smith, *Apolipoprotein E allele-specific antioxidant activity and effects on cytotoxicity by oxidative insults and beta-amyloid peptides*. Nat Genet, 1996. **14**(1): p. 55-61.
208. Getz, G.S. and C.A. Reardon, *Apoprotein E and Reverse Cholesterol Transport*. Int J Mol Sci, 2018. **19**(11).
209. Bellosta, S., et al., *Macrophage-specific expression of human apolipoprotein E reduces atherosclerosis in hypercholesterolemic apolipoprotein E-null mice*. J Clin Invest, 1995. **96**(5): p. 2170-9.
210. Wei, E., et al., *Loss of TGH/Ces3 in mice decreases blood lipids, improves glucose tolerance, and increases energy expenditure*. Cell Metab, 2010. **11**(3): p. 183-93.
211. Sniderman, A.D., A.M. Navar, and G. Thanassoulis, *Apolipoprotein B vs Low-Density Lipoprotein Cholesterol and Non-High-Density Lipoprotein Cholesterol as the Primary Measure of Apolipoprotein B Lipoprotein-Related Risk: The Debate Is Over*. JAMA Cardiol, 2021.
212. Marston, N.A., et al., *Association of Apolipoprotein B-Containing Lipoproteins and Risk of Myocardial Infarction in Individuals With and Without Atherosclerosis: Distinguishing Between Particle Concentration, Type, and Content*. JAMA Cardiol, 2021.
213. Colgan, S.M., et al., *Endoplasmic reticulum stress causes the activation of sterol regulatory element binding protein-2*. Int J Biochem Cell Biol, 2007. **39**(10): p. 1843-51.